Electronic Supplementary Material (ESI) for Organic Chemistry Frontiers.

Electronic Supplementary Information

Highly efficient synthesis of hydrogen-bonded aromatic tetramers as macrocyclic receptors for selective recognition of lithium ion

Xuwen Guo, Yizhou Yang, Zhiyong Peng, Yimin Cai, Wen Feng and Lihua Yuan*

College of Chemistry, Key Laboratory for Radiation Physics and Technology of Ministry of Education, Sichuan University, Chengdu 610064, Sichuan, China

E-mail: lhyuan@scu.edu.cn

Table of Contents

1. General Methods

All chemicals were obtained from commercial suppliers and were used as received unless other-wise noted. All reactions were conducted with oven-dried glassware under atmosphere or nitrogen. Solvents were dried and distilled following usual protocols. Column chromatography was carried out using silica gel (300-400 mesh). Solvents for extraction and chromatography were reagent grade. $CDCl_3$, CD_3CN and CD_3OD were from Cambridge Isotope Laboratories (CIL).

Analytical NMR spectra were recorded on Bruker AVANCE AV II-400 MHz or AVANCE AV II-600 MHz, at a constant temperature of 298 K, if not specifically indicated. Chemical shifts are reported in δ values in ppm using tetramethylsilane (TMS) or residual solvent as internal standard and coupling constants (*J*) are denoted in Hz. Multiplicities are denoted as follows: s = singlet, d = doublet, t = triplet, dd = double doublet and m = multiplet. MALDI-TOF MS spectra were recorded on a Bruker Autoflex III MS and AXIMA Performance spectrometer, matrix is α-cyano-4-hydroxycinnamic acid (CCA), 2,6-dihydroxyacetophenone (DHAP) and 2,5-dihydroxybenzoic acid (DHB). ESI mass spectra were recorded on a Bruker Daltonics MicroTOF-Q II. ESI-MS were obtained on a Thermo-ITQ. UV-vis spectra were measured by SHIMADZU UV-2450. Fourier transform Infrared (FT-IR) data were collected by a Thermal Nicolet NEXUS 670 FT-IR spectrophotometer.

2. Synthetic Protocols

Synthetic routes of building blocks

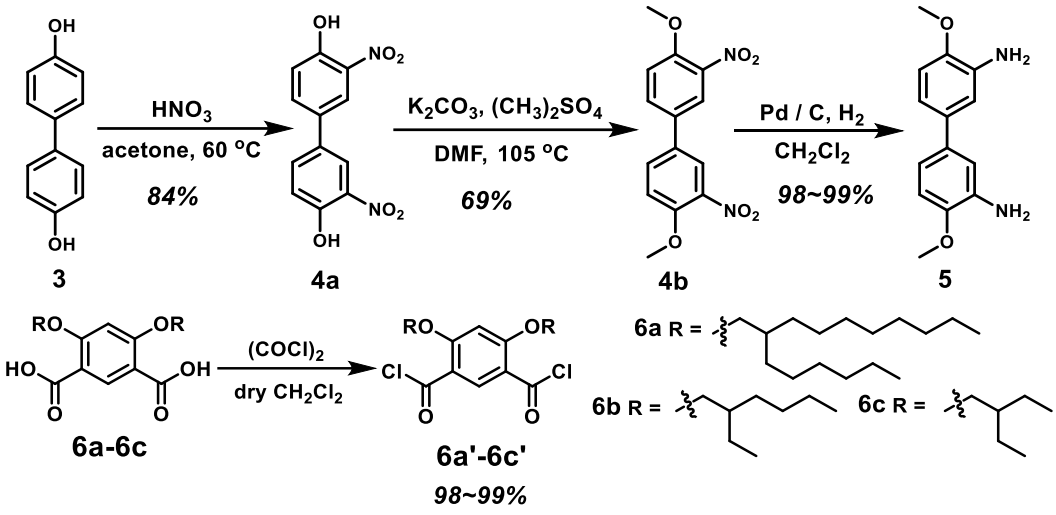

Scheme S1 Synthetic routes of building blocks

Compounds **6a-6c** were prepared according to literature procedures. [1-3]

Synthesis of compound 4a

Compound **4a** was prepared according to literature procedures.[4,5]
Compound **3** (3.05 g, 16.4 mmol) and acetone (150 ml) were added into a two-neck flask equipped with a condenser and mechanical stirrer. The mixture was heated to 60 ℃, and nitric acid (2.0 ml of 69.3% nitric acid, 32.8 mmol) was added dropwise. The solution was kept at 60 ℃ for 6 h and then filtered. The residue was washed with excess acetone to afford compound **4a** as a yellow powder (3.81 g, yield 84.2%).

^{1}H NMR (400 MHz, 298 K, DMSO-d_6) δ 11.15 (s, 1H), 8.15 (d, J = 2.4 Hz, 1H), 7.88 (dd, J = 8.7, 2.4 Hz, 1H), 7.21 (d, J = 8.7 Hz, 1H).

Synthesis of compound 4b

Compound **4a** (3.00 g, 10.9 mmol) and potassium carbonate (8.99 g, 65.4 mmol) were dissolved in DMF (100 mL) at 80 ℃ for 30 min, to which dimethyl sulfate (5.47 g, 43.4 mmol) was added dropwise. The solution was heated to 120 ℃ for 11 h and filtered. After removing the solvent under vacuum, the crude product was extracted with CH_2Cl_2 and water, NaOH and HCl solution three times (3 × 40 mL), respectively. The organic layer was dried by anhydrous Na_2SO_4. After removing the solvent, the residue was subjected to column chromatography separation (pure CH_2Cl_2). Compound **4b** was provided as a light

yellow solid (2.28 g, yield 69.1 %).

^{1}H NMR (400 MHz, 298 K, $CDCl_3$) δ 8.05 (d, J = 2.4 Hz, 1H), 7.73 (dd, J = 8.8, 2.4 Hz, 1H), 7.19 (d, J = 8.8 Hz, 1H), 4.02 (s, 3H); ^{13}C NMR (100 MHz, 298 K, $CDCl_3$) δ 152.63, 139.94, 132.10, 130.95, 123.77, 114.26, 77.34, 77.02, 76.70, 56.76, 1.03, 0.00. ESI-MS (m/z) calcd. for $C_{14}H_{12}N_2O_6$ $[M+H]^+$ 305.0773, found $[M+H]^+$ 305.1705.

Synthesis of compound 5

Compound **4b** (300 mg, 0.99 mmol) was hydrogenated in the presence of 20% Pd/C (60 mg) in CH_2Cl_2 (60 mL) for 10 h at room temperature. The solution was filtered in darkness followed by immediate removal of the solvent to afford the reduced diamine **5** as a white powder (239 mg, yield 99 %).

^{1}H NMR (400 MHz, 298 K, $CDCl_3$) δ 6.90 (s, 1H), 6.88 (d, J = 2.1 Hz, 1H), 6.81 (d, J = 8.1 Hz, 1H), 3.88 (s, 3H), 3.83 (s, 2H); ^{13}C NMR (100 MHz, 298 K, $CDCl_3$/CD_3OD =9:1 (v/v)) δ 146.93, 135.72, 134.45, 117.43, 114.15, 110.76, 77.58, 77.26, 76.94, 55.71, 49.66, 49.45, 49.24, 49.02, 48.81, -0.00; MALDI-TOF-HRMS (m/z) calcd. for $C_{14}H_{16}N_2O_2$ $[M]^+$ 244.1212, found $[M]^+$ 244.2848.

Synthesis of 1a-c *via* one pot approach

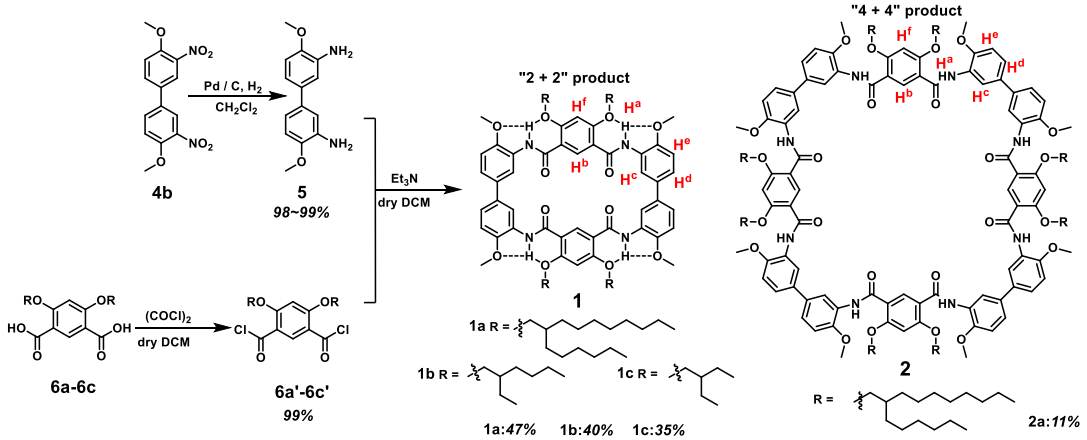

Scheme S2 Synthetic routes of one-pot method

Compound **4b** (300 mg, 0.99 mmol) was hydrogenated in the presence of 20% Pd/C (60 mg) in CH_2Cl_2 (60 mL) for 10 h at room temperature. The solution was filtered in darkness followed by immediate removal of the solvent. The reduced diamine **5** was used for the immediate macrocyclization reaction. DMF (10 μL) was added to a solution of compound **6a** (638 mg, 0.986 mmol) and oxalyl chloride (0.3 mL, 3.46 mmol) in CH_2Cl_2. The mixture was stirred for an hour at room temperature. The solvent was evaporated and the resulting

acid chloride was dried in vacuum at room temperature for 30 min to afford compound **6'a**. Compound **6'a** was dissolved in CH_2Cl_2 (30 mL) and added dropwise to a mixture of the above **5** and Et_3N (0.822 mL, 5.92 mmol) in CH_2Cl_2 (100 mL) at -20 °C. The solution was stirred under argon for 8 h. The organic layer was washed with water (30 mL × 3) and dried over anhydrous Na_2SO_4. The crude product was purified by chromatography on silica gel (eluent: CH_2Cl_2/MeOH = 35: 1) to provide the macrocycle **2a** as a white solid (90 mg, 11%) and (eluent: CH_2Cl_2/MeOH = 20: 1) to provide the macrocycle **1a** as a white solid (397 mg, yield 47 %).

1a: ^{1}H NMR (400 MHz, 298 K, $CDCl_3$) δ 9.61 (s, 4H), 9.46 (s, 2H), 9.19 (s, 4H), 7.33 (dd, *J* = 8.5, 2.3 Hz, 4H), 6.91 (d, *J* = 8.4 Hz, 3H), 6.52 (s, 2H), 4.12 (s, 7H), 3.91 (s, 12H), 2.12 (s, 3H), 1.95 (d, *J* = 46.3 Hz, 3H), 1.79 (d, *J* = 40.2 Hz, 9H), 1.53 (d, *J* = 9.7 Hz, 16H), 1.41 (d, *J* = 17.7 Hz, 18H), 1.27 (dt, *J* = 13.9, 7.3 Hz, 87H), 0.85 (t, *J* = 6.7 Hz, 33H); ^{13}C NMR (100 MHz, 298 K, $CDCl_3$:CD_3CN(5:1)) δ 168.67, 166.50, 152.77, 136.87, 132.58, 125.45, 118.62, 115.02, 101.93, 82.82, 82.50, 82.18, 78.58, 60.80, 42.70, 36.97, 36.93, 35.88, 35.75, 35.56, 35.36, 35.23, 35.17, 34.98, 34.90, 34.79, 34.70, 34.59, 34.45, 31.57, 27.75, 19.15, 19.13, 5.03. MALDI-TOF-MS (m/z) calcd. for $C_{108}H_{164}N_4O_{12}$ $[M+H]^+$ 1711.242, found $[M+H]^+$ 1711.113.

2a: ^{1}H NMR (400 MHz, 298 K, $CDCl_3$) δ 9.77 (s, 8H), 9.11 (s, 4H), 8.92 (d, J = 2.3 Hz, 8H), 7.30 (dd, J = 8.3, 2.2 Hz, 9H), 6.86 (d, J = 8.5 Hz, 8H), 6.54 (s, 4H), 4.10 (d, J = 6.4 Hz, 16H), 3.86 (s, 24H), 2.08 - 2.00 (m, 10H), 1.47-1.42 (m, 25H), 1.28 - 1.18 (m, 148H), 0.90 - 0.77 (m, 63H), 0.07 (s, 32H). ^{13}C NMR (101 MHz, 298 K, $CDCl_3$: CD_3OD (9:1)) δ 159.36, 146.66, 141.08, 136.49, 132.81, 126.98, 121.06, 118.55, 114.92, 109.12, 104.94, 95.89, 76.51, 76.19, 75.87, 72.31, 69.49, 54.66, 48.79, 48.58, 48.37, 48.16, 47.94, 47.73, 47.52, 36.59, 30.87, 30.80, 30.10, 29.04, 28.70, 28.58, 28.32, 25.71, 25.64, 21.66, 21.63, 13.05, 13.02, -0.00. MALDI-TOF-MS (m/z) calcd. for $C_{216}H_{328}N_8O_{24}$ $[M+H]^+$ 3421.962, found $[M+H]^+$ 3421.761.

1b was synthesized according to the above general procedure using compound **4b** (300 mg, 0.99 mmol) and **6b** (417 mg, 0.986 mmol). The solution was stirred under argon for 8 h. The organic layer was washed with water (3 ×30 mL) and dried over anhydrous Na_2SO_4. The crude product was purified by chromatography on silica gel (CH_2Cl_2/MeOH = 20: 1) to provide the macrocycle **1b** as a white solid (248 mg, yield 40%).

1b: ^{1}H NMR (400 MHz, 298 K, $CDCl_3$) δ 9.66 (s, 4H), 9.33 (s, 2H), 9.12 (s, 4H), 7.35 (s, 4H), 6.86 (d, *J* = 7.0 Hz, 4H), 6.24 (s, 4H), 3.89 (d, *J* = 7.9 Hz, 17H), 3.62 (d, *J* = 8.2 Hz, 4H), 2.16 (d, *J* = 6.5 Hz, 26H), 2.08 – 1.89 (m, 21H), 1.67 (s, 3H), 1.52 – 1.03 (m, 71H), 0.97 – 0.65 (m, 40H); ^{13}C NMR (100 MHz, 298 K, $CDCl_3$) δ 162.74, 160.31, 146.93, 137.85, 130.91, 126.38, 120.22, 119.67, 112.91, 109.13, 95.58, 76.53, 76.21, 75.96, 75.89, 71.95, 54.70, 48.52, 48.30, 48.09, 47.88, 47.66, 41.92, 37.73, 28.88, 28.69,

27.79, 22.31, 22.07, 13.01, 10.06, 9.45, 0.00. MALDI-TOF-MS (m/z) calcd. for $C_{76}H_{100}N_4O_{12}$ $[M+H]^+$ 1261.741, found $[M+H]^+$ 1261.875.

1c was synthesized according to the above general procedure using compound **4b** (300 mg, 0.99 mmol) and **6c** (362 mg, 0.986 mmol). The reaction mixture containing a small amount of $LiClO_4$ was purified by chromatography on silica gel (CH_2Cl_2/MeOH = 20: 1) to provide the macrocycle **1c** as a white solid (198 mg, yield 35%).

1c ⊃ $LiClO_4$: ^{1}H NMR (400 MHz, 298 K, $CDCl_3$) δ 9.86 (s, 4H), 9.31 (s, 2H), 9.07 (d, *J* = 2.1 Hz, 4H), 7.37 (s, 14H), 6.92 (d, *J* = 8.1 Hz, 4H), 6.44 (s, 2H), 5.35 (d, *J* = 1.1 Hz, 3H), 4.05 (d, *J* = 6.2 Hz, 7H), 3.95 (s, 10H), 3.73 (s, 2H), 2.41 (s, 15H), 1.99 (p, *J* = 2.4 Hz, 12H), 1.56 (t, *J* = 7.1 Hz, 16H), 1.26 (s, 14H), 1.00 (t, *J* = 7.3 Hz, 24H), 0.86 (s, 7H), 0.09 (s, 2H), 0.07 (s, 32H); ^{13}C NMR (100 MHz, 298 K, $CDCl_3$/CD_3OD=9:1(v/v)) δ 163.88, 161.52, 148.10, 138.95, 132.21, 127.46, 121.55, 120.96, 114.10, 110.27, 108.10, 77.57, 77.25, 76.94, 72.76, 55.75, 49.63, 49.42, 49.20, 48.99, 48.78, 48.56, 40.26, 29.78, 29.40, 22.92, 10.76, 1.07, 1.07, 0.00; MALDI-TOF-HRMS (m/z) calcd. for $C_{68}H_{84}N_4O_{12}$ $[M+Li]^+$ 1155.6236, found $[M+Li]^+$ 1155.1378.

Synthesis of 1a-b *via* fragment coupling approach

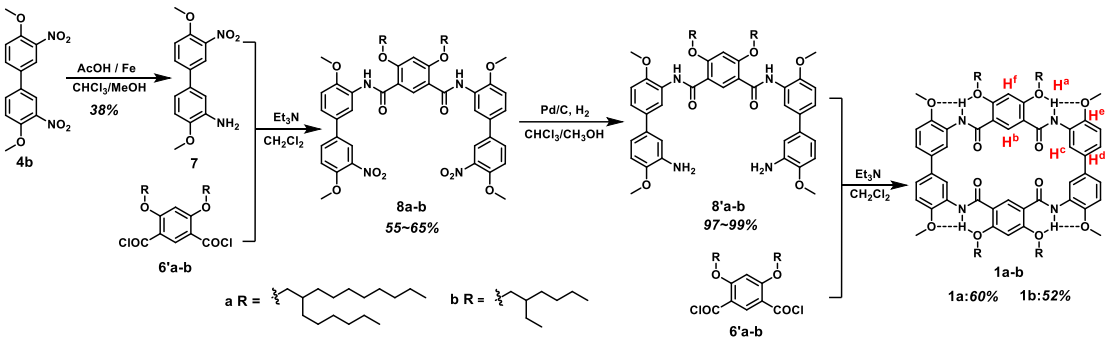

Scheme S3 Synthetic routes of fragment coupling method

Synthesis of compound 7

Compound **4b** (500 mg, 1.65 mmol) and reduced iron powder (276 mg, 4.94 mmol) were added into a mixed solvent of $CHCl_3$/MeOH (120 mL, v:v = 5:1) with AcOH (5 mL) and then stirred at 65 °C under reflux for 6 hours. The solution was filtered in darkness as fast as possible followed by immediate removal of the solvent. The crude product was washed with CH_2Cl_2 and water for three times followed by separation with column chromatography (DCM) to recycle start material **4b** 287 mg and provide the reduced monoamine **7** as a yellow powder (173 mg, yield 38.4 %).

^{1}H NMR(400 MHz, 298 K, $CDCl_3$) δ 8.02 (d, *J* = 2.3 Hz, 1H), 7.69 (dd, *J* = 8.7, 2.4 Hz, 1H), 7.11 (d, *J* = 8.7 Hz, 1H), 6.91 (dq, *J* = 5.0, 2.2 Hz, 2H), 6.85 (d, *J* = 8.9 Hz, 1H),

3.99 (s, 3H), 3.90 (s, 5H); ^{13}C NMR (100 MHz, 298 K, $CDCl_3$) δ 151.72, 147.31, 136.68, 134.06, 132.09, 131.38, 123.62, 116.75, 113.78, 113.07, 110.71, 77.34, 77.02, 76.71, 56.66, 55.64, 1.03, -0.00; ESI-HRMS (m/z) calcd. for $C_{14}H_{14}N_2O_4$ $[M+H]^+$ 275.1032, found $[M+H]^+$ 275.1021.

Synthesis of compound 8a-b

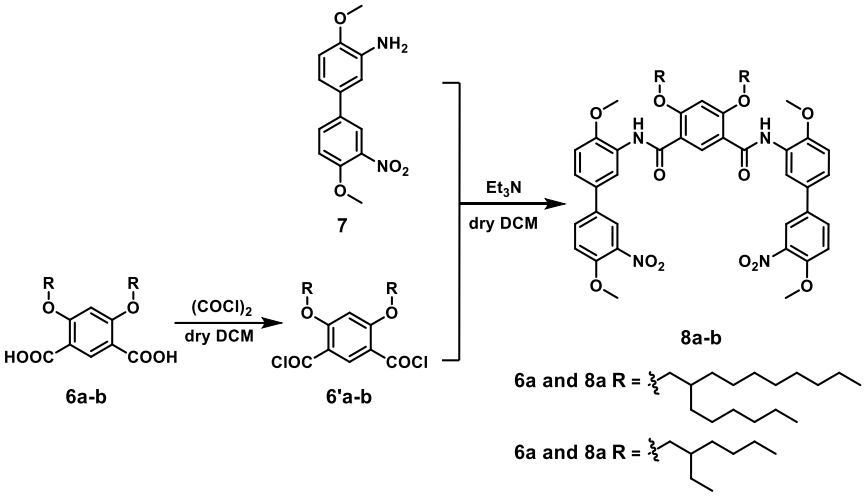

Scheme S4 Synthesis of compound **8a-b**

DMF (10 μL) was added to a solution of compound **6a** (236 mg, 0.365 mmol) and oxalyl chloride (144 μL, 1.46 mmol) in CH_2Cl_2 (40 mL). The mixture was stirred for an hour at room temperature. The solvent and residual oxalyl chloride was then removed under vacuum to produce yellow oil **6'a**. Compound **6'a** was dissolved in CH_2Cl_2 (30 mL) and added dropwise to a mixture of monoamine **7** (200 mg, 0.730 mmol) and Et_3N (270 μ mL, 2.19 mmol) in dry CH_2Cl_2 (40 mL) at room temperature. The solution was stirred under N_2 for 3 hours. The organic layer was washed with water for three times (3 × 20 mL). The crude product was purified by chromatography on silica gel (CH_2Cl_2/EA = 20:1) to provide the product **8a** as a yellow solid (251 mg, yield 59.5 %).

^{1}H NMR (400 MHz, 298 K, $CDCl_3$) δ 9.92 (s, 2H), 9.16 (s, 1H), 8.91 (d, *J* = 2.3 Hz, 2H), 8.08 (d, *J* = 2.4 Hz, 2H), 7.85 (dd, *J* = 8.7, 2.4 Hz, 2H), 7.24 (ddd, *J* = 8.5, 2.5, 1.2 Hz, 2H), 7.14 (d, *J* = 8.8 Hz, 2H), 6.97 (d, *J* = 8.5 Hz, 2H), 6.60 (s, 1H), 4.15 (d, *J* = 6.2 Hz, 4H), 4.00 (s, 6H), 3.94 (s, 6H), 2.08 – 2.01 (m, 2H), 1.52 – 1.13 (m, 48H), 0.83 (q, 12H); ^{13}C NMR (100 MHz, 298 K, $CDCl_3$) δ 162.52, 160.34, 151.85, 148.21, 139.72, 137.67, 133.70, 132.62, 131.32, 128.75, 123.60, 121.63, 119.28, 116.10, 113.87, 110.29, 96.83, 77.35, 77.04, 76.72, 73.28, 56.68, 55.78, 37.68, 31.84, 31.78, 31.16, 30.01, 29.71, 29.67, 29.55, 29.30, 26.73, 26.70, 22.64, 22.63, 14.08, 14.06, 1.03, -0.00. MALDI-TOF-HRMS (m/z) calcd. for $C_{68}H_{94}N_4O_{12}$ $[M+Na]^+$ 1182.4834, found $[M+ Na]^+$ 1183.2583.

8b was synthesized according to the above general procedure using compound **6b** (154 mg, 0.365 mmol) and monoamine **7** (200 mg, 0.730 mmol). The solution was stirred under N_2 for 3 hours. The organic layer was washed with water for three times (3 × 20 mL). The crude product was purified by chromatography on silica gel (CH_2Cl_2/EA = 20:1) to provide the product **8b** as a yellow solid (254 mg, yield 74.5 %).

^{1}H NMR (400 MHz, 298 K, $CDCl_3$) δ 9.89 (s, 2H), 9.15 (s, 1H), 8.91 (d, *J* = 2.3 Hz, 2H), 8.09 (d, *J* = 2.4 Hz, 2H), 7.86 (dd, *J* = 8.7, 2.4 Hz, 2H), 7.27 (d, *J* = 2.3 Hz, 3H), 7.25 (d, *J* = 2.3 Hz, 1H), 7.15 (d, *J* = 8.8 Hz, 2H), 6.98 (d, *J* = 8.5 Hz, 2H), 6.60 (s, 1H), 4.20 – 4.11 (m, 4H), 4.00 (s, 7H), 3.94 (s, 6H), 2.02 (p, *J* = 6.2 Hz, 2H), 1.60 (d, *J* = 14.2 Hz, 7H), 1.58 – 1.51 (m, 4H), 1.51 – 1.40 (m, 5H), 1.39 – 1.24 (m, 11H), 0.96 (t, *J* = 7.4 Hz, 7H), 0.87 (t, *J* = 7.0 Hz, 7H).; ^{13}C NMR (100 MHz, 298 K, $CDCl_3$) δ 162.53, 160.38, 151.83, 148.20, 139.69, 137.66, 133.67, 132.59, 131.18, 128.77, 123.55, 121.58, 119.18, 115.92, 113.89, 110.28, 96.72, 77.40, 77.08, 76.76, 72.80, 60.39, 56.68, 55.74, 53.48, 38.79, 30.14, 28.92, 23.53, 23.01, 21.05, 14.20, 14.00, 10.69, 0.00; MALDI-TOF-HRMS (m/z) calcd. for $C_{52}H_{62}N_4O_{12}$ $[M+Na]^+$ 958.0582, found $[M+Na]^+$ 958.4551.

Synthesis of 1a-b *via* fragment coupling approach

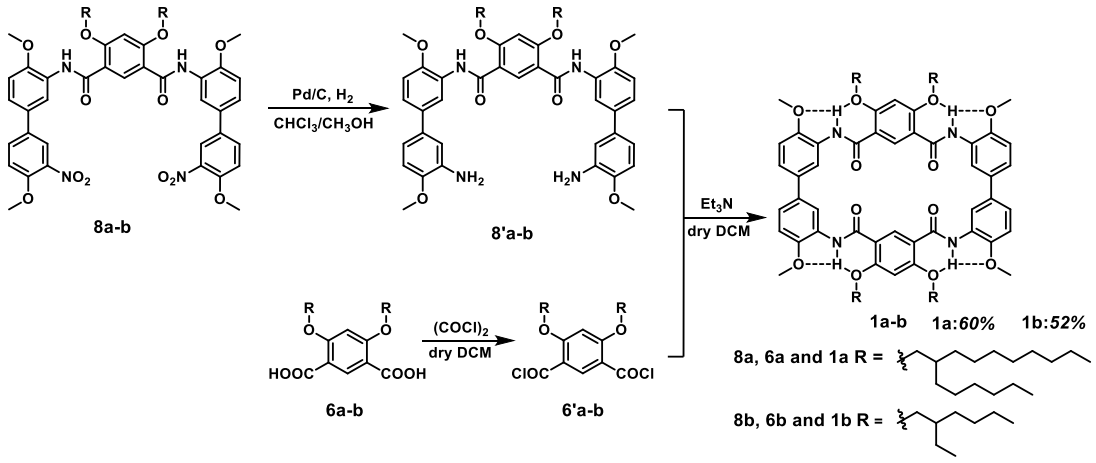

Scheme S5 Synthesis of **1a-b** *via* fragment coupling approach

Compound **8a** (100 mg, 0.087 mmol) was hydrogenated in the presence of 20% Pd/C (60 mg) in mixed solvent of $CHCl_3$ and MeOH (50 mL, v/v=5:1) for 10 h at 50 °C. The solution was filtered in darkness as fast as possible followed by immediate removal of the solvent to produce the diamine **8'a**. DMF (10 μL) was added to a solution of compound **6a** (56.0 mg, 0.087 mmol) and oxalyl chloride (30 μL, 0.35 mmol) in CH_2Cl_2 (20 mL). The mixture was stirred for an hour at room temperature. The solvent and residual oxalyl chloride was then removed under vacuum to afford yellow oil **6'a**. Compound **6'a** was dissolved in CH_2Cl_2 (20 mL) and added dropwise to a mixture of the above **5** and Et_3N (72 μL, 0.525

mmol) in dry CH_2Cl_2 (40 mL) at -20 °C. The solution was stirred under argon for 3 hours. The reaction mixture was quenched with MeOH (1 mL), washed with water three times and reprecipitaed with CH_2Cl_2 and CH_3OH. Then the crude product was purified with column chromatography (CH_2Cl_2/CH_3OH = 20:1) to provide the macrocycle **1a** as a white solid (89 mg, yield 60 %).

1b was synthesized according to the above general procedure using compound **8b** (250 mg, 0.267 mmol) and compound **6b** (113 mg, 0.267 mmol). The reaction mixture was quenched with MeOH (1 mL), washed with water three times and reprecipitaed with CH_2Cl_2 and CH_3OH. Then the crude product was purified with column chromatography (CH_2Cl_2/CH_3OH = 20:1) to provide the macrocycle **1b** as a white solid (175 mg, yield 52 %).

Synthesis of 1a-c *via* one pot approach with $LiClO_4$ as template

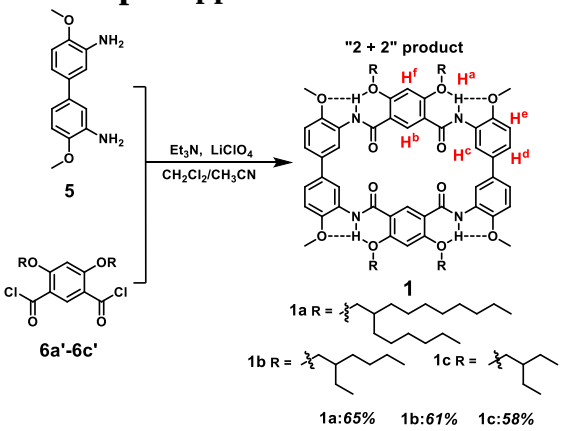

Scheme S6 Synthesis of **1a-1c** *via* one pot approach with $LiClO_4$ as template.

Compound **4b** (300 mg, 0.99 mmol) was hydrogenated in the presence of 20% Pd/C (60 mg) in CH_2Cl_2 (60 mL) for 10 h at room temperature. The solution was filtered in darkness followed by immediate removal of the solvent. The reduced diamine **5** was used for the immediate macrocyclization reaction. DMF (10 μL) was added to a solution of compound **6a** (638 mg, 0.986 mmol) and oxalyl chloride (300 μL, 3.46 mmol) in CH_2Cl_2 (40 mL). The mixture was stirred for an hour at room temperature. The solvent was evaporated and the resulting acid chloride was dried in vacuum at room temperature for 30 min to afford compound **6'a**. Compound **6'a** was dissolved in CH_2Cl_2 (30 mL) and added dropwise to a mixture of the above **5**, Et_3N (0.411 mL, 2.96 mmol) and $LiClO_4$ (106 mg, 0.99 mmol) in CH_2Cl_2/CH_3CN (100 mL, 7:3, v/v) at -20 °C. The solution was stirred under argon for 3 hours. The reaction mixture was quenched with MeOH (1 mL), washed with water three times and reprecipitaed with CH_2Cl_2 and CH_3OH. Then the crude product was purified by chromatography on silica gel (CH_2Cl_2/MeOH = 20: 1) to provide the complex **1a** ⊃ **$LiClO_4$** as a white solid (550 mg, 65%).

The complex **1b** ⊃ **LiClO$_4$** was synthesized according to the above general procedure using compound **4b** (300 mg, 0.99 mmol), **6b** (416 mg, 0.986 mmol) and $LiClO_4$ (106 mg, 0.99 mmol). The reaction mixture was quenched with MeOH (1 mL), washed with water three times and reprecipitaed with CH_2Cl_2 and CH_3OH. Then the crude product was purified by chromatography on silica gel (CH_2Cl_2/MeOH = 20: 1) to provide the complex **1b** ⊃ **LiClO$_4$** as a white solid (381 mg, 61%).

The complex **1c** ⊃ **LiClO$_4$** was synthesized according to the above general procedure using compound **4b** (300 mg, 0.99 mmol), **6c** (362 mg, 0.986 mmol) and $LiClO_4$ (106 mg, 0.99 mmol). The reaction mixture was quenched with MeOH (1 mL), washed with water three times and reprecipitaed with CH_2Cl_2 and CH_3OH. Then the crude product was purified by chromatography on silica gel (CH_2Cl_2/MeOH = 20: 1) to provide the complex **1c** ⊃ **LiClO$_4$** as a white solid (329 mg, 58%).

Synthesis of 1a *via* fragment coupling approach with LiClO$_4$ as template

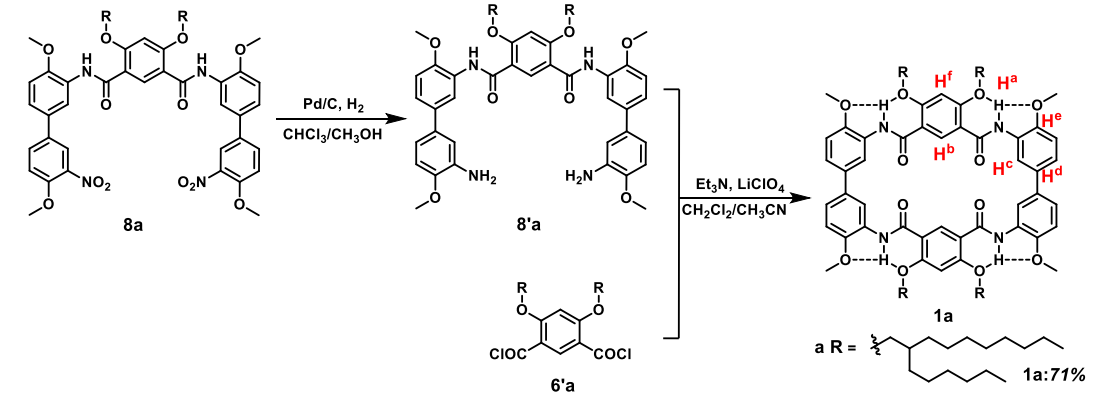

Scheme S7 Synthesis of **1a** *via* fragment coupling approach with $LiClO_4$ as template.

The complex **1a** ⊃ **LiClO$_4$** was synthesized according to the above general procedure using compound **8a** (100 mg, 0.087 mmol), **6a** (56 mg, 0.087 mmol) and $LiClO_4$ (9.5 mg, 0.087 mmol). The crude product was purified by chromatography on silica gel (CH_2Cl_2/MeOH = 20: 1) to provide the complex **1a** ⊃ **LiClO$_4$** as a white solid (112 mg, 71%).

Synthesis of compound 9

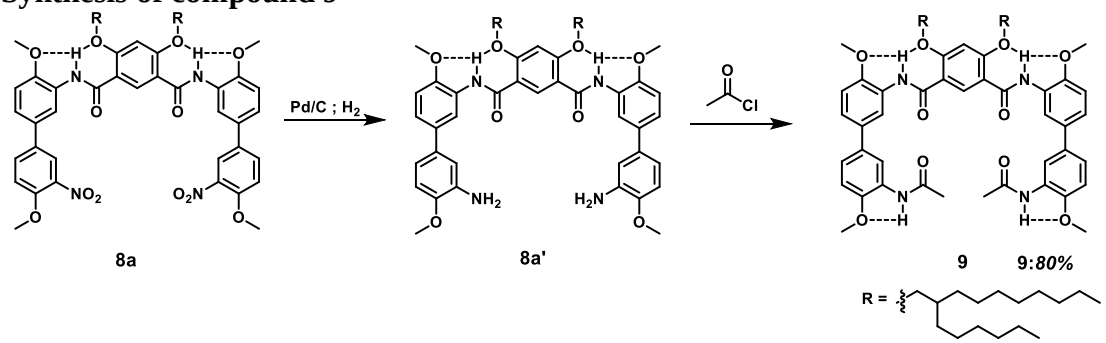

Scheme S8 Synthesis of compound **9**

Trimer **8a** (500 mg, 0.435 mmol) was hydrogenated in the presence of 20% Pd/C (100 mg) in mixed solvent of $CHCl_3$/MeOH (100 mL, v/v=5:1) for 10 h at 50 °C. The solution was filtered in darkness as fast as possible followed by immediate removal of the solvent. The reduced diamine **8'a** (Scheme S7) was used for the direct coupling reaction. Dissolved acetic chloride (0.135 mL, 1.74 mmol) with 10 mL CH_2Cl_2 was added dropwise to a mixture comprising **8'a** and Et_3N (0.72 mL, 5.15 mmol) in CH_2Cl_2 (50 mL). The solution was stirred under N_2 for 3 hours. The organic layer was washed with water for three times (3 × 20 mL). The crude product was purified by chromatography on silica gel (CH_2Cl_2/CH_3OH = 20:1) to provide the product **9** as a white solid (511 mg, yield 80 %).

^{1}H NMR (400 MHz, 298 K, $CDCl_3$) δ 9.86 (s, 2H), 9.17 (s, 1H), 8.88 (d, *J* = 2.3 Hz, 2H), 8.64 (d, *J* = 2.2 Hz, 2H), 7.76 (s, 2H), 7.39 (dd, *J* = 8.5, 2.3 Hz, 2H), 7.33 (dd, *J* = 8.5, 2.3 Hz, 2H), 6.93 (dd, *J* = 8.5, 3.8 Hz, 4H), 6.57 (s, 1H), 4.13 (d, *J* = 6.2 Hz, 4H), 3.91 (s, 11H), 2.22 (s, 5H), 2.10 – 2.00 (m, 2H), 1.45 (dp, *J* = 13.6, 7.2, 6.5 Hz, 8H), 1.35 (h, *J* = 7.9, 7.2 Hz, 8H), 1.26 (d, *J* = 2.6 Hz, 9H), 1.22 (d, *J* = 6.3 Hz, 18H), 0.92 – 0.79 (m, 14H), 0.07 (s, 5H); ^{13}C NMR (100 MHz, 298 K, $CDCl_3$) δ 160.19, 147.67, 146.91, 146.89, 134.02, 133.77, 128.29, 127.64, 122.41, 119.63, 118.30, 110.13, 77.34, 77.02, 76.70, 73.15, 55.83, 55.70, 37.65, 31.85, 31.80, 31.13, 30.01, 29.67, 29.57, 29.31, 26.68, 22.65, 22.63, 14.09, 14.07, 1.03, 0.00; ESI-HRMS (m/z) calcd. for $C_{72}H_{102}N_4O_{10}$ $[M+Na]^+$ 1207.7650, found $[M+Na]^+$ 1207.4383.

Synthesis of compound 11

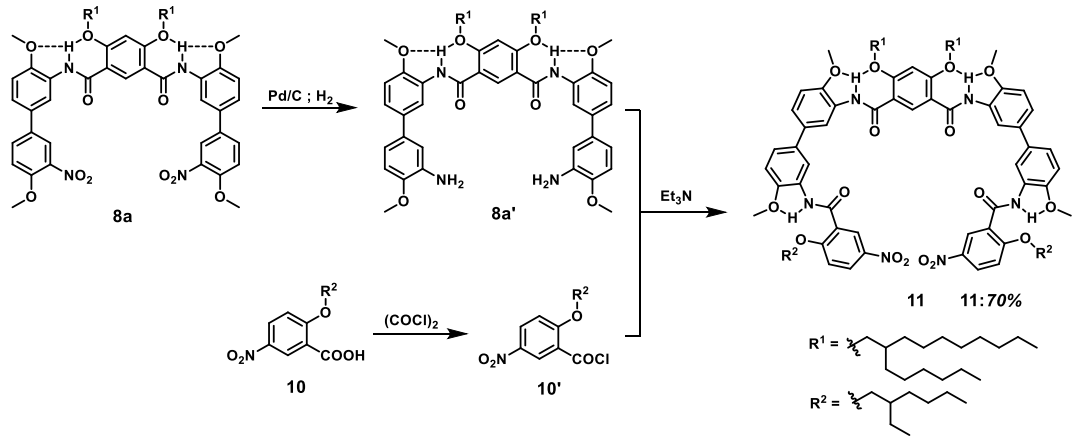

Scheme S9 Synthesis of compound **11**

Compound **10** was prepared according to literature procedures. [6]

Trimer **8a** (500 mg, 0.435 mmol) was hydrogenated in the presence of 20% Pd/C (100 mg) in mixed solvent of $CHCl_3$/MeOH (100 mL, v/v=5:1) for 10 h at 50 °C. The solution was filtered in darkness as fast as possible followed by immediate removal of the solvent. The

reduced diamine **8'a** (Scheme S8) was used for the direct coupling reaction. DMF (10 μL) was added to a suspension of compound **10** (255 mg, 0.86 mmol) and oxalyl chloride (0.292 mL, 3.41 mmol) in dry CH_2Cl_2 (40 mL). The mixture was stirred for 40 minutes at room temperature. The solvent was evaporated and the resulting acyl chloride **10'** was dried in vacuum at room temperature for 30 minutes. Compound **10'** was dissolved in dry CH_2Cl_2 (40 mL) and the solution was added dropwise to a mixture comprising **8'a** and Et_3N (0.72 mL, 5.15 mmol) in CH_2Cl_2 (50 mL). The solution was stirred under N_2 for 3 hours. The organic layer was washed with water for three times (3 × 20 mL). The crude product was purified by chromatography on silica gel (CH_2Cl_2/CH_3OH = 20:1) to provide the product **11** as a yellow solid (720 mg, yield 70 %).

^{1}H NMR (400 MHz, 298 K, $CDCl_3$) δ 9.97 (s, 1H), 9.90 (s, 1H), 9.19 (d, *J* = 2.7 Hz, 1H), 8.91 (d, *J* = 2.3 Hz, 1H), 8.86 (d, *J* = 2.2 Hz, 1H), 8.31 (dd, *J* = 9.1, 3.0 Hz, 1H), 7.42 (ddd, *J* = 19.5, 8.5, 2.3 Hz, 2H), 7.13 (d, *J* = 9.2 Hz, 1H), 6.95 (dd, *J* = 8.6, 4.8 Hz, 2H), 6.58 (s, 1H), 4.20 (dt, *J* = 6.8, 3.4 Hz, 2H), 4.14 (d, *J* = 6.2 Hz, 2H), 3.93 (d, *J* = 2.7 Hz, 6H), 2.04 (dhept, *J* = 12.6, 6.4 Hz, 2H), 1.75 (s, 2H), 1.61 – 1.51 (m, 2H), 1.48 (dd, *J* = 14.7, 7.5 Hz, 4H), 1.43 (d, *J* = 6.8 Hz, 2H), 1.38 – 1.33 (m, 4H), 1.23 (t, *J* = 10.7 Hz, 21H), 0.93 (t, *J* = 7.5 Hz, 3H), 0.84 (dp, *J* = 6.7, 3.3 Hz, 9H); ^{13}C NMR (100 MHz, 298 K, $CDCl_3$) δ 162.41, 161.21, 160.98, 160.23, 147.73, 147.63, 141.79, 134.07, 133.68, 128.75, 128.35, 128.03, 127.44, 123.53, 123.08, 122.09, 119.64, 119.58, 116.29, 112.77, 110.22, 110.10, 77.34, 77.03, 76.71, 73.57, 55.73, 38.64, 37.65, 31.86, 31.81, 31.13, 30.02, 29.68, 29.58, 29.32, 28.77, 26.73, 26.68, 23.44, 22.98, 22.66, 22.64, 14.10, 14.08, 13.99, 10.58, -0.00. ESI-HRMS (m/z) calcd. for $C_{98}H_{136}N_6O_{16}$ $[M]^+$ 1654.0012, found $[M]^+$ 1654.0068.

References

[1] Yuan, L.; Feng, W.; Yamato, K.; Sanford, A. R.; Xu, D.; Guo, H.; Gong, B., *J. Am. Chem. Soc.* 2004, **126**, 11120.

[2] Yang, Y.; Feng, W.; Hu, J.; Zou, S.; Gao, R.; Yamato, K.; Kline, M.; Cai, Z.; Gao, Y.; Wang, Y.; Li, Y.; Yang, Y.; Yuan, L.; Zeng, X. C.; Gong, B., *J. Am. Chem. Soc.* 2011, **133**, 18590.

[3] Hu, J.; Chen, L.; Ren, Y.; Deng, P.; Li, X.; Wang, Y.; Jia, Y.; Luo, J.; Yang, X.; Feng, W.; Yuan, L., *Org. Lett*. 2013, 15, 4670.

[4] D. Oberoi, P. Dagar, U. Shankar, G. Vyas, A. Kumar, S. Sahu and A. Bandyopadhyay, *New J. Chem.*, 2018, **42**, 19090-19100.

[5] Liu, Q.; Borjigin, H.; Paul, D. R.; Riffle, J. S.; McGrath, J. E.; Freeman, B. D. *J. Memb. Sci.* 2016, **518**, 88.

[6] J. Hu, L. Chen, J. Shen, J. Luo, P. Deng, Y. Ren, H. Zeng, W. Feng and L. Yuan, *Chem. Commun.*, 2014, **50**, 8024-8027.

3. Spectroscopic Characterization

3.1 ^{1}H and ^{13}C NMR spectra of novel compounds

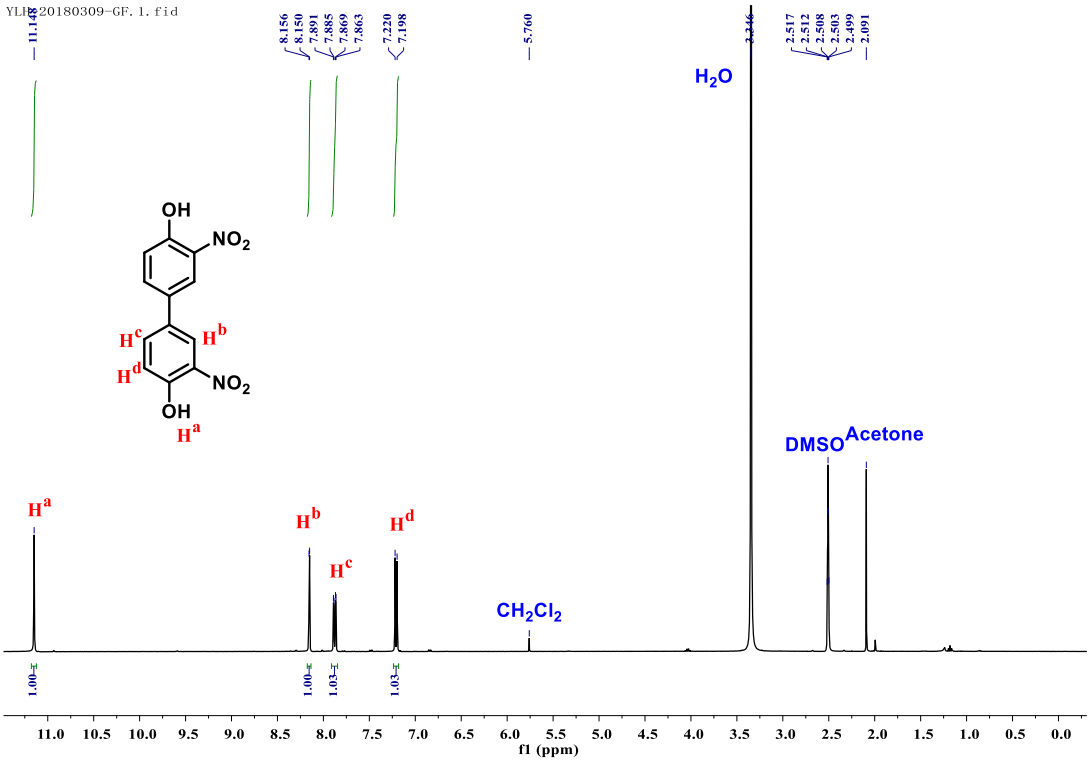

Figure S1. ^{1}H NMR spectrum of **4a** in DMSO-d_6 (400 MHz, 298 K).

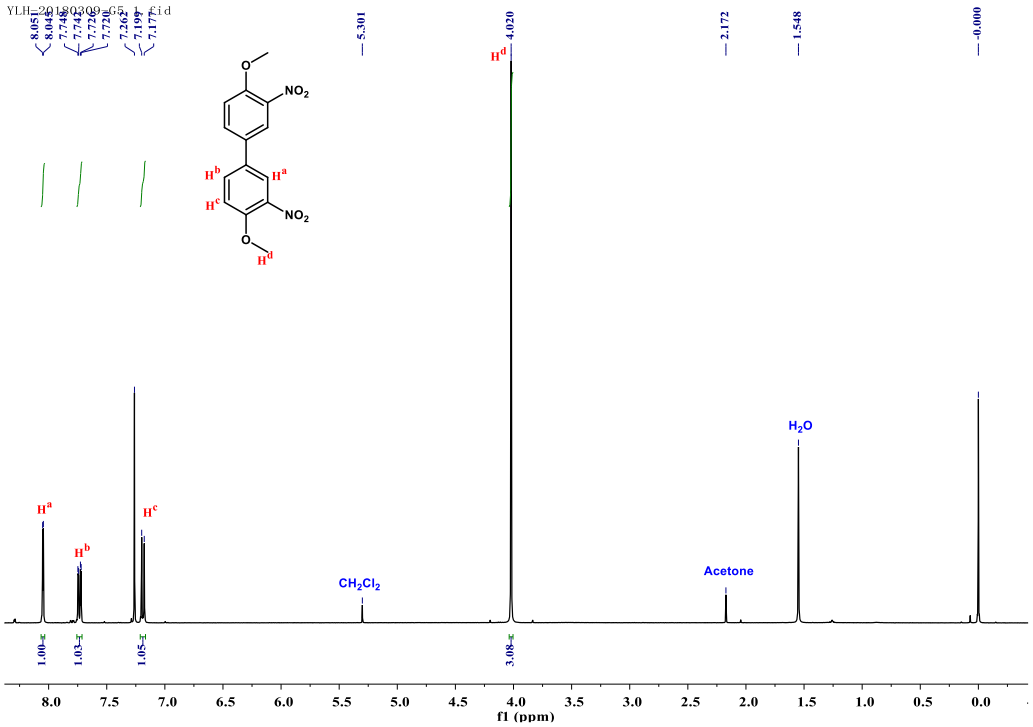

Figure S2. ^{1}H NMR spectrum of **4b** (400 MHz, 298 K, $CDCl_3$).

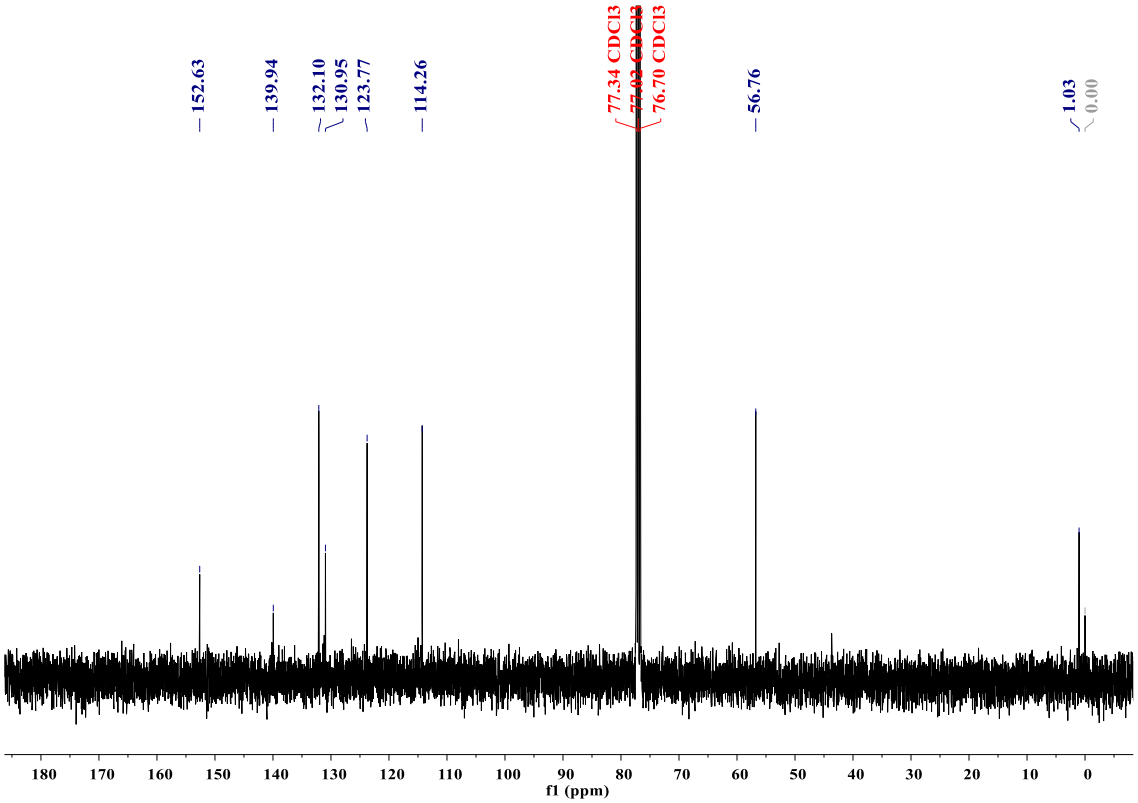

Figure S3. ^{13}C NMR spectrum of **4b** (100 MHz, 298 K, $CDCl_3$).

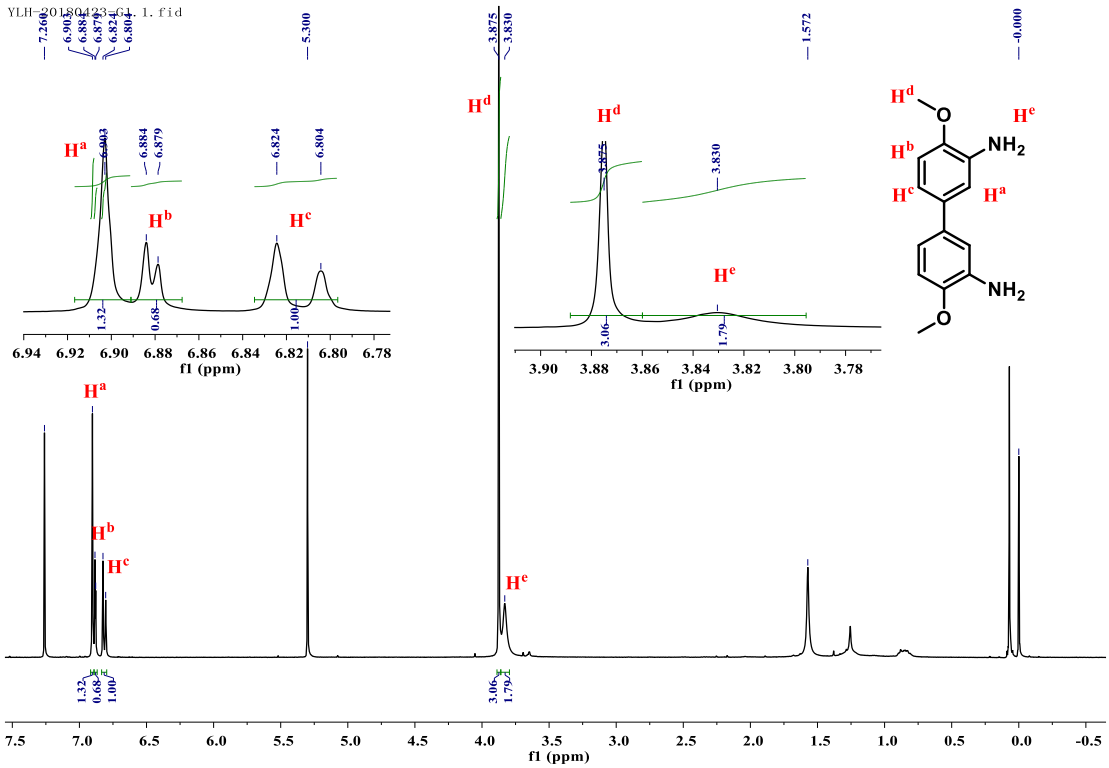

Figure S4. ^{1}H NMR spectrum of **5** (400 MHz, 298 K, $CDCl_3$).

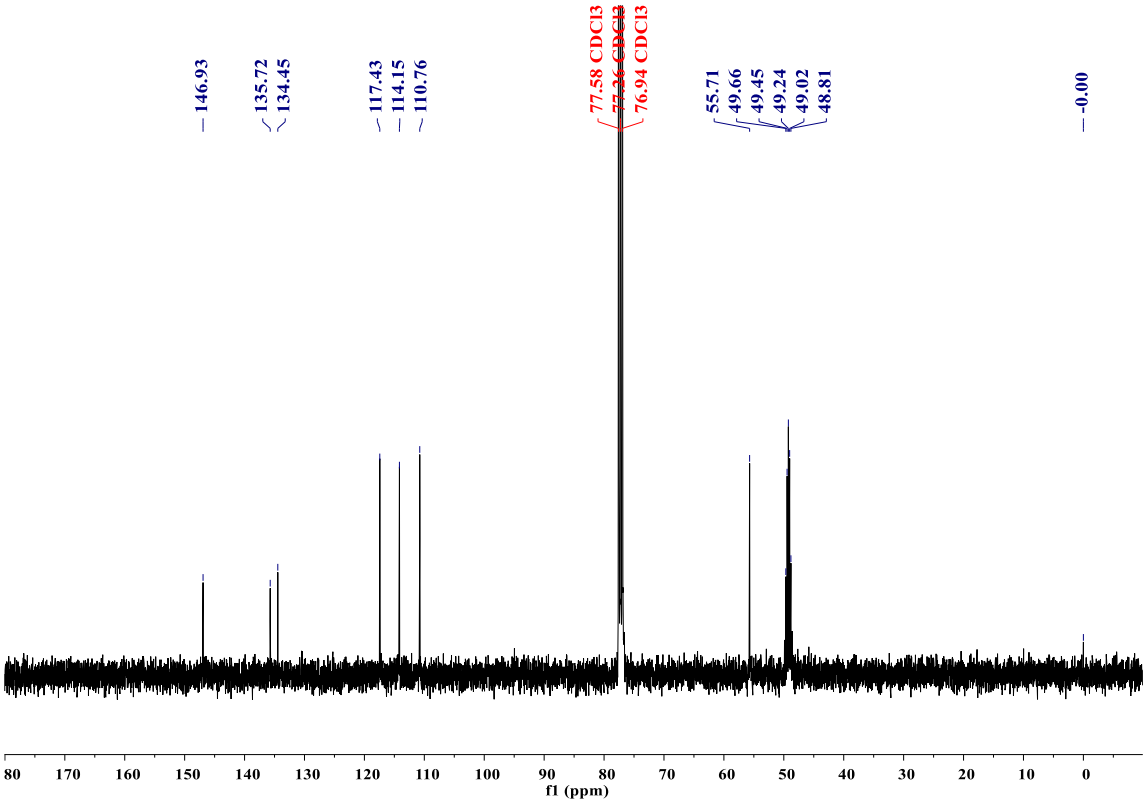

Figure S5. ^{13}C NMR spectrum of **5** (100 MHz, 298 K, $CDCl_3/CD_3OD$=9:1(v/v)).

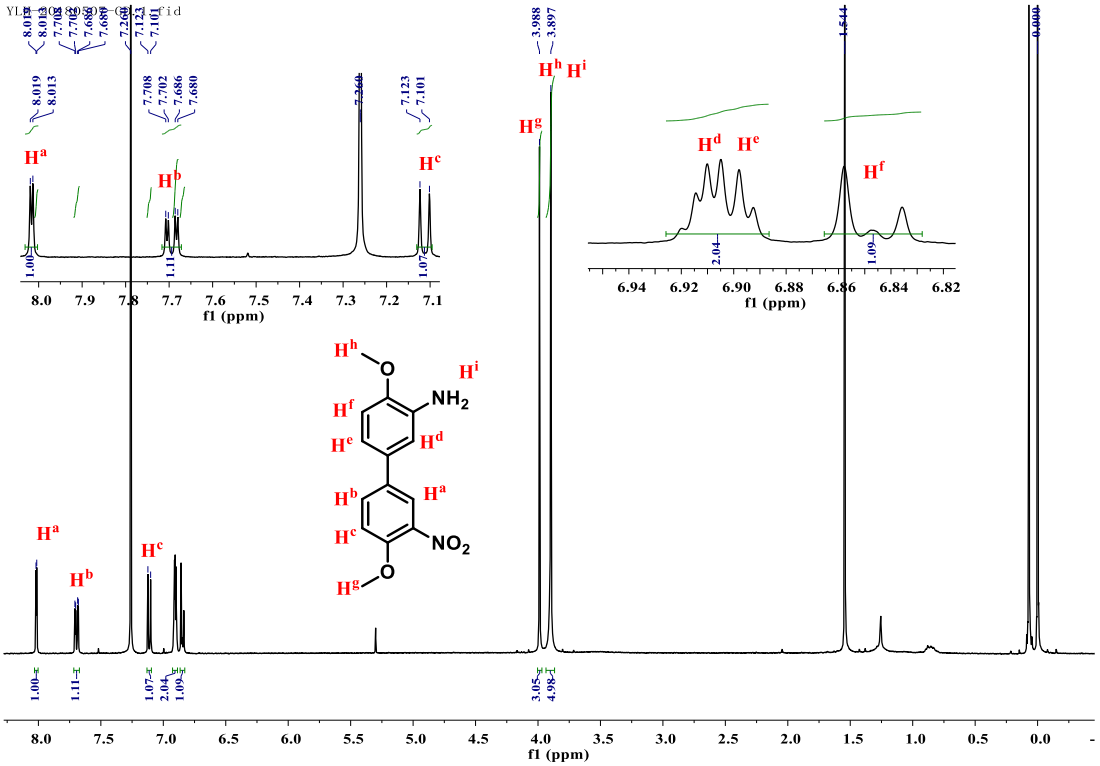

Figure S6. ^{1}H NMR spectrum of **7** (400 MHz, 298 K, $CDCl_3$).

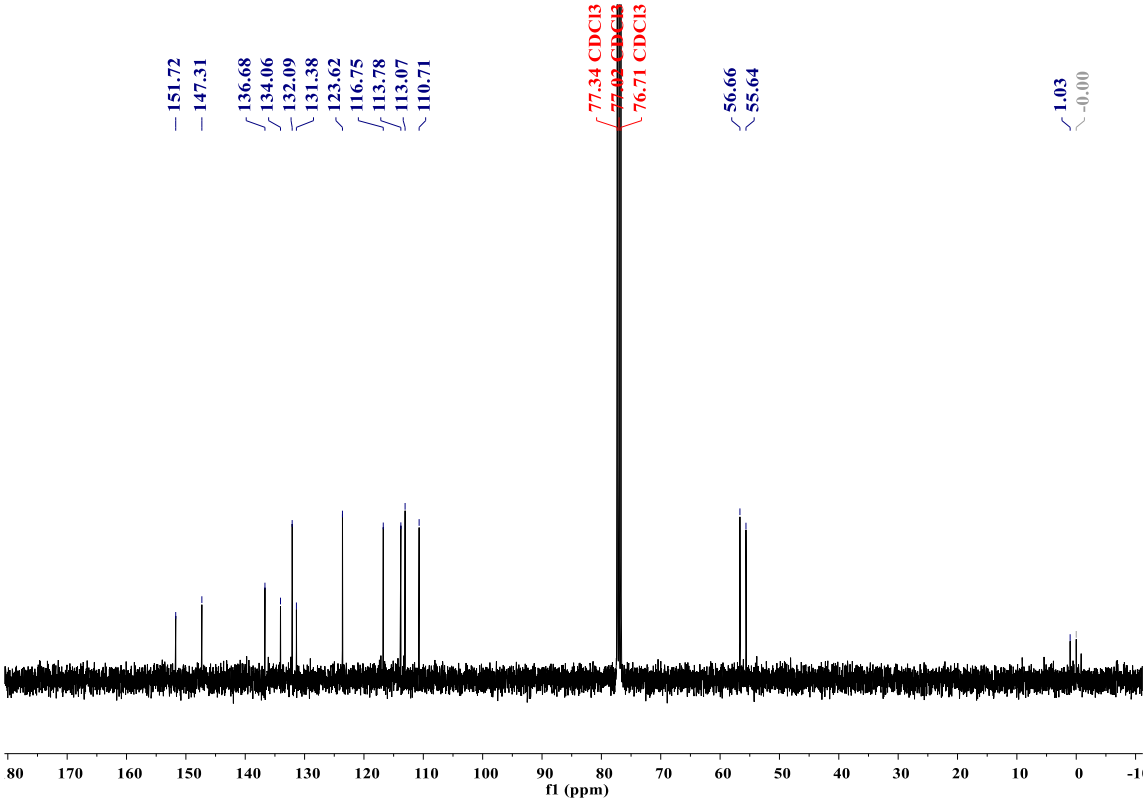

Figure S7. ^{13}C NMR spectrum of **7** (100 MHz, 298 K, $CDCl_3$).

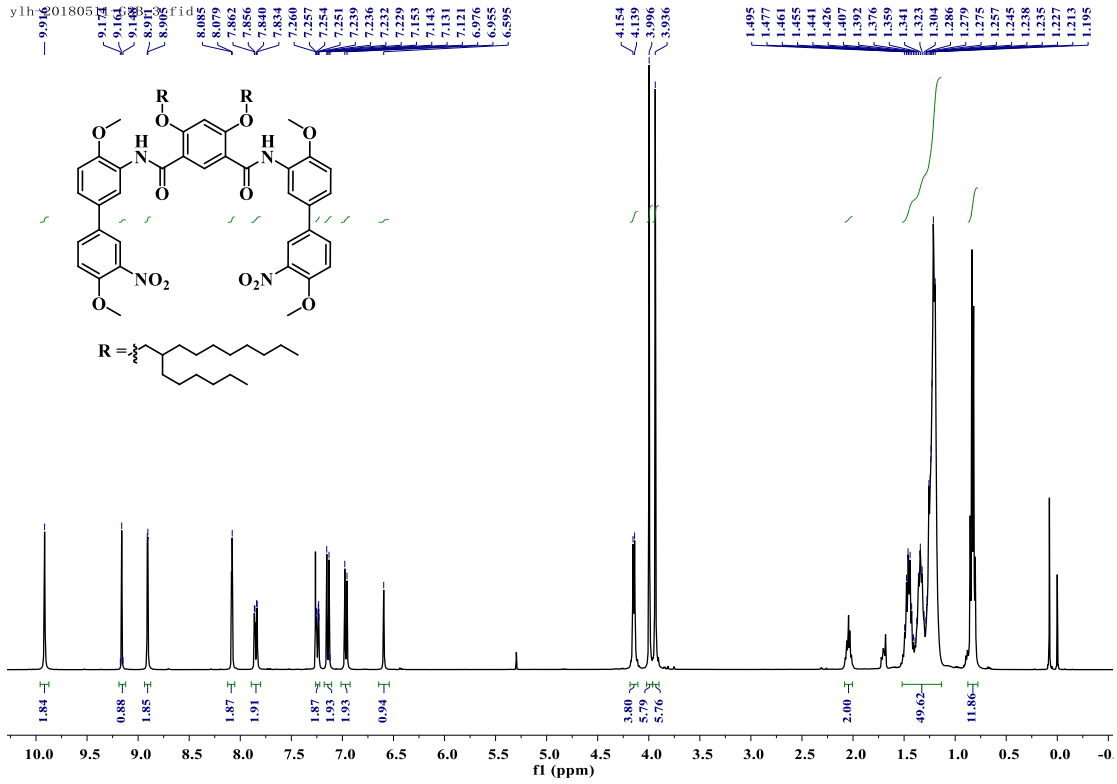

Figure S8. ^{1}H NMR spectrum of **8a** (400 MHz, 298 K, $CDCl_3$).

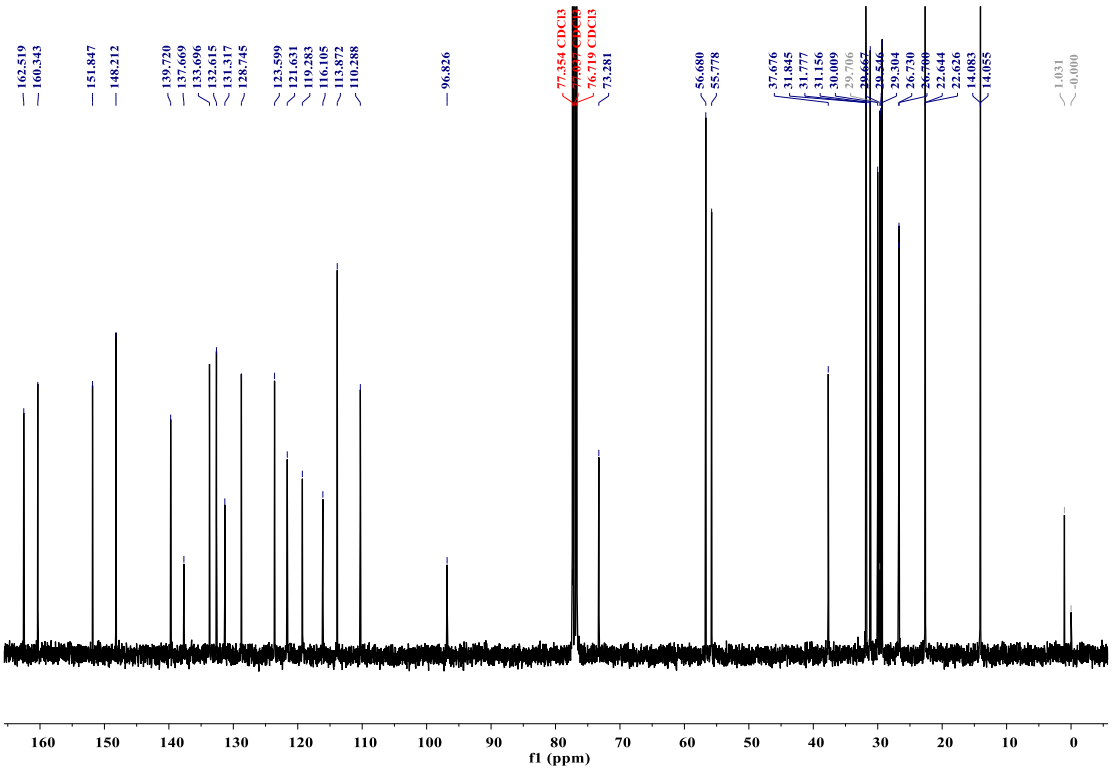

Figure S9. ^{13}C NMR spectrum of **8a** (100 MHz, 298 K, $CDCl_3$).

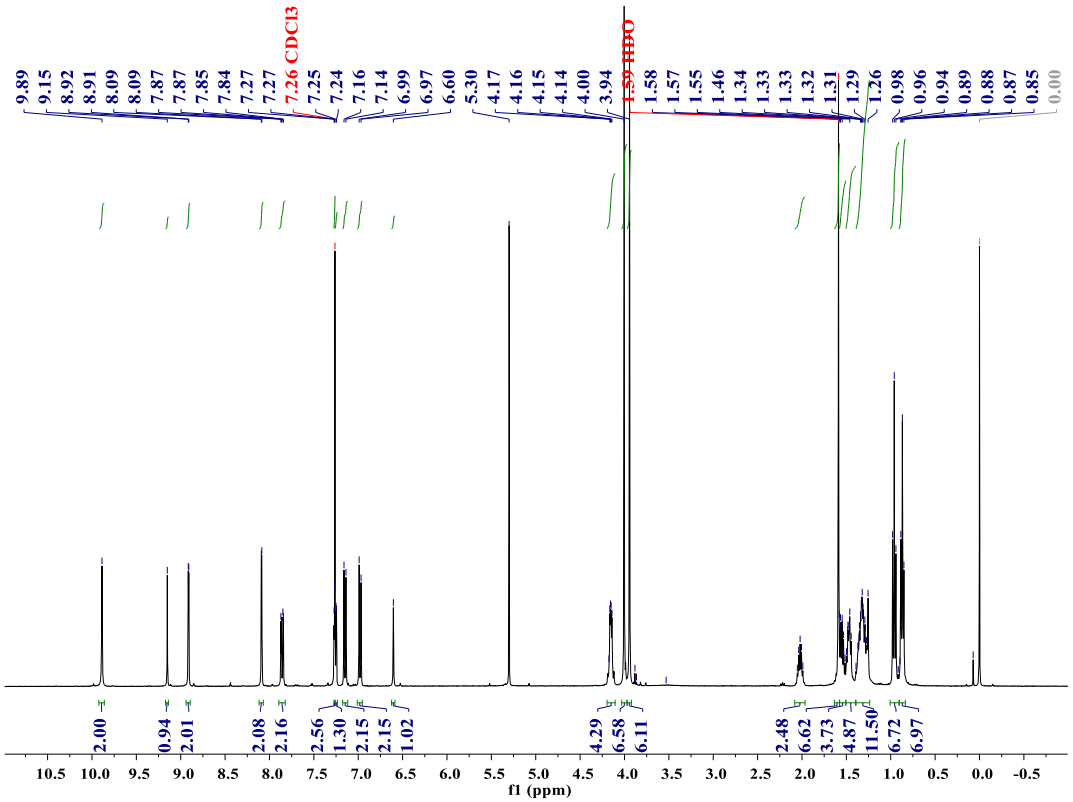

Figure S10. ^{1}H NMR spectrum of compound **8b** (400 MHz, 298 K, $CDCl_3$).

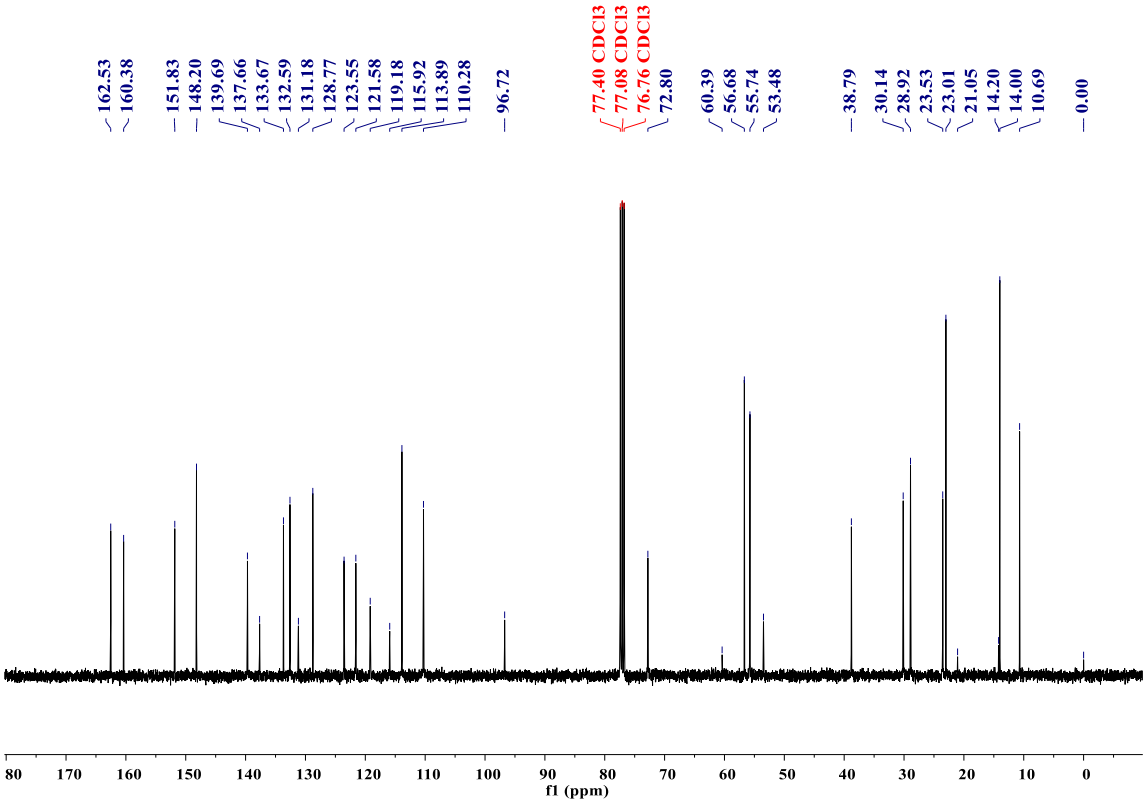

Figure S11. ^{13}C NMR spectrum of **8b** (100 MHz, 298 K, $CDCl_3$).

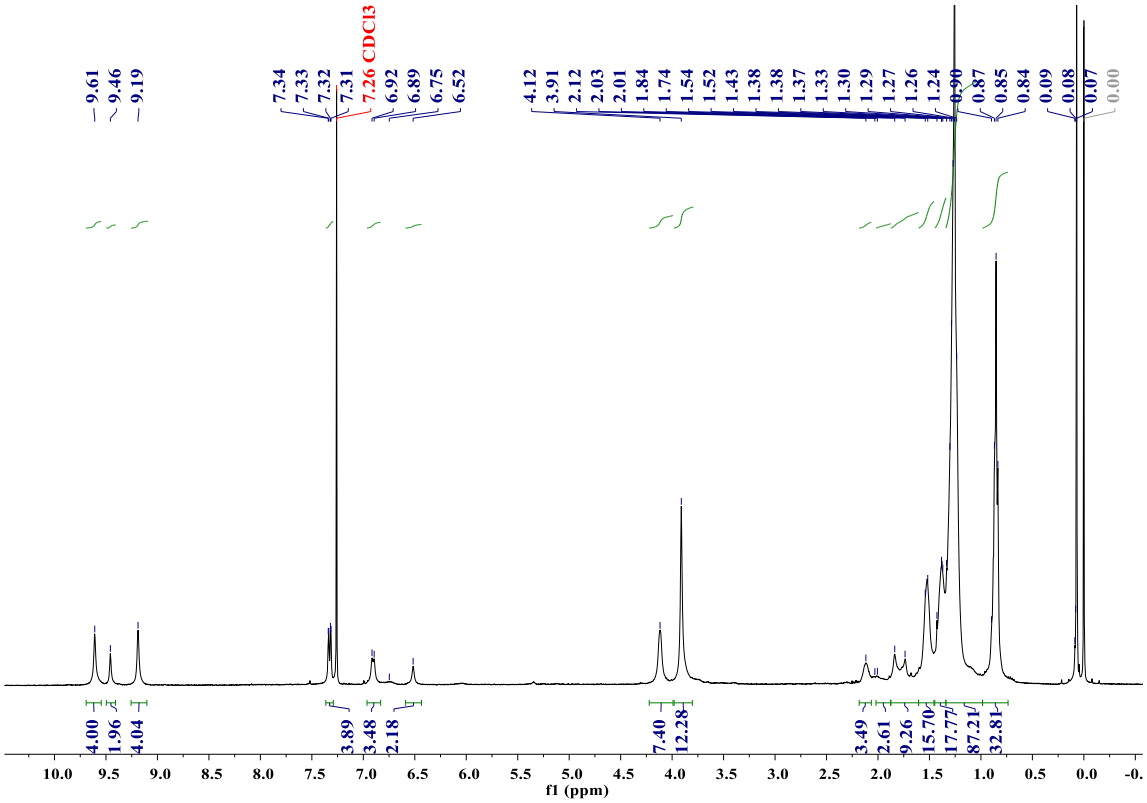

Figure S12. ^{1}H NMR spectrum of **1a** (400 MHz, 298 K, $CDCl_3$).

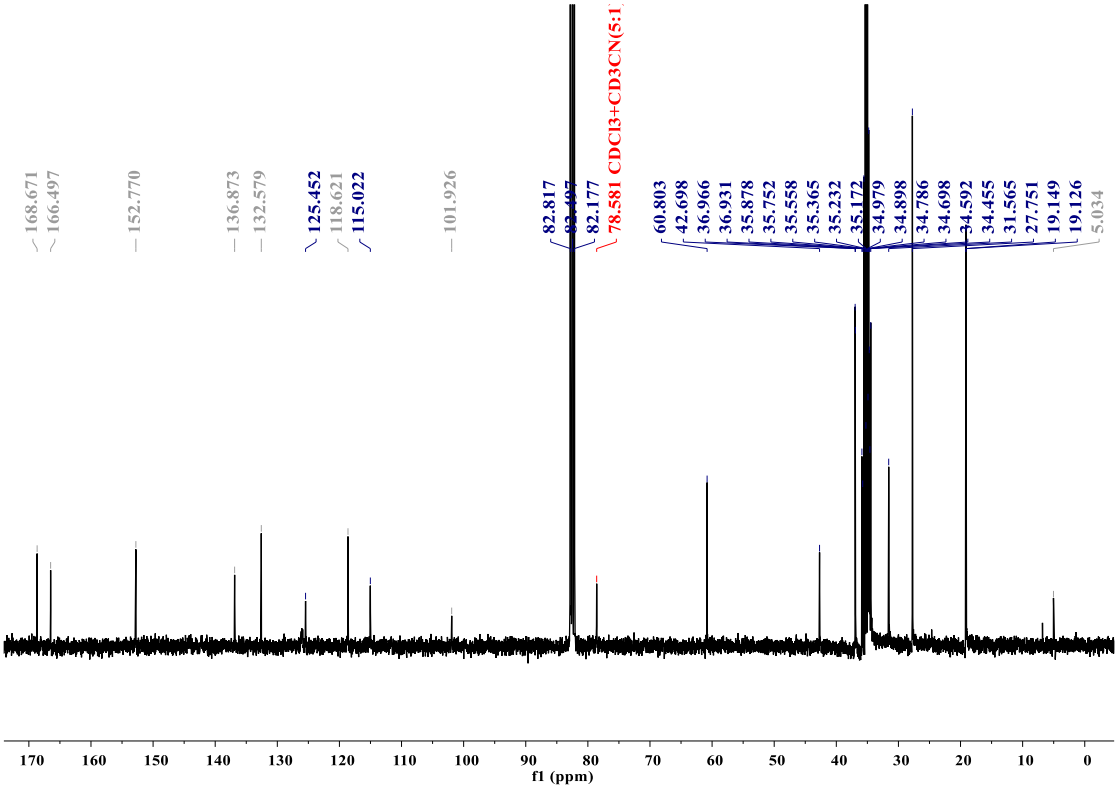

Figure S13. ^{13}C NMR spectrum of **1a** ⊃ **LiClO$_4$** (400 MHz, 298 K, $CDCl_3/CD_3CN$ = 5:1 (v/v)).

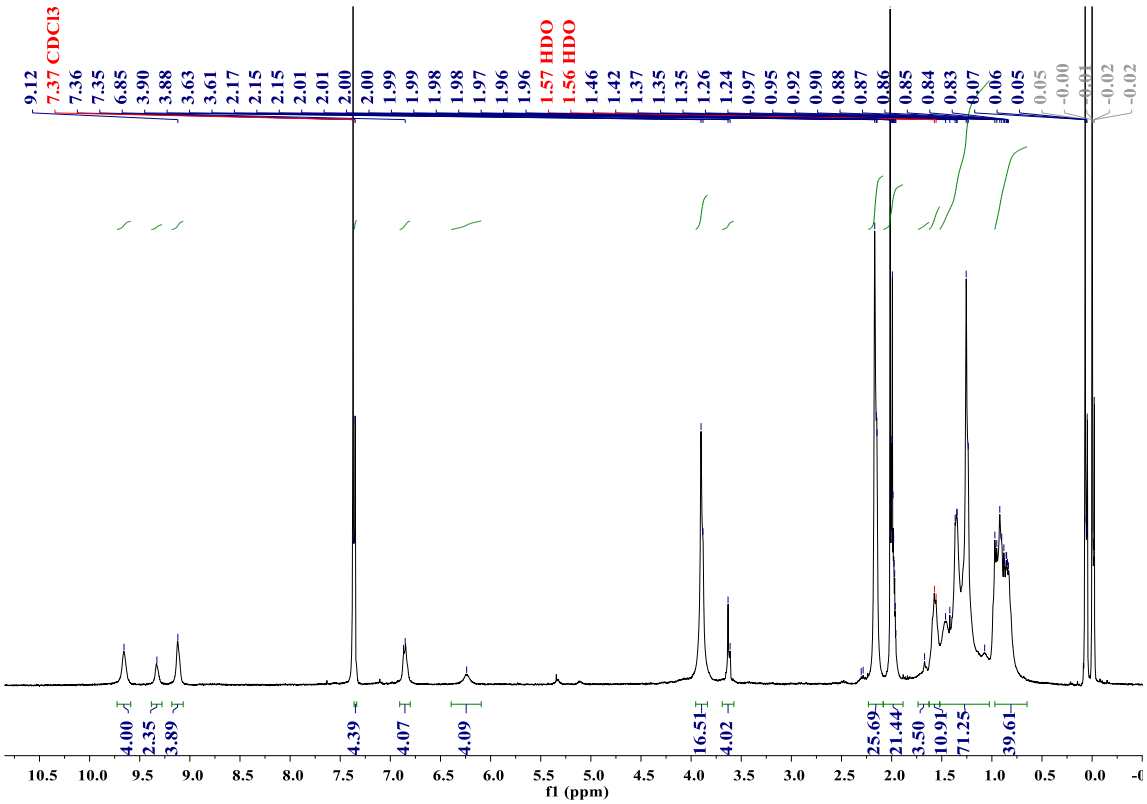

Figure S14. ^{1}H NMR spectrum of **1b** (400 MHz, 298 K, $CDCl_3$).

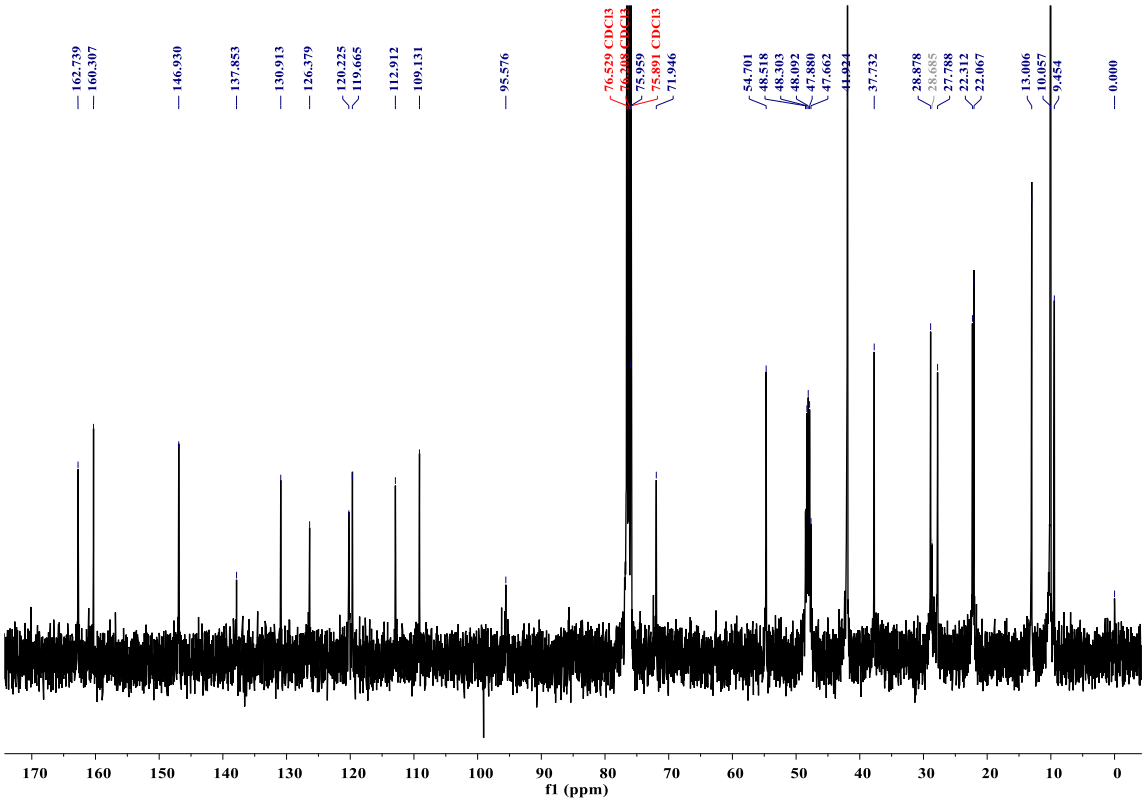

Figure S15. ^{13}C NMR spectrum of **1b ⊃ LiClO$_4$** (100 MHz, 298 K, $CDCl_3/CD_3OD$ = 9:1(v/v)).

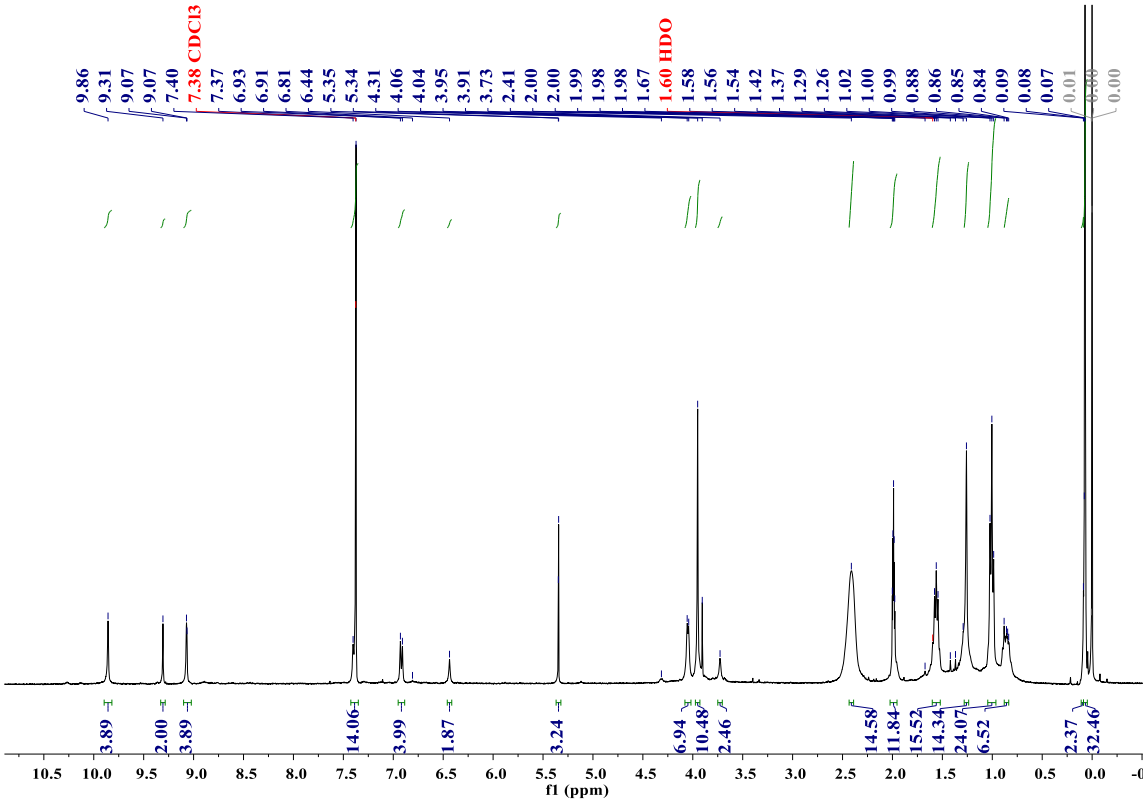

Figure S16. ^{1}H NMR spectrum of **1c ⊃ LiClO$_4$** (400 MHz, 298 K, $CDCl_3$).

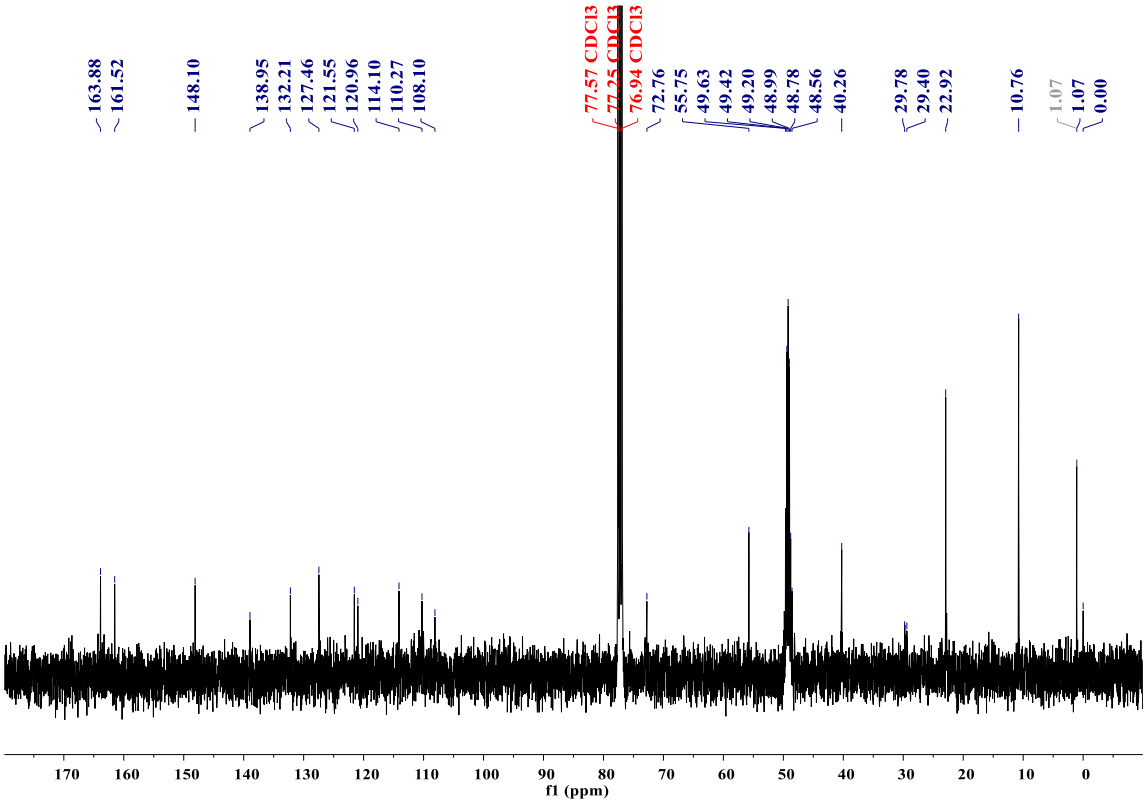

Figure S17. ^{13}C NMR spectrum of **1c** ⊃ **LiClO$_4$** (100 MHz, 298 K, $CDCl_3/CD_3OD$ = 9:1(v/v)).

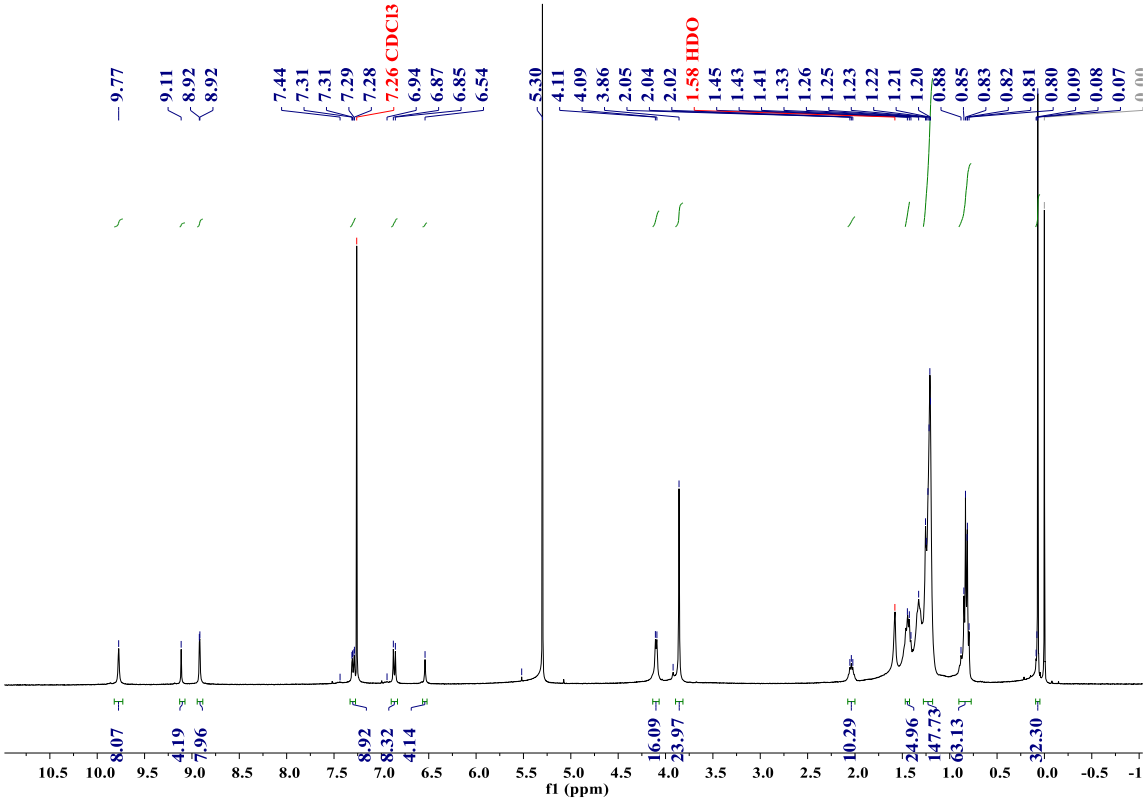

Figure S18. ^{1}H NMR spectrum of **2a**. (400 MHz, 298 K, $CDCl_3$).

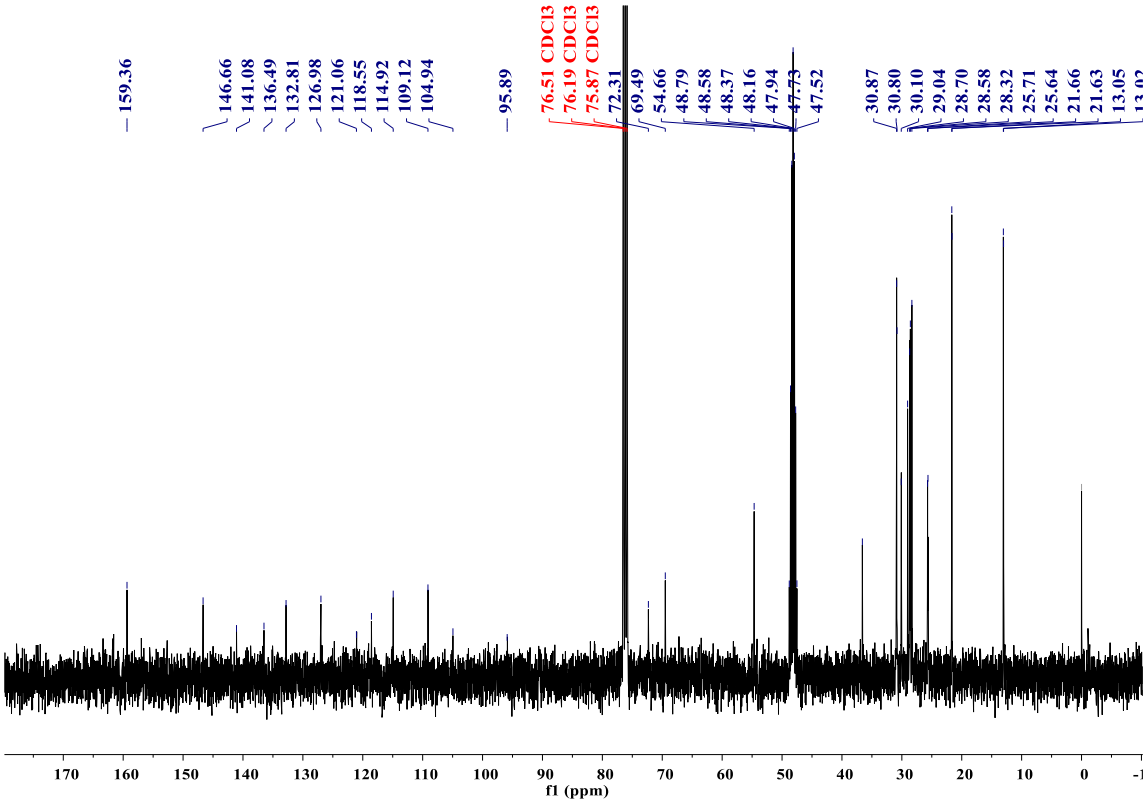

Figure S19. ^{13}C NMR spectrum of **2a** (100 MHz, 298 K, $CDCl_3$ / CD_3OD = 9:1(v/v)).

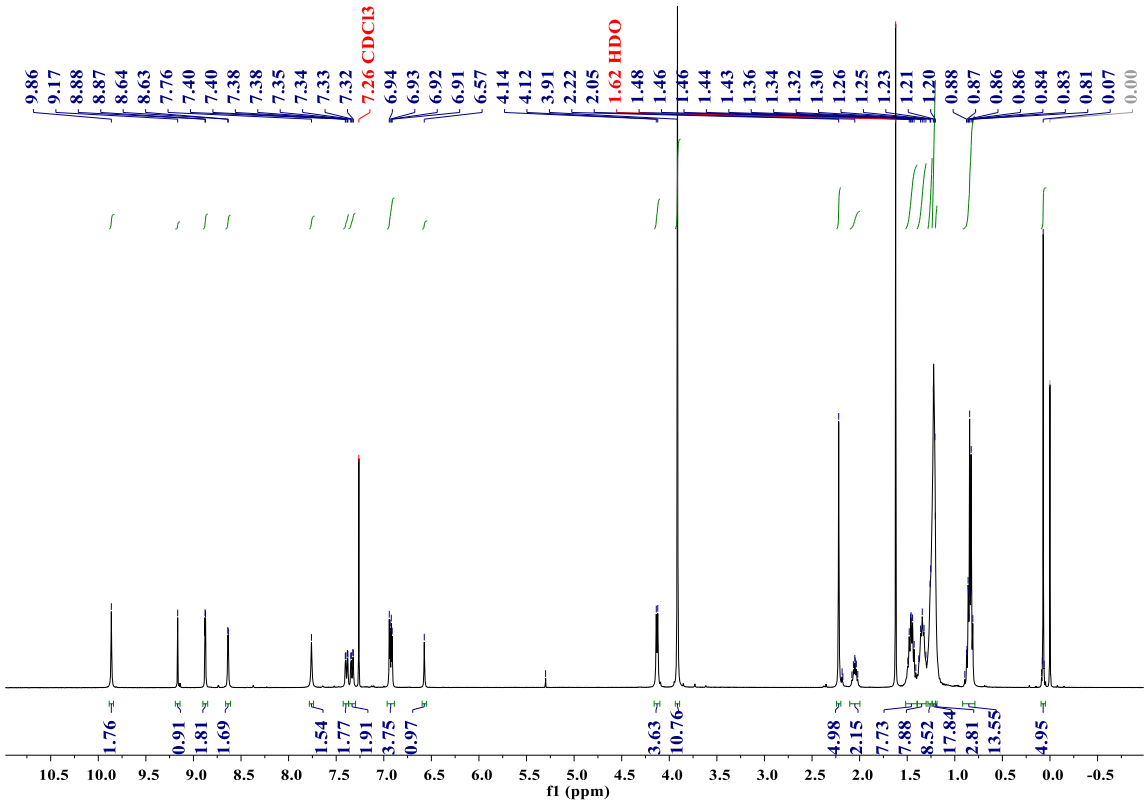

Figure S20. ^{1}H NMR spectrum of **9** (400 MHz, 298 K, $CDCl_3$).

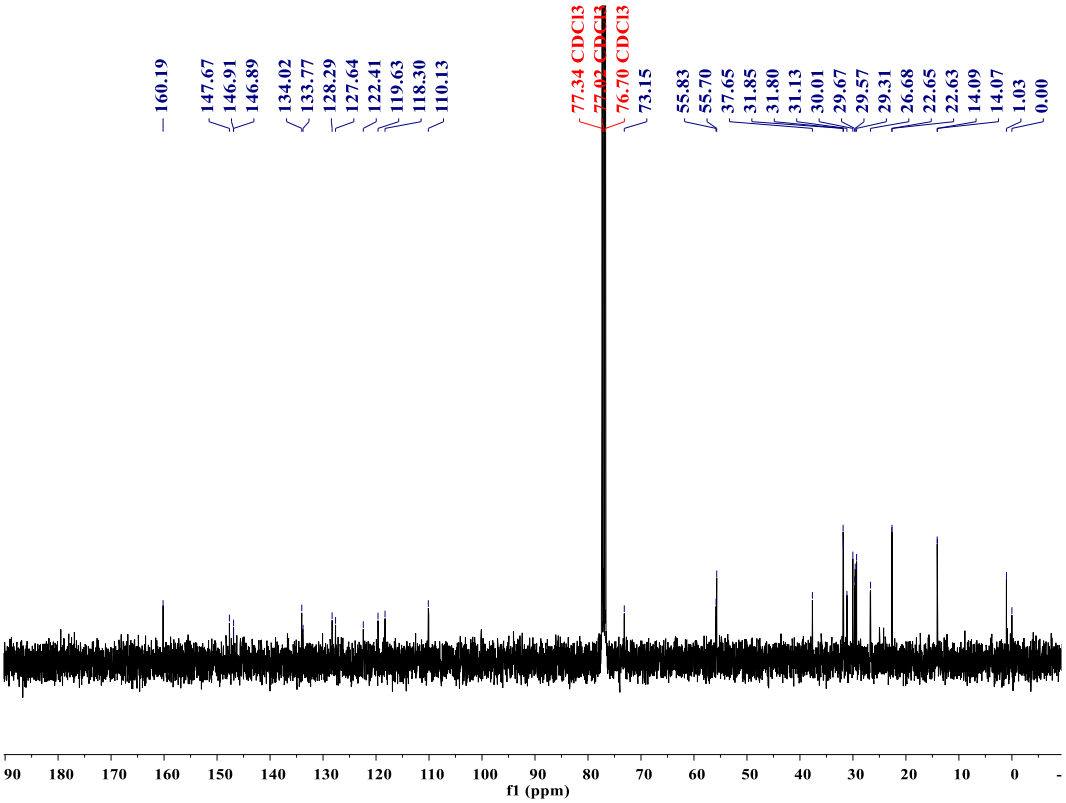

Figure S21. ^{13}C NMR spectrum of **9** (100 MHz, 298 K, $CDCl_3$).

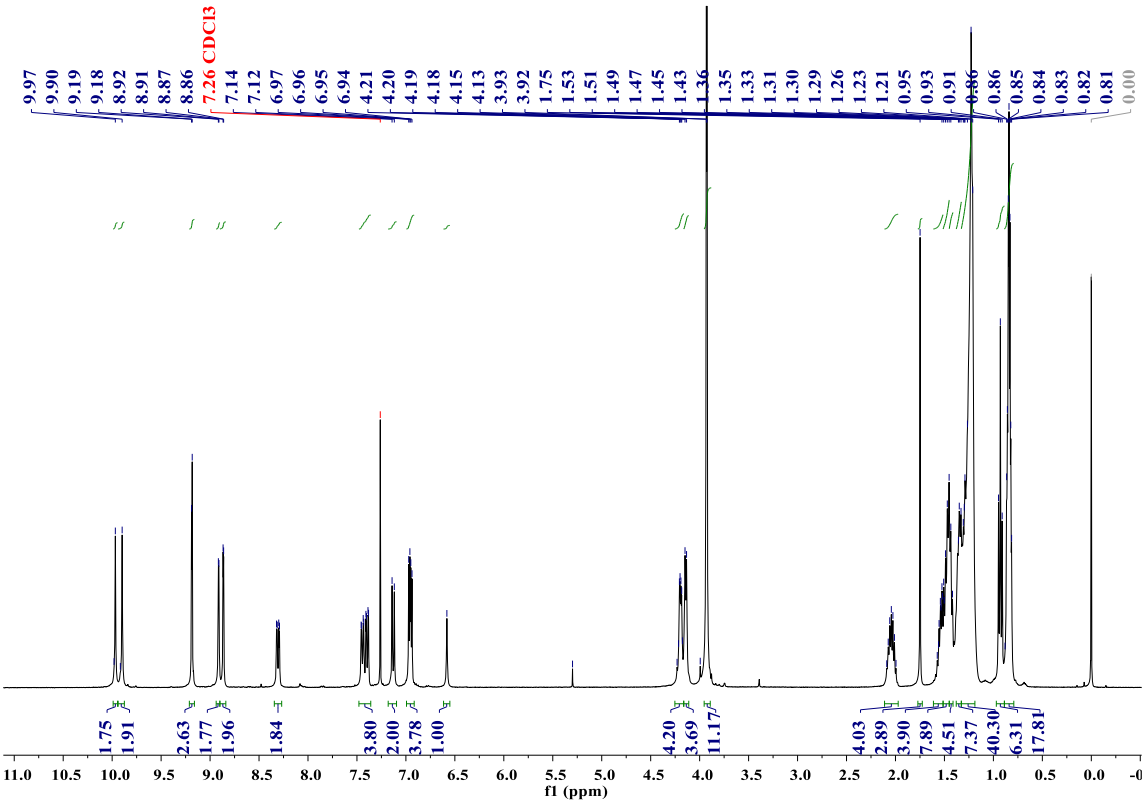

Figure S22. ^{1}H NMR spectrum of **11** (400 MHz, 298 K, $CDCl_3$).

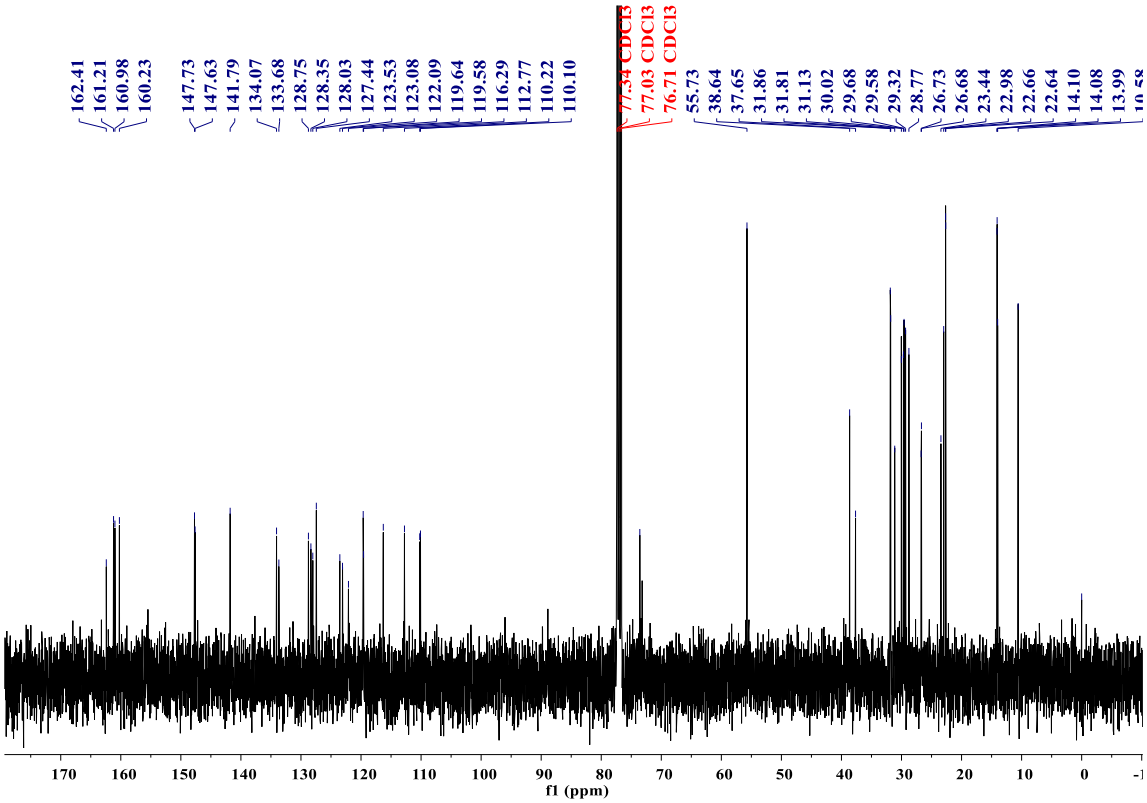

Figure S23. ^{13}C NMR spectrum of **11** (100 MHz, 298 K, $CDCl_3$).

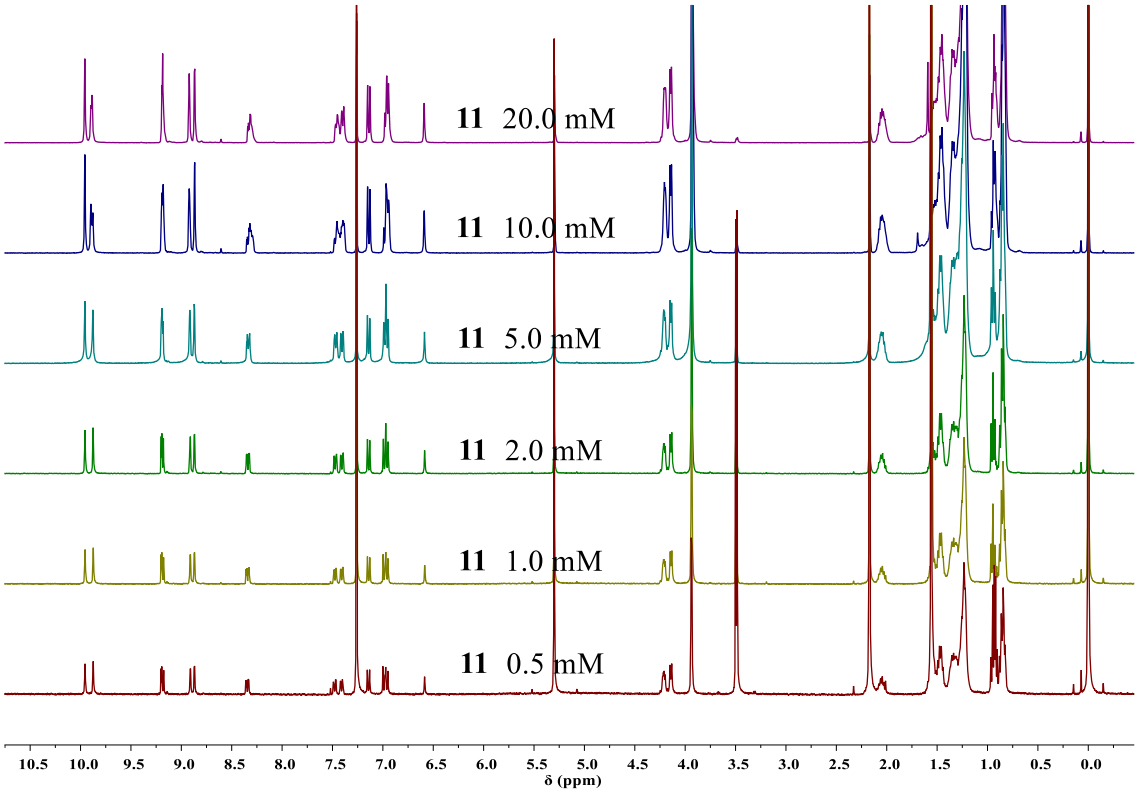

Figure S24. Stacked ^{1}H NMR spectra (400 MHz, $CDCl_3$, 298 K) of **11** at different concentrations (0.5~20 mM).

3.2 MALDI-TOF-MS or ESI-HRMS spectra of novel compounds

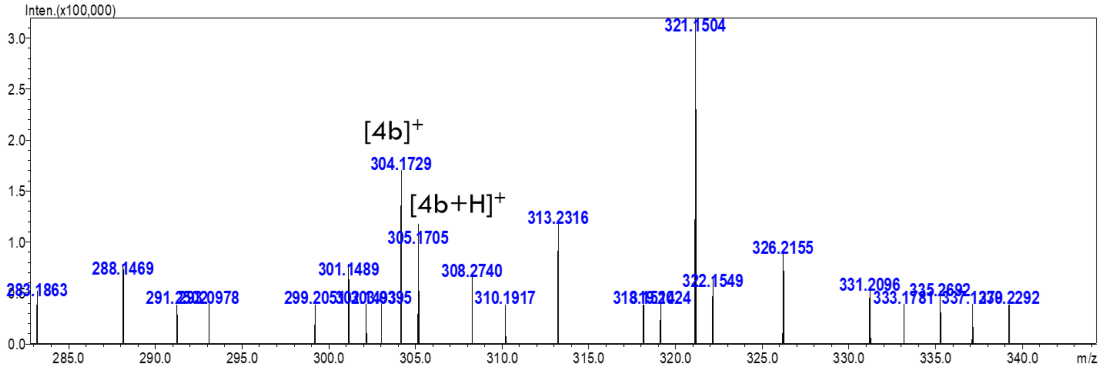

Figure S25. ESI-HR mass spectrum of compound **4b.**

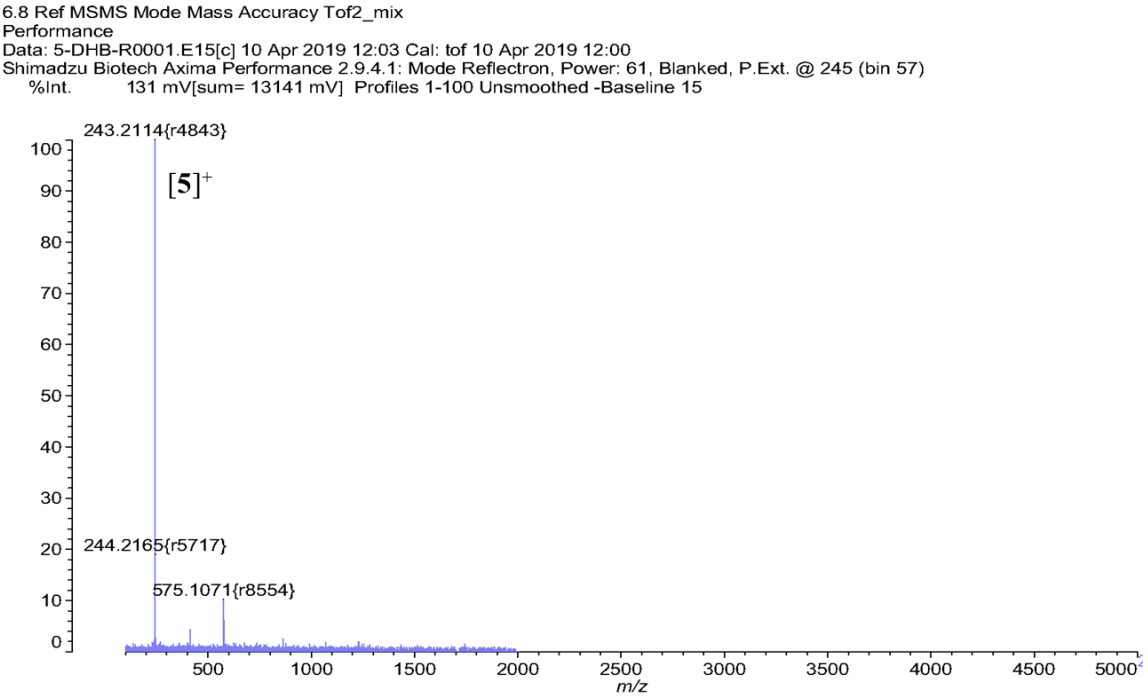

Figure S26. MALDI-TOF mass spectrum of compound **5** (Matrix: DHB).

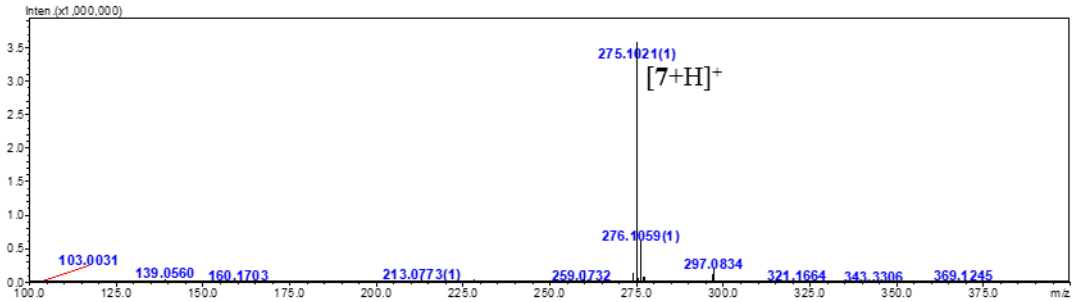

Figure S27. ESI-HR mass spectrum of compound **7**.

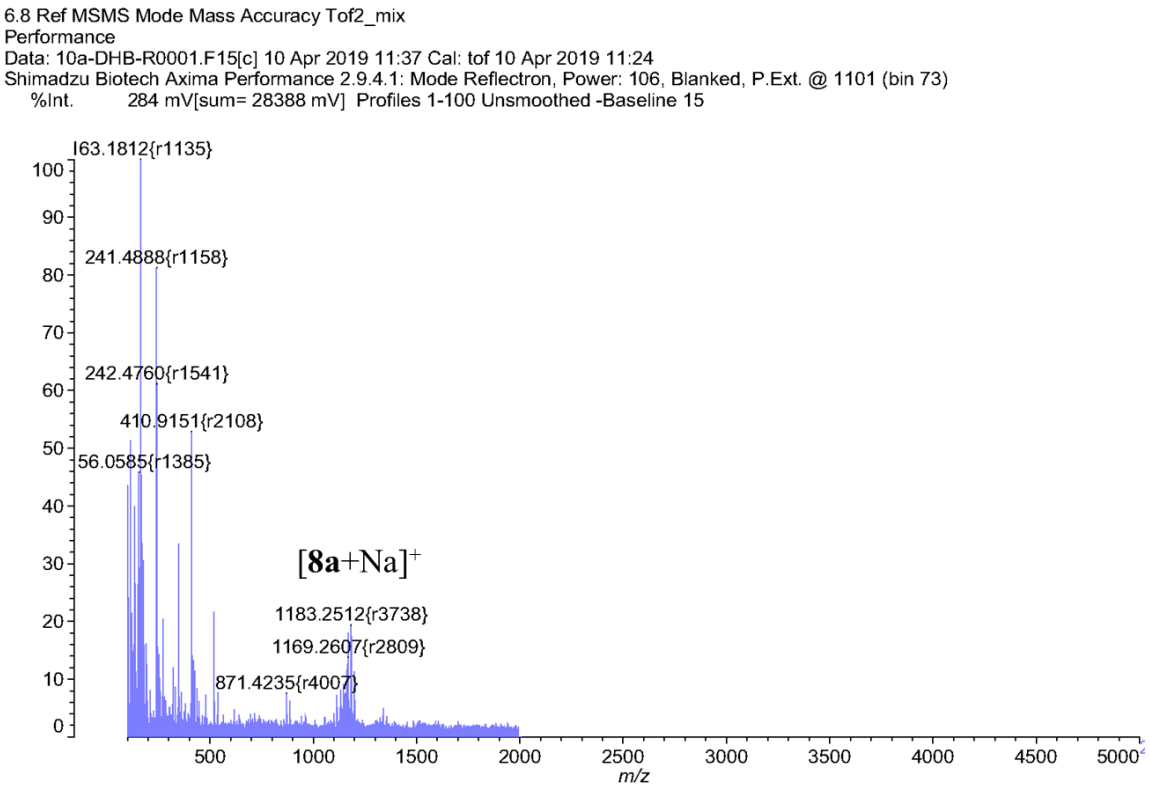

Figure S28. MALDI-TOF mass spectrum of **8a** (Matrix: DHB).

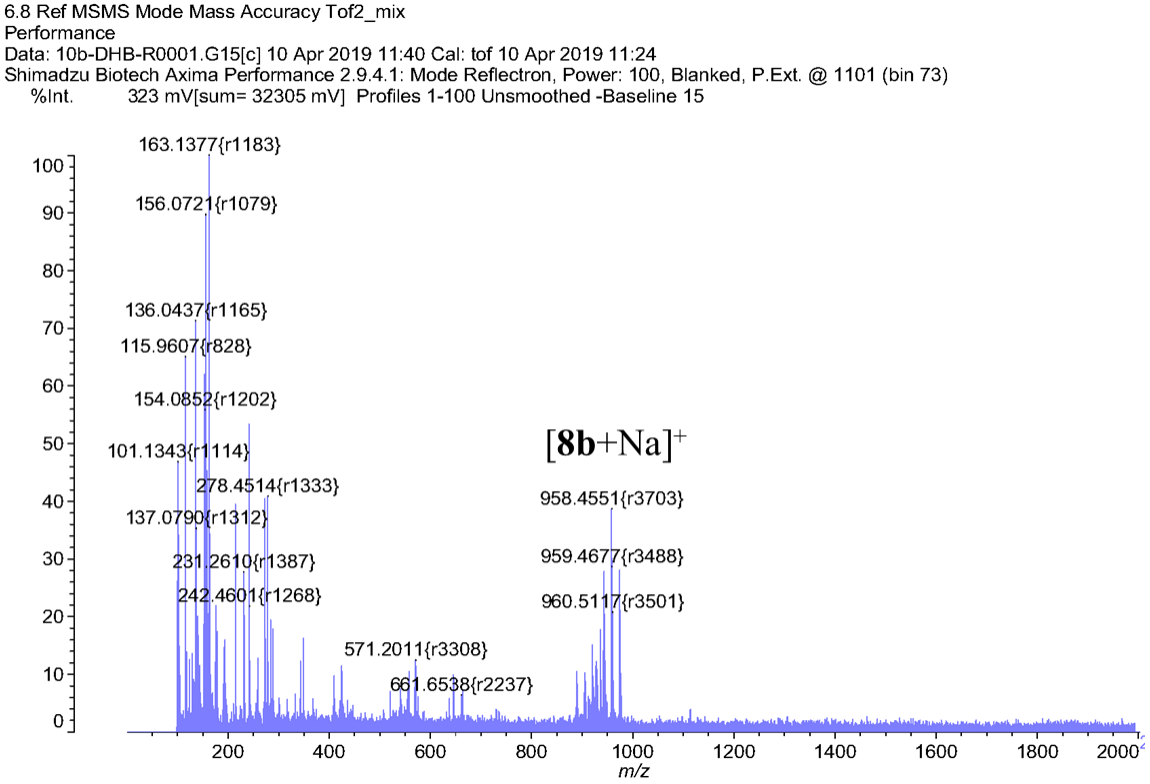

Figure S29. MALDI-TOF mass spectrum of **8b** (Matrix: DHB).

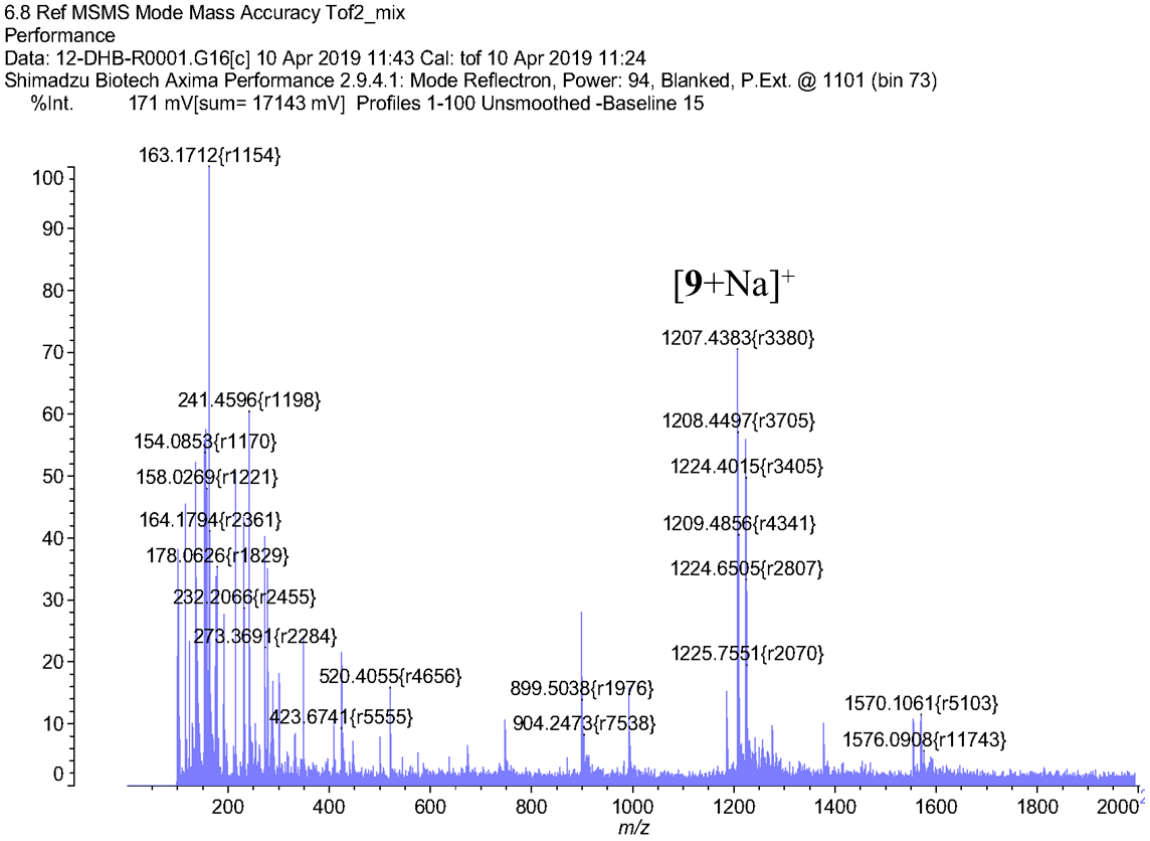

Figure S30. MALDI-TOF mass spectrum of compound **9** (Matrix: DHB).

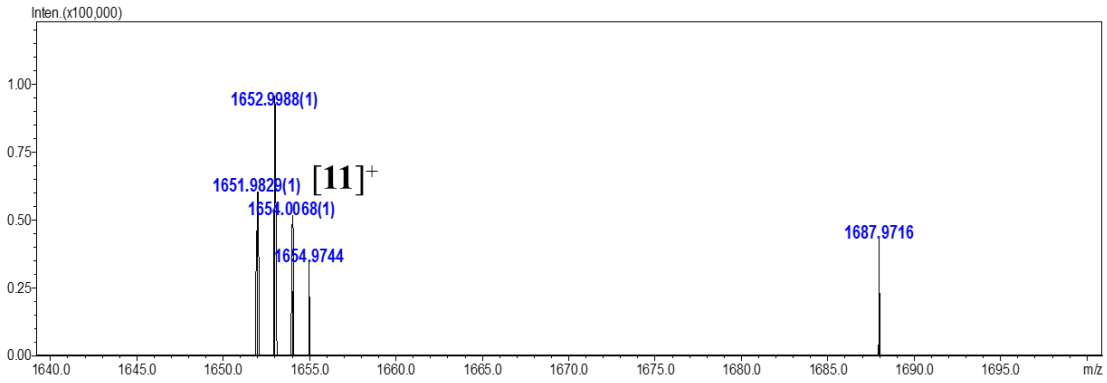

Figure S31. ESI-HR mass spectrum of compound **11**.

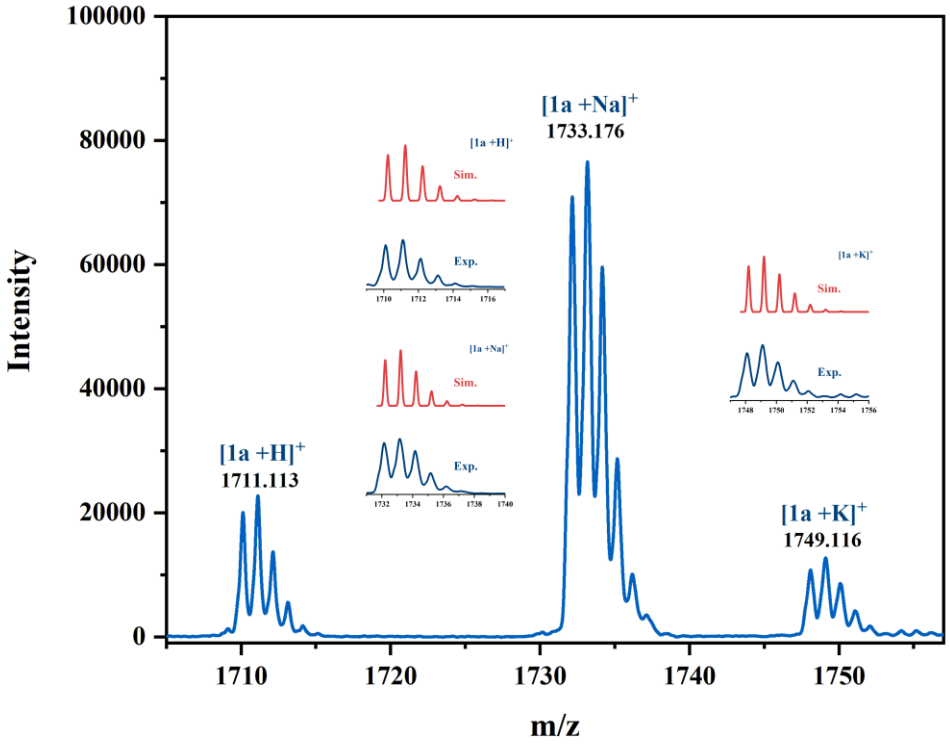

Figure S32. Partial MALDI-TOF mass spectrum of **1a** (insert: experimental isotope distribution (blue) and computer simulation (red)). (Matrix: CCA(NaCl))

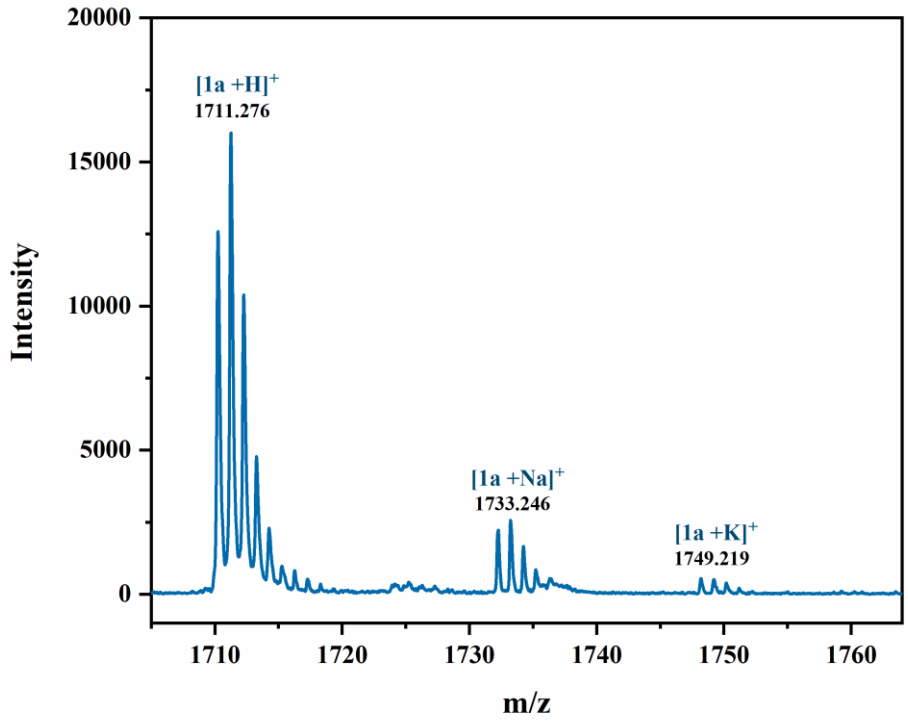

Figure S33. Partial MALDI-TOF mass spectrum of **1a**. (Matrix: DHAP)

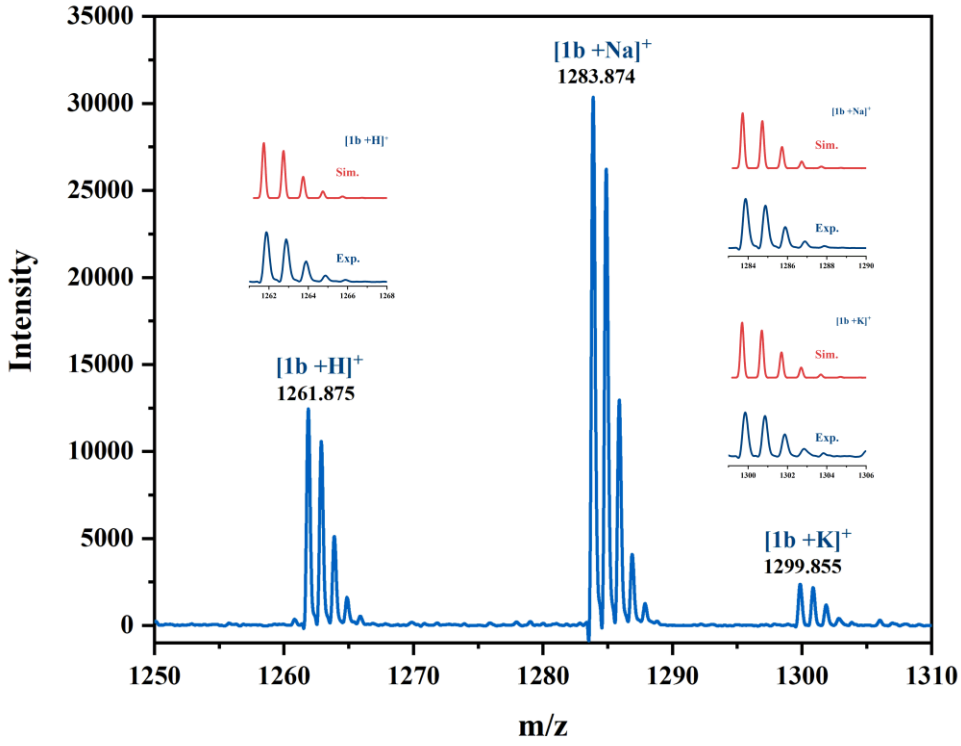

Figure S34. Partial MALDI-TOF mass spectrum of **1b** (insert: experimental isotope distribution (blue) and computer simulation (red)). (Matrix: DHAP)

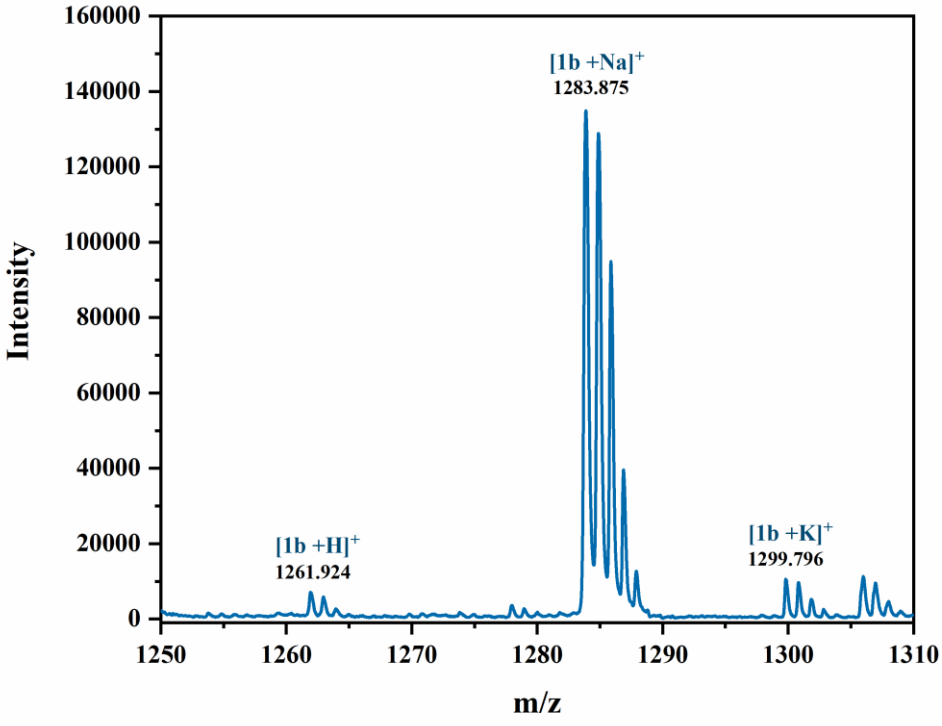

Figure S35. Partial MALDI-TOF mass spectrum of **1b**. (Matrix: CCA(NaCl))

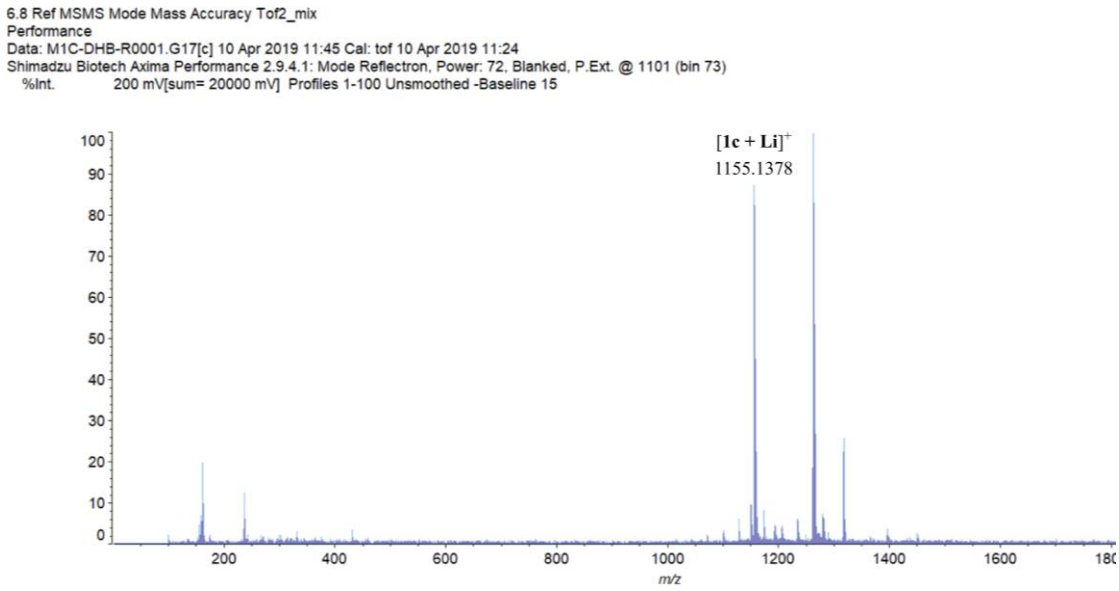

Figure S36. MALDI-TOF mass spectrum of **1c ⊃ $LiClO_4$** (Matrix: DHB).

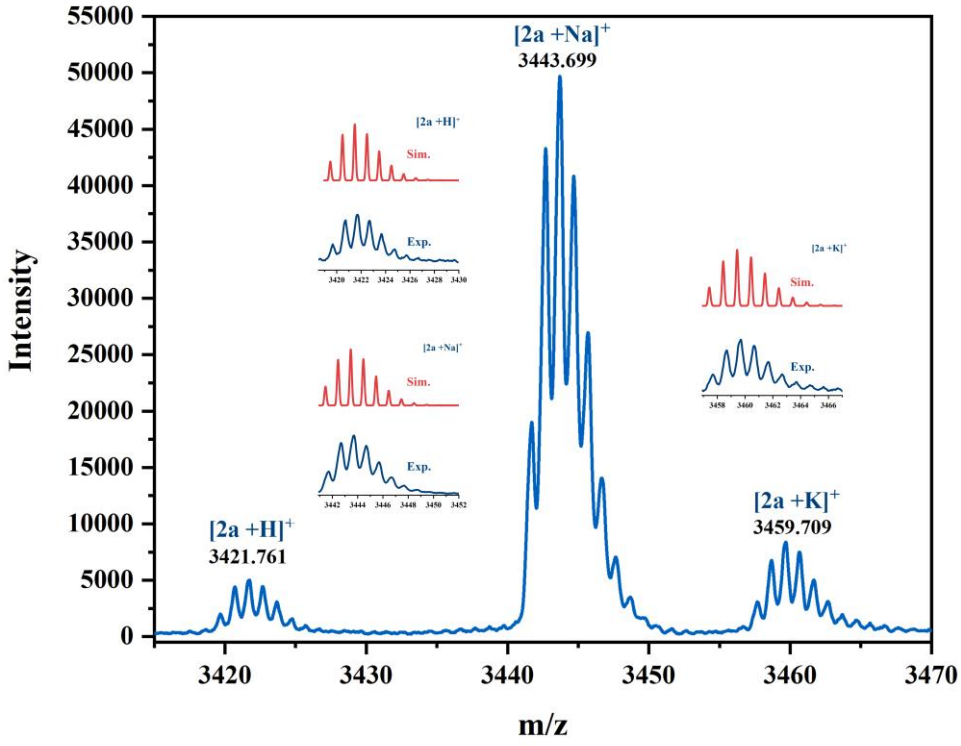

Figure S37. Partial MALDI-TOF mass spectrum of **2a** (insert: experimental isotope distribution (blue) and computer simulation (red)).(Matrix: CCA(NaCl))

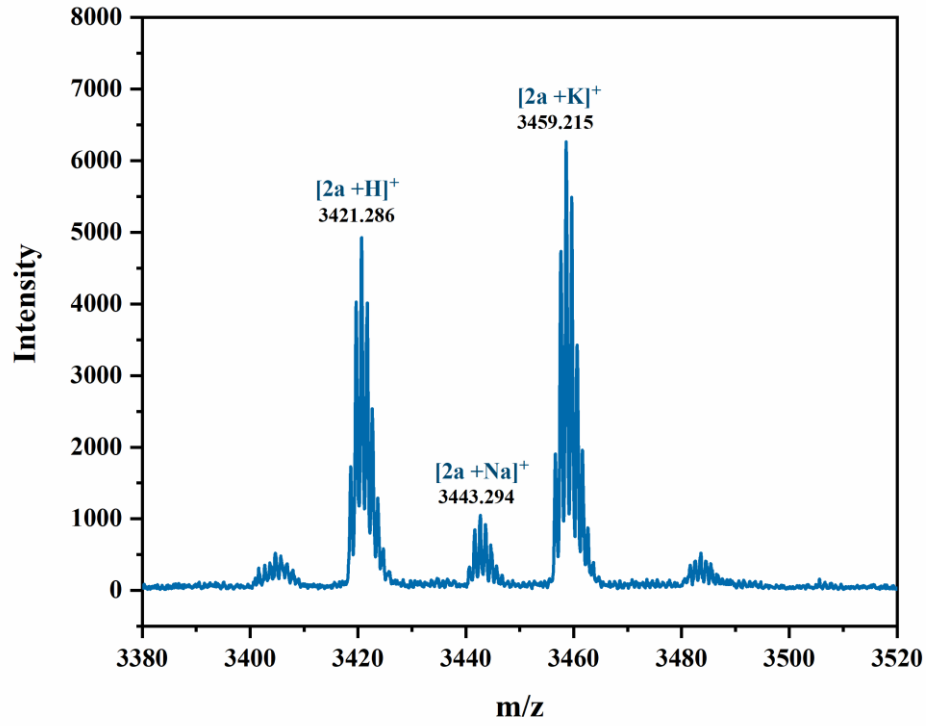

Figure S38. Partial MALDI-TOF mass spectrum of **2a**. (Matrix: DHAP)

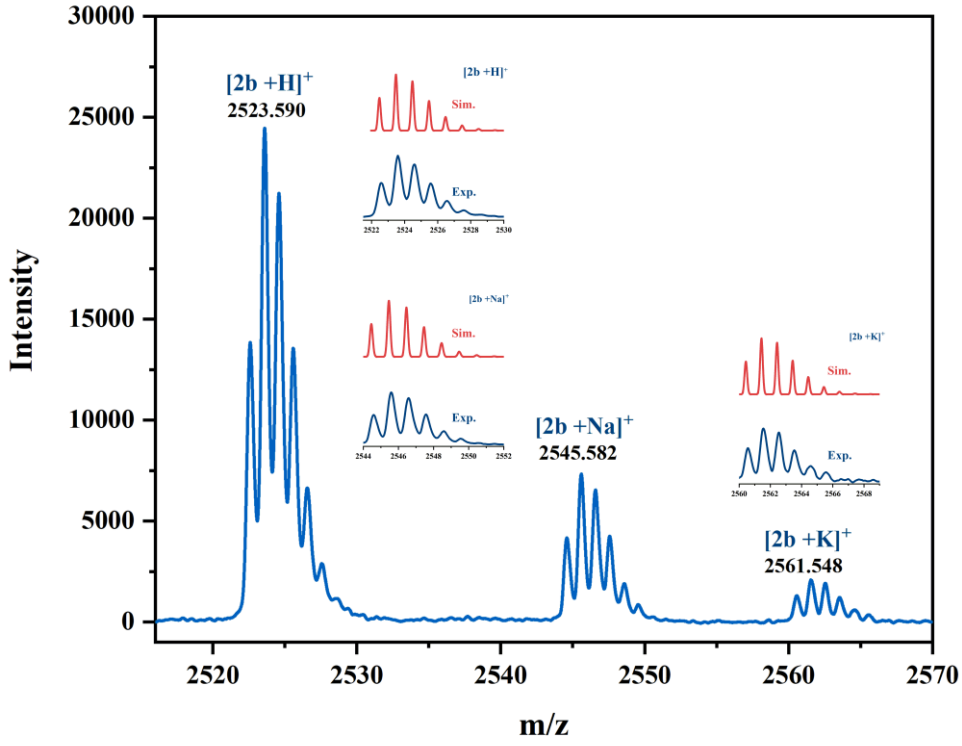

Figure S39. Partial MALDI-TOF mass spectrum of **2b** (insert: experimental isotope distribution (blue) and computer simulation (red)). (Matrix: DHAP)

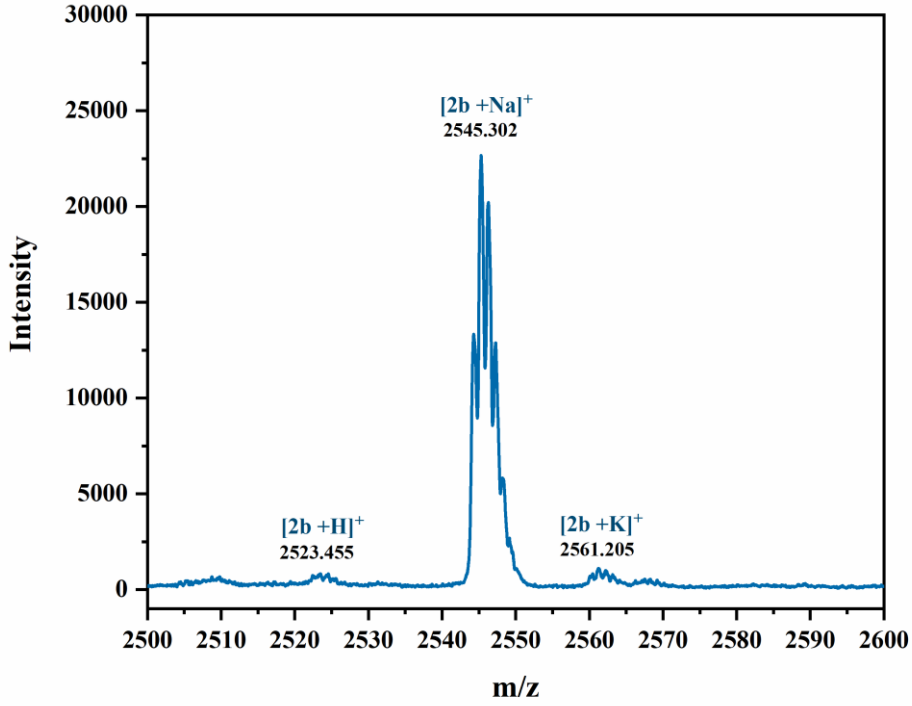

Figure S40. Partial MALDI-TOF mass spectrum of **2b**. (Matrix: CCA(NaCl))

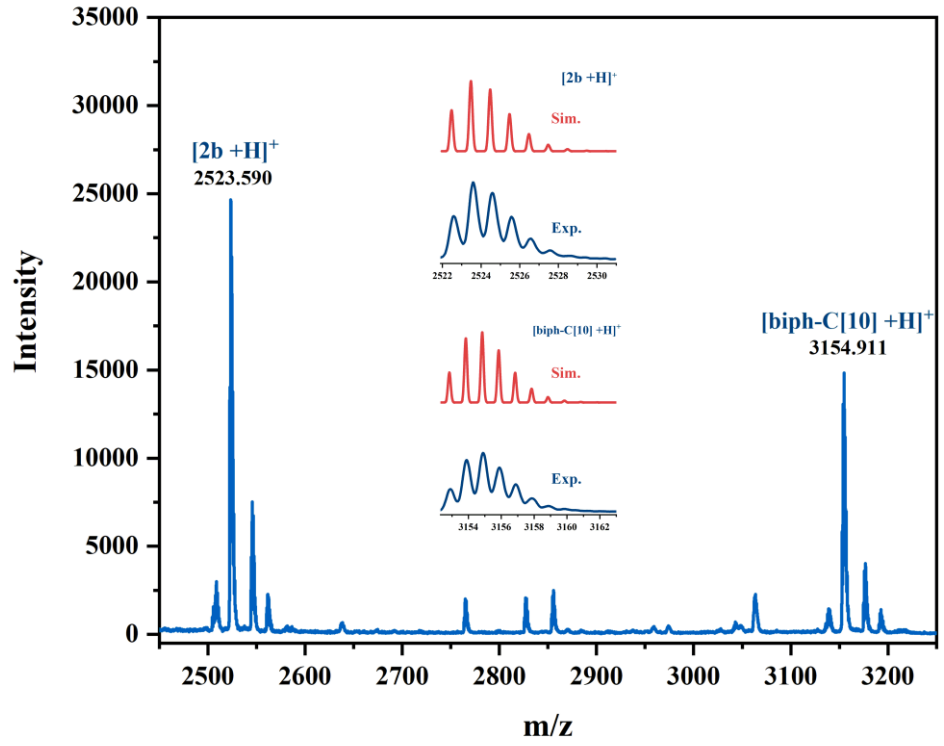

Figure S41. Partial MALDI-TOF mass spectrum of **2b** and biphenyl-cyclo[10]aramide (insert: experimental isotope distribution (blue) and computer simulation (red)). (Matrix: DHAP)

3.3 2D NOESY spectrum of 1a

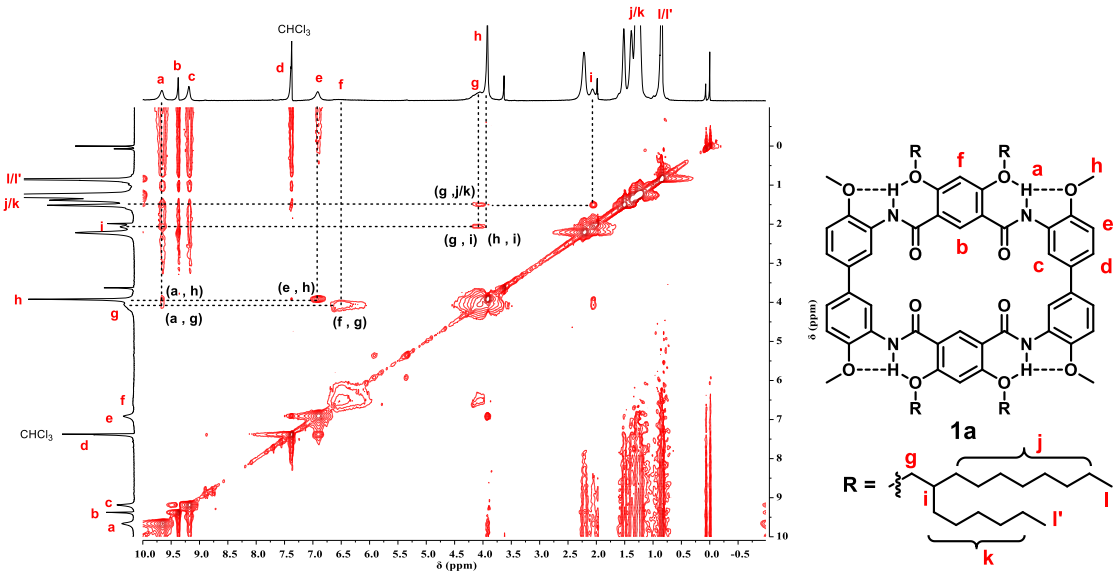

Figure S42. 2D NOESY spectrum of **1a** in $CDCl_3/CD_3CN$ = 5/1 (v/v) at 298 K (600 MHz, 10 mM; mixing time: 0.4 s).

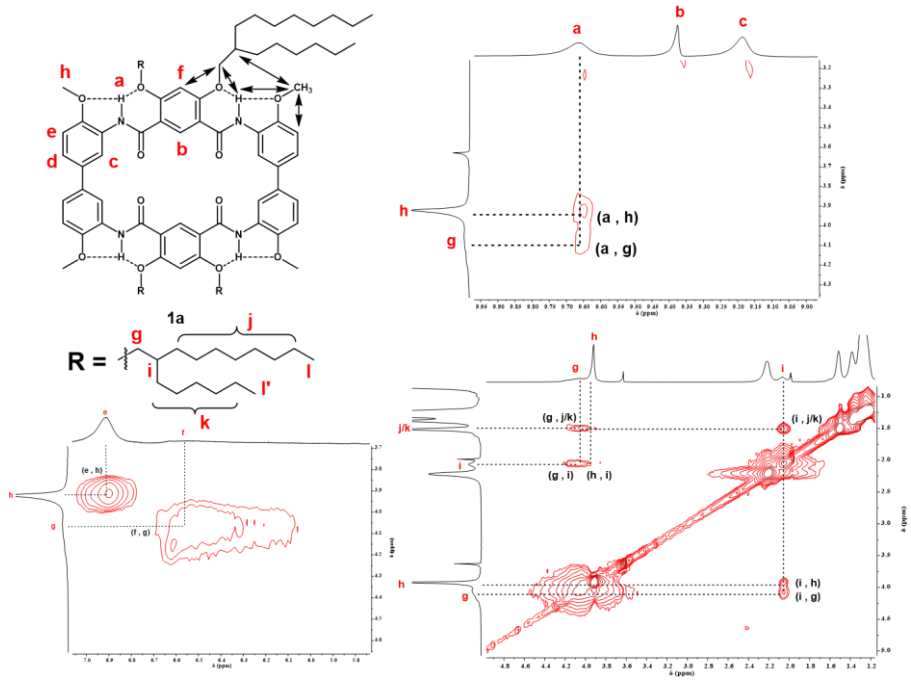

Figure S43. Expanded 2D NOESY spectrum of **1a** in $CDCl_3/CD_3CN$ = 5/1 (v/v) at 298 K (600 MHz, 10 mM; mixing time: 0.4 s).

4. Host-Guest Complexation of 1a and Different Guests

4.1 NMR spectra of complexation

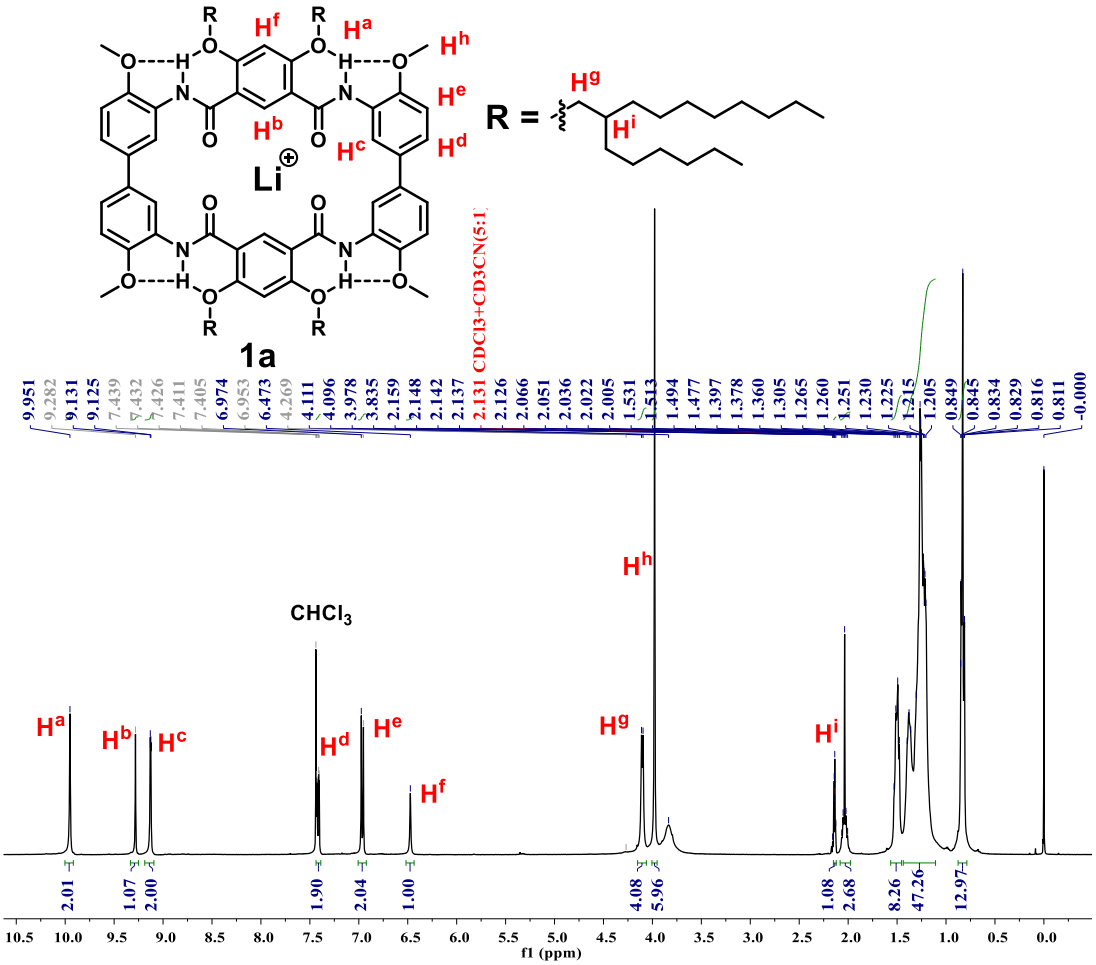

Figure S44. ^{1}H NMR spectrum of **1a** ⊃ **LiClO$_4$** (400 MHz, 298 K, $CDCl_3$ / CD_3CN = 5:1 (v/v)).

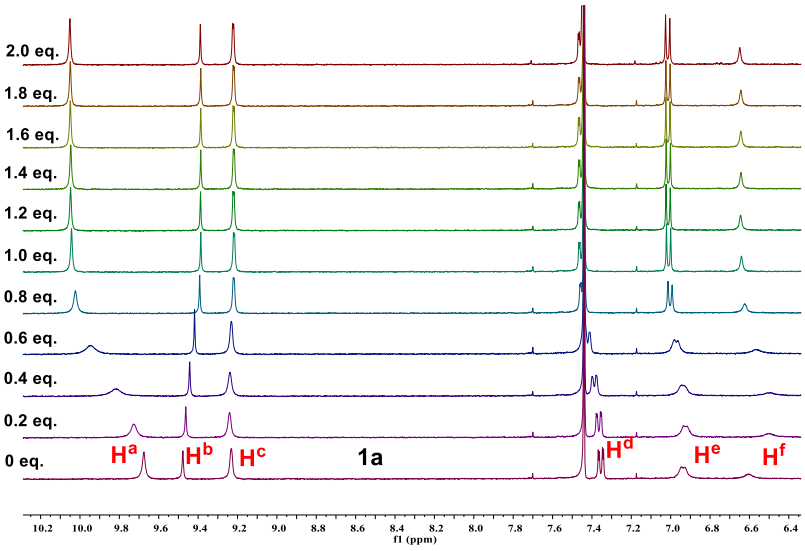

Figure S45. Stacked ^{1}H NMR spectra of **1a** ⊃ **LiClO$_4$** (1 mM) in aromatic area (400 MHz, 298 K, $CDCl_3$ / CD_3CN = 5:1 (v/v)).

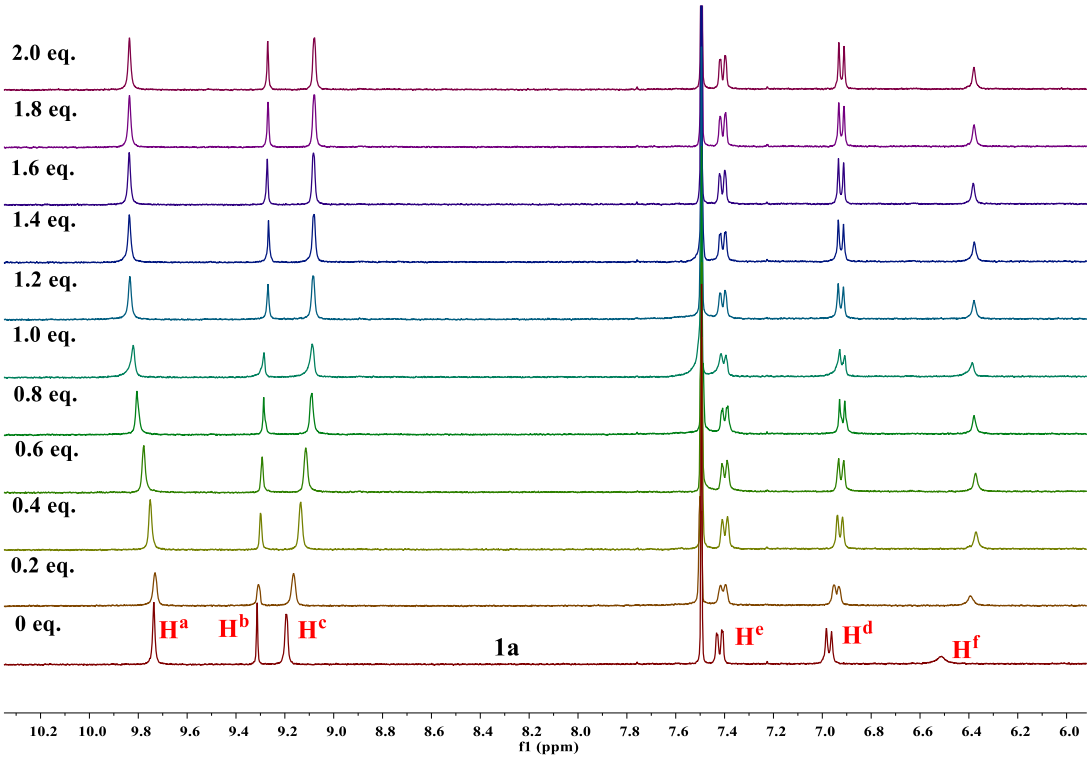

Figure S46. Stacked ^{1}H NMR spectra of **1a** ⊃ **LiClO$_4$** (1 mM) at aromatic area (400 MHz, 298 K, $CDCl_3$ / CD_3CN = 1:1 (v/v)).

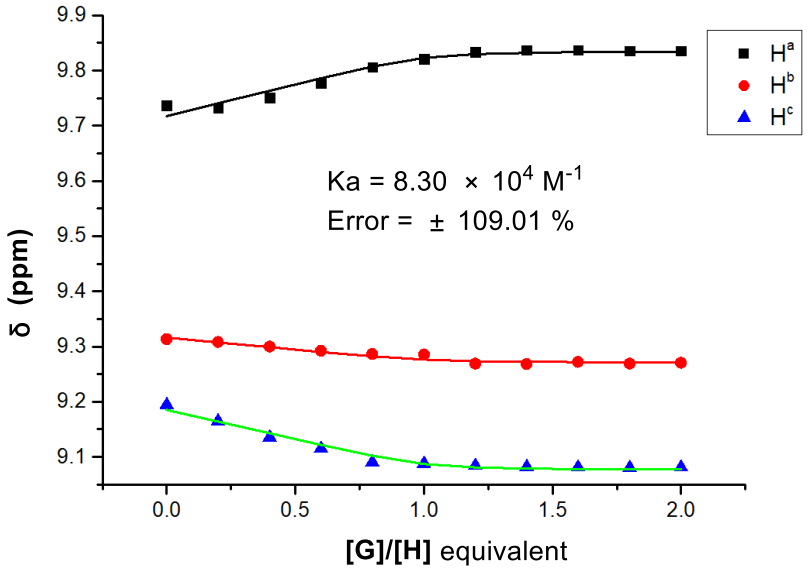

Figure S47. Determination of the binding constant of **1a** ⊃ **LiClO$_4$** in $CDCl_3$ / CD_3CN (1/1, v/v) at 298 K.

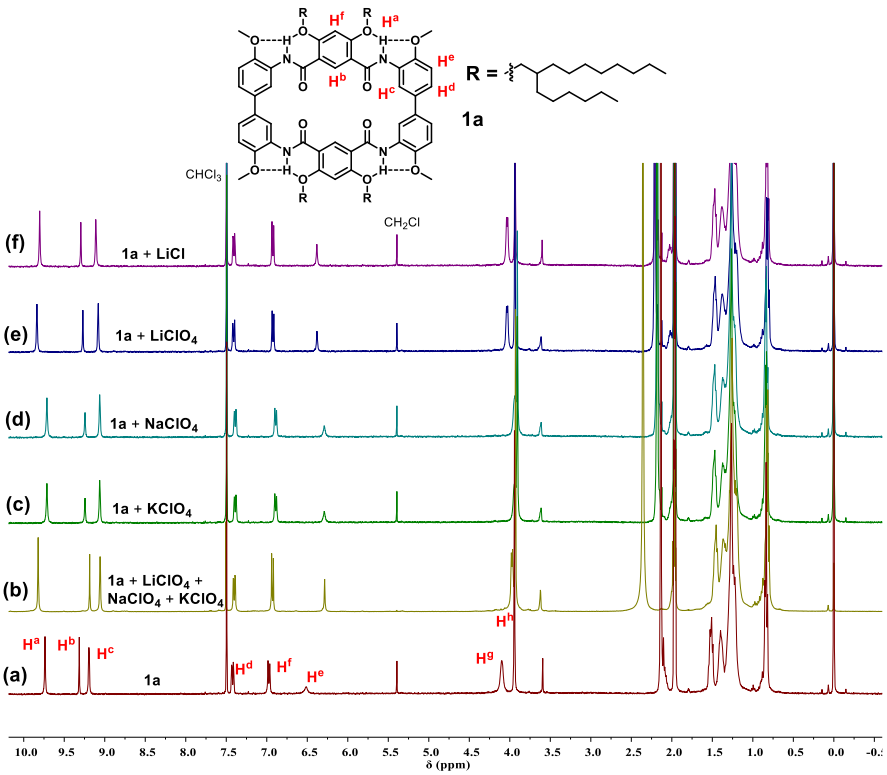

Figure S48. Stacked ^{1}H NMR spectra (400MHz, 298 K, $CDCl_3$:CD_3CN, 1:1) of **1a** in the presence of excess of Li^+, Na^+ and K^+.

4.2 Determination of stoichiometry and binding constant

Determination of stoichiometry and binding constant of 1a ⊃ di-n-butylammonium hexafluorophosphate

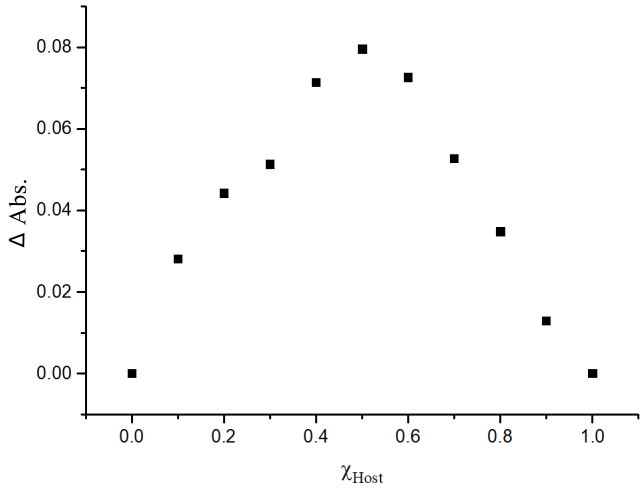

Figure S49. Job plots for **1a** ⊃ di-n-butylammonium hexafluorophosphate in $CHCl_3/CH_3CN$ (5/1, v/v) were obtained by UV-vis spectroscopy indicating a 1:1 stoichiometry.

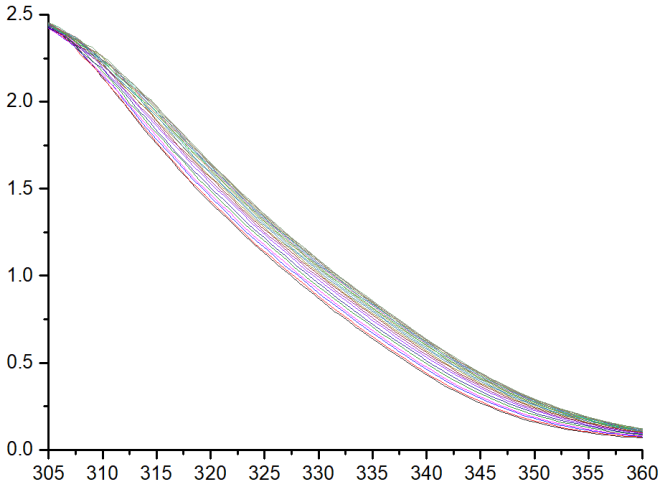

Figure S50. Stacked UV-vis spectra of **1a** (50 μM) titrated with di-n-butylammonium hexafluorophosphate in $CHCl_3/CH_3CN$ (5/1, v/v) from 0 equiv. to 3.0 equiv. at 298 K.

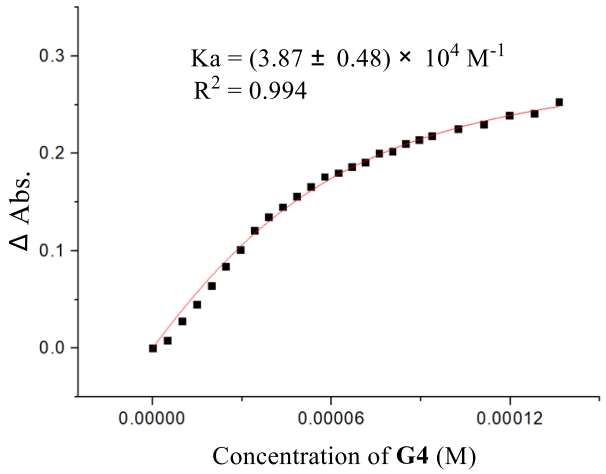

Figure S51. Determination of the binding constant of **1a** ⊃ di-n-butylammonium hexafluorophosphate in $CHCl_3/CH_3CN$ (5/1, v/v) at 298 K. Fitting result based on the absorbance at 330 nm. **1a** (50 μM) titrated with di-n-butylammonium hexafluorophosphate.

Determination of stoichiometry and binding constant of 1a ⊃ $LiClO_4$

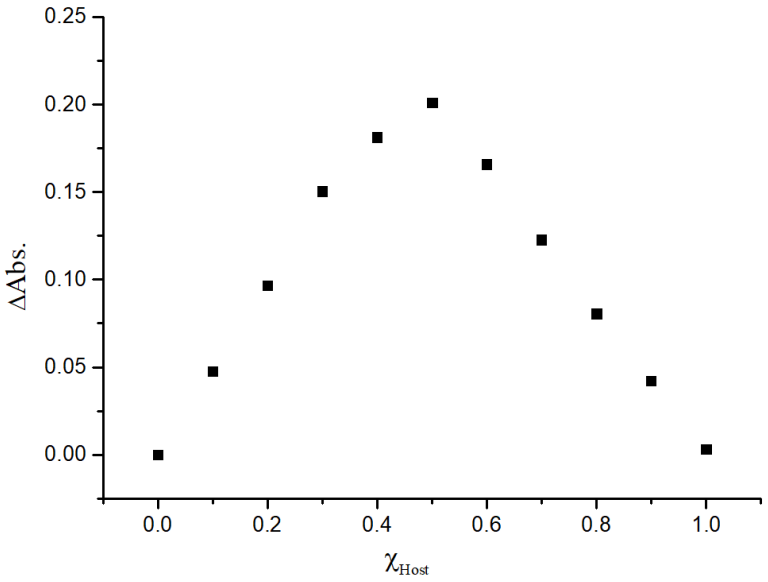

Figure S52. Job plots for **1a** ⊃ **$LiClO_4$** in $CHCl_3/CH_3CN$ (5/1, v/v) were obtained by UV-vis spectroscopy indicating a 1:1 stoichiometry.

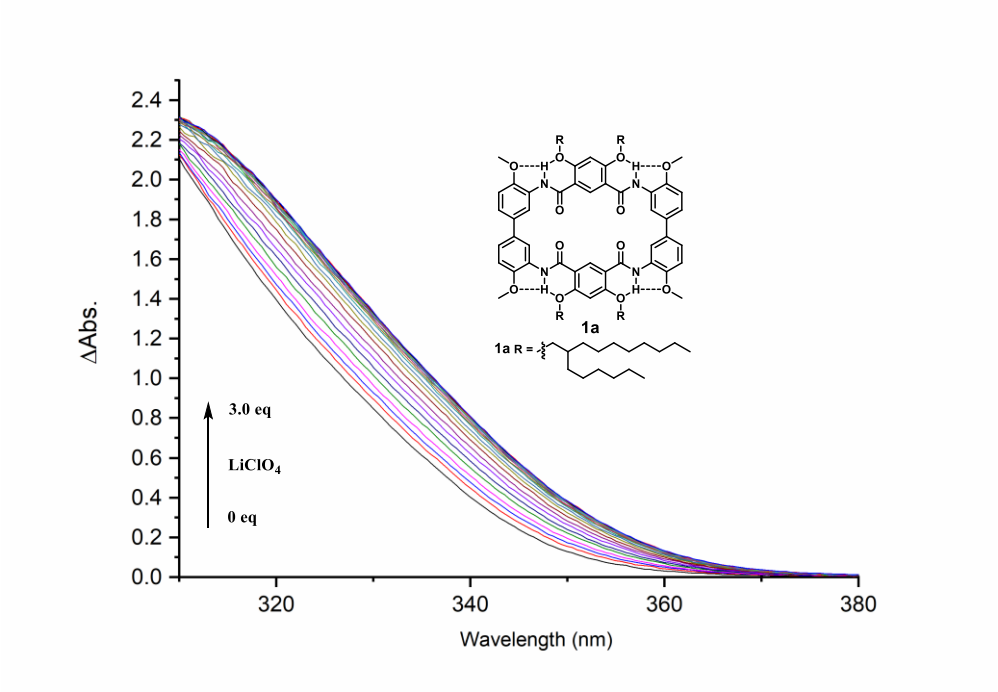

Figure S53. Stacked UV-vis spectra of **1a** (50 μM) titrated with $LiClO_4$ in $CHCl_3/CH_3CN$ (5/1, v/v) from 0 equiv. to 3.0 equiv. at 298 K.

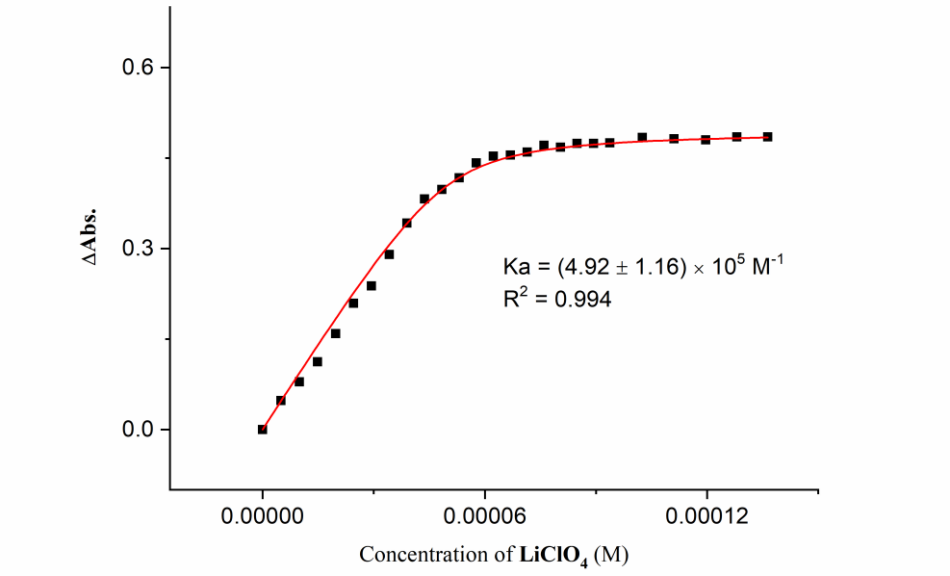

Figure S54. Determination of the binding constant of **1a** ⊃ **$LiClO_4$** in $CHCl_3/CH_3CN$ (5/1, v/v) at 298 K. Fitting result based on the absorbance at 330 nm. **1a** (50 μM) titrated with $LiClO_4$.

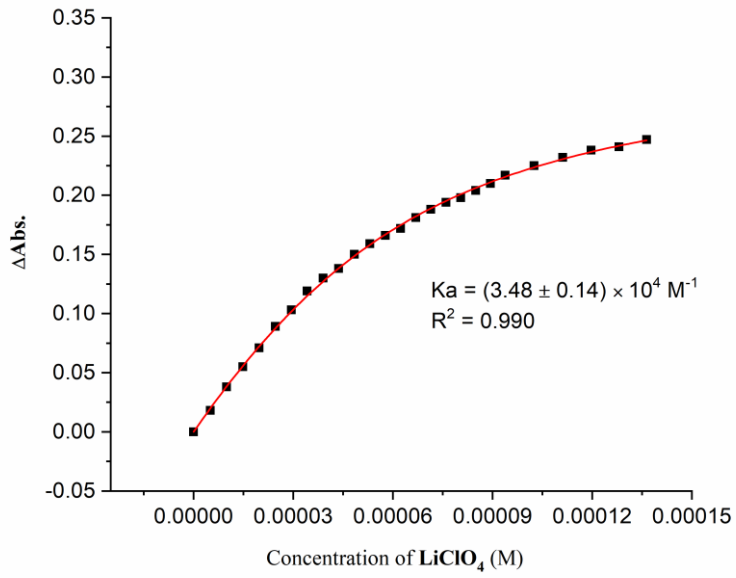

Figure S55. Determination of the binding constant of **1a** ⊃ **LiClO4** in $CHCl_3/CH_3CN$ (1/1, v/v) at 298 K. Fitting result based on the absorbance at 330 nm. **1a** (50 μM) titrated with $LiClO_4$.

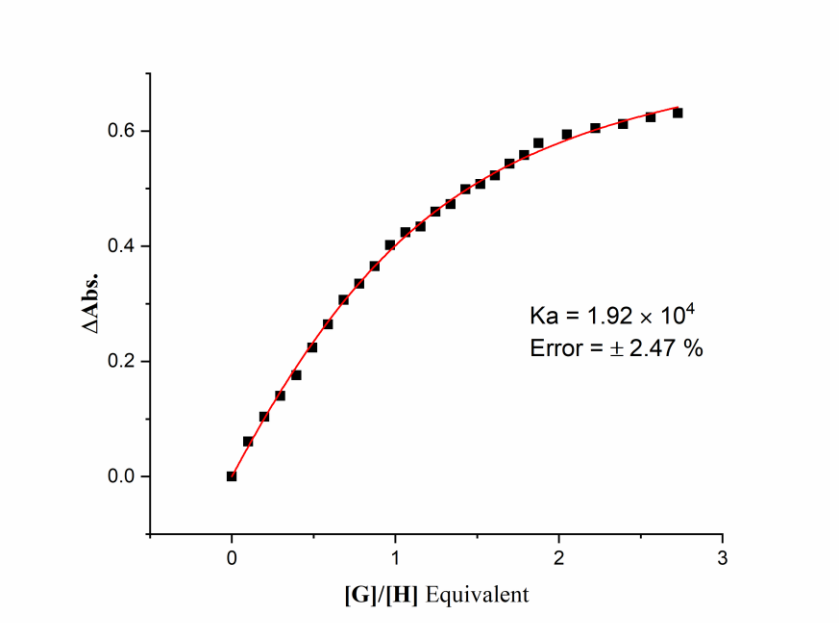

Figure S56. Determination of the binding constant of **1a** ⊃ **LiClO4** in $CHCl_3/CH_3CN$ (1/1, v/v) at 298 K. Fitting result based on the absorbance at 330 nm. **1a** (100 μM) titrated with $LiClO_4$.

Determination of stoichiometry and binding constant of 1a ⊃ $NaClO_4$

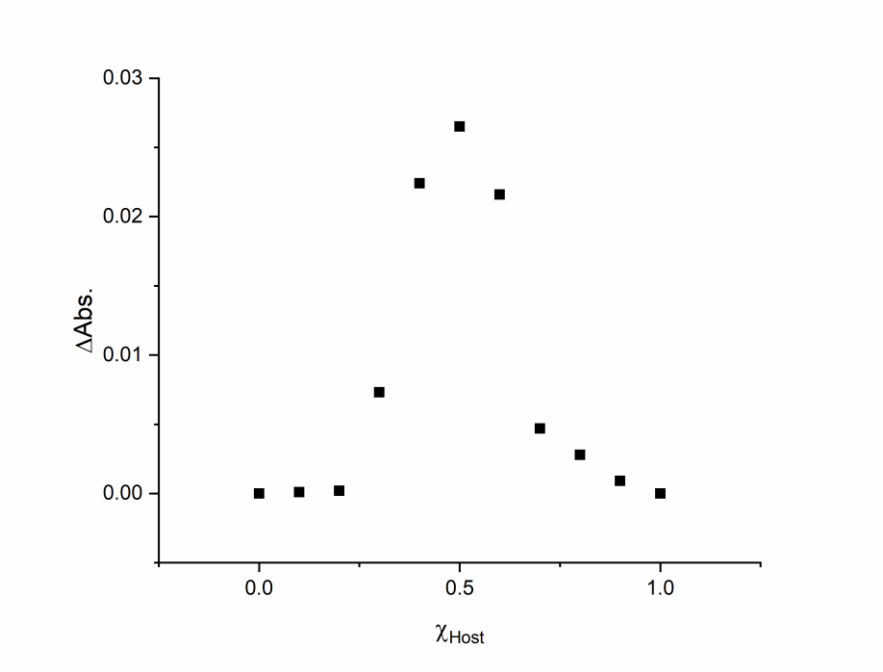

Figure S57. Job plots for **1a ⊃ $NaClO_4$** $CHCl_3/CH_3CN$ (1/1, v/v) were obtained by UV-vis spectroscopy indicating a 1:1 stoichiometry.

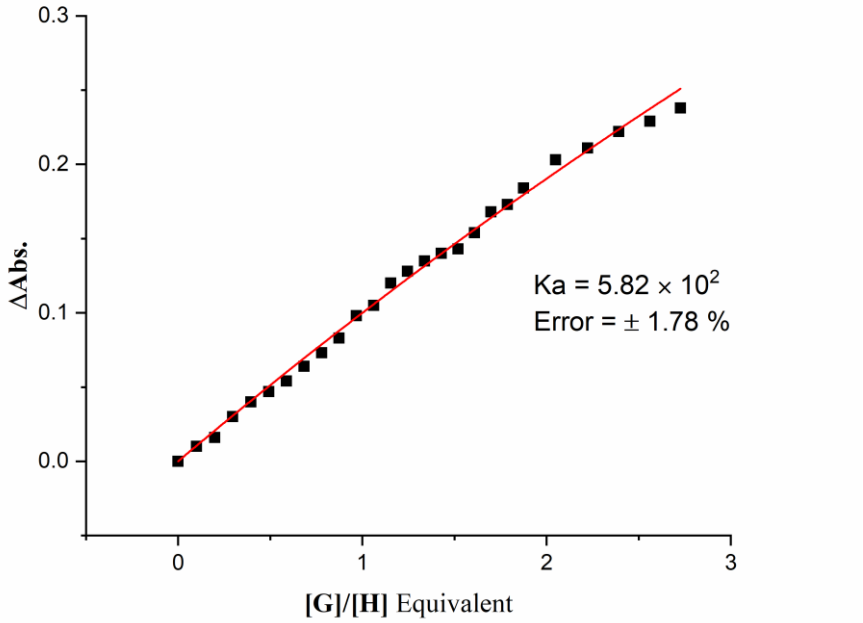

Figure S58. Determination of the binding constant of **1a ⊃ NaClO4** in $CHCl_3/CH_3CN$ (1/1, v/v) at 298 K. Fitting result based on the absorbance at 330 nm. **1a** (100 μM) titrated with $NaClO_4$.

Determination of stoichiometry and binding constant of 1a ⊃ $KClO_4$

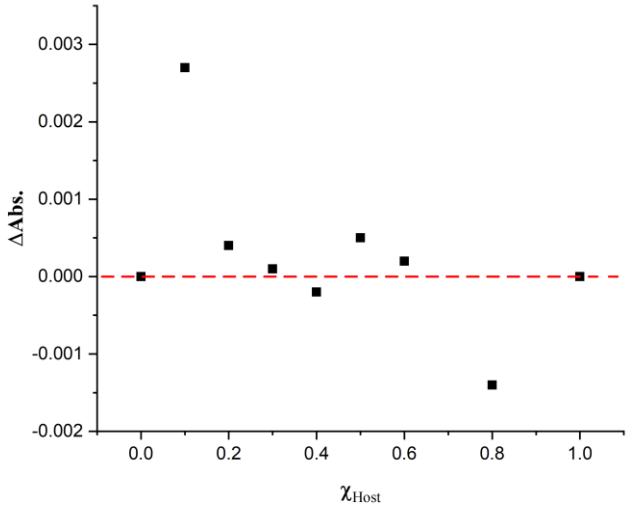

Figure S59. Job plots for **1a ⊃ $KClO_4$** $CHCl_3/CH_3CN$ (1/1, v/v) were obtained by UV-vis spectroscopy. The stoichiometry cannot be determined due to the weak association.

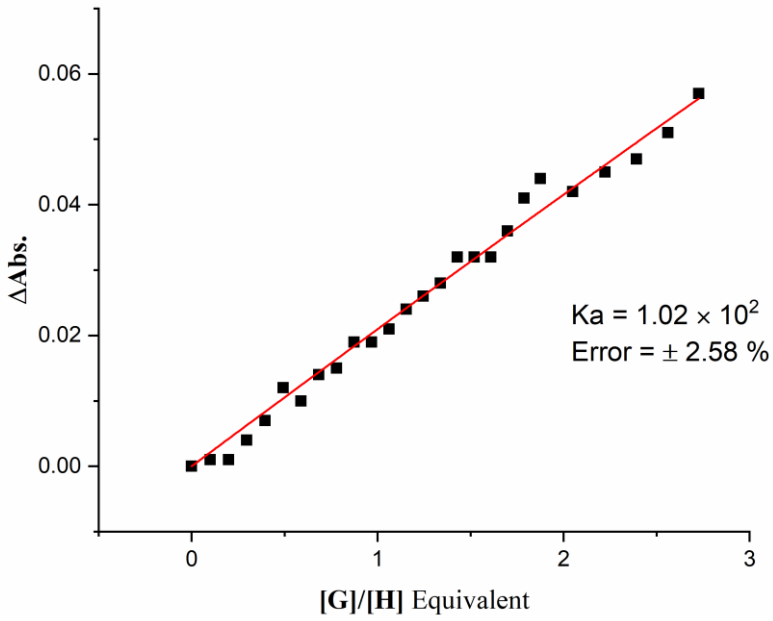

Figure S60. Determination of the binding constant of **1a ⊃ KClO4** in $CHCl_3/CH_3CN$ (1/1, v/v) at 298 K. Fitting result based on the absorbance at 330 nm. **1a** (100 μM) titrated with $KClO_4$.

Determination of stoichiometry and binding constant of 9 ⊃ $LiClO_4$

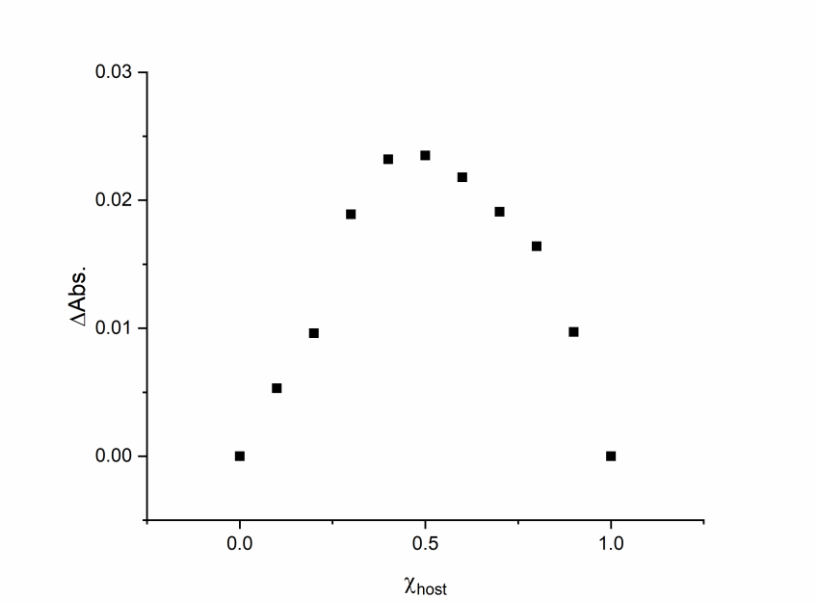

Figure S61. Job plots experiment for the complexation of **9** ⊃ $LiClO_4$ in $CHCl_3/CH_3CN$ (5/1, v/v) based on the absorbance at 330 nm, indicating a 1:1 stoichiometry. The total concentration is 50 μM.

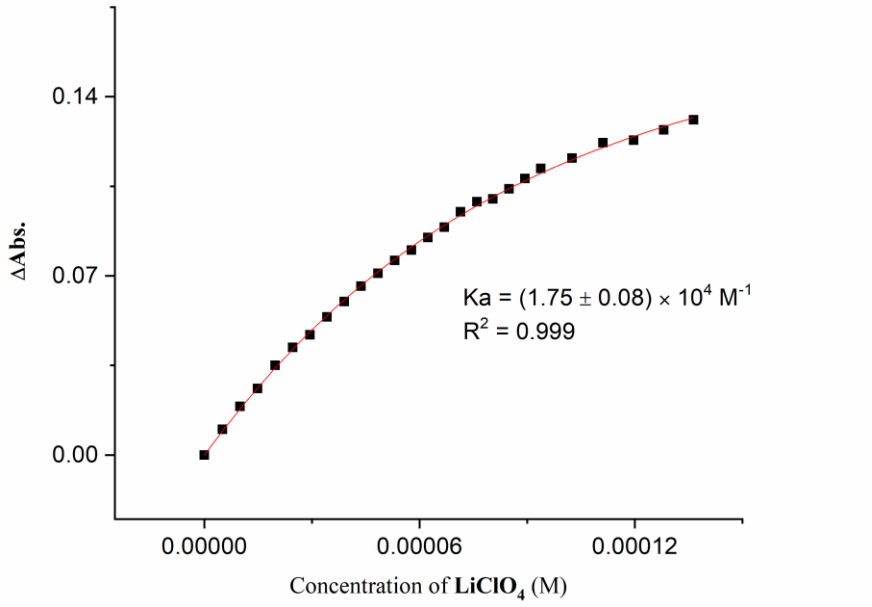

Figure S62. Determination of the binding constant of **9** ⊃ $LiClO_4$ in $CHCl_3/CH_3CN$ (5/1, v/v) at 298 K. Fitting result based on the absorbance at 330 nm. **9** (50 μM) titrated with $LiClO_4$.

Determination of stoichiometry and binding constant of 11 ⊃ $LiClO_4$

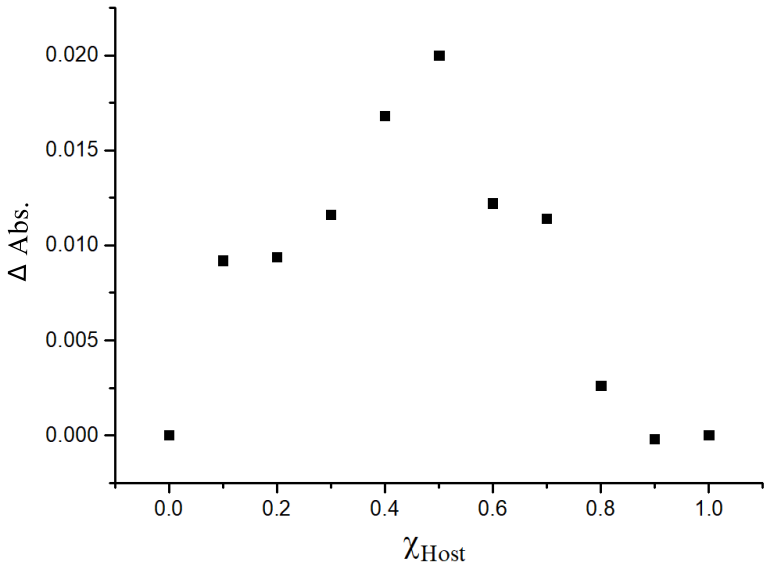

Figure S63. Job plots experiment for the complexation of **11** ⊃ $LiClO_4$ in $CHCl_3/CH_3CN$ (5/1, v/v) based on the absorbance at 330 nm, indicating a 1:1 stoichiometry. The total concentration is 50 μM.

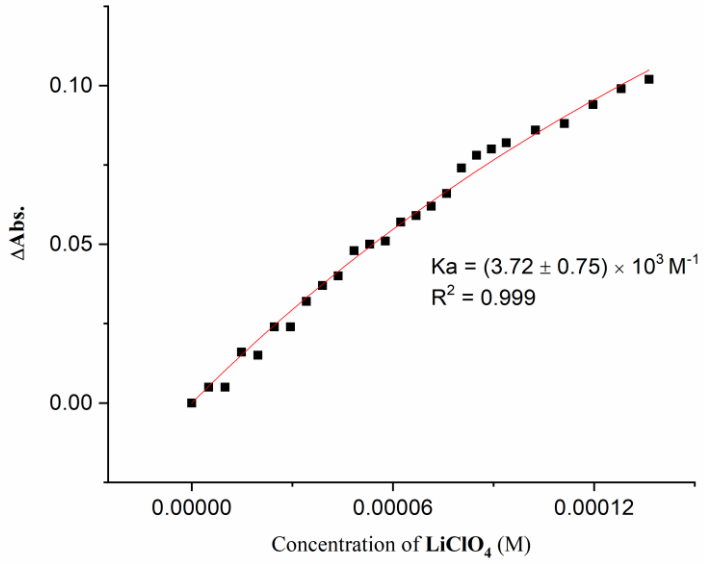

Figure S64. Determination of the binding constant of **11** ⊃ $LiClO_4$ in $CHCl_3/CH_3CN$ (5/1, v/v) at 298 K. Fitting result based on the absorbance at 340 nm. **11** (50 μM) titrated with $LiClO_4$.

4.3 MALDI-TOF mass spectra of complexes

MALDI-TOF mass spectra of 1a⊃ $LiClO_4$

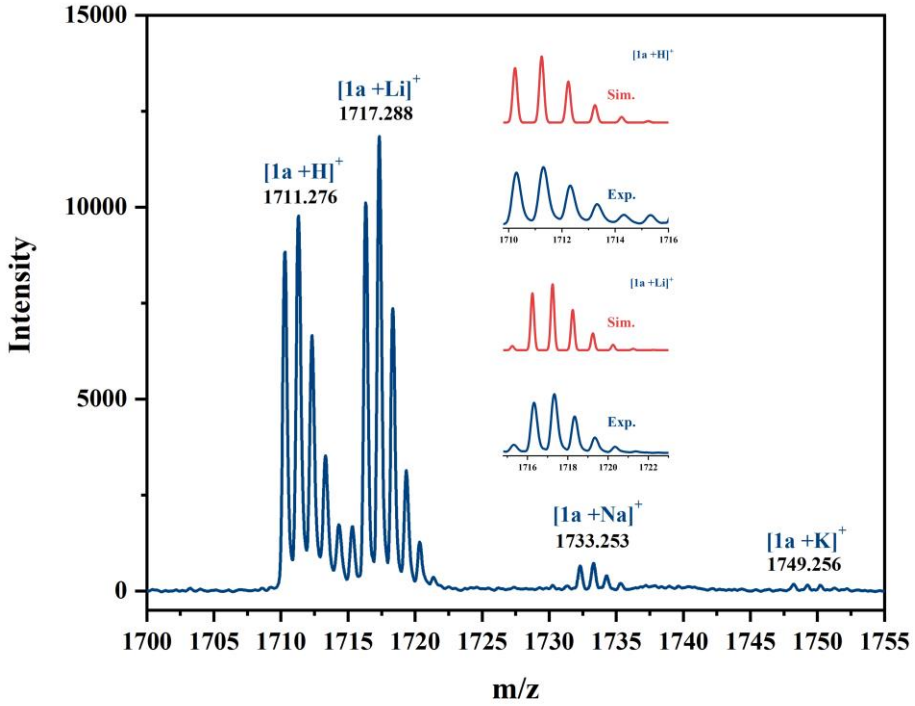

Figure S65. Partial MALDI-TOF mass spectrum of **1a** ⊃ $LiClO_4$ (insert: experimental isotope distribution (blue) and computer simulation (red)). (Matrix: DHAP)

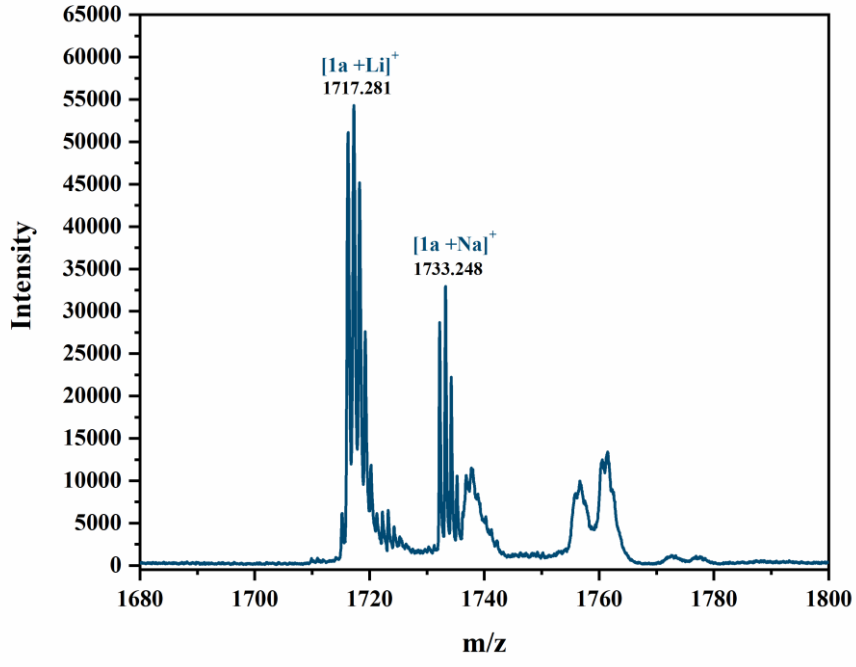

Figure S66. Partial MALDI-TOF mass spectrum of **1a** ⊃ $LiClO_4$. (Matrix: CCA(NaCl))

4.4 Fluorescence emission spectra of complex

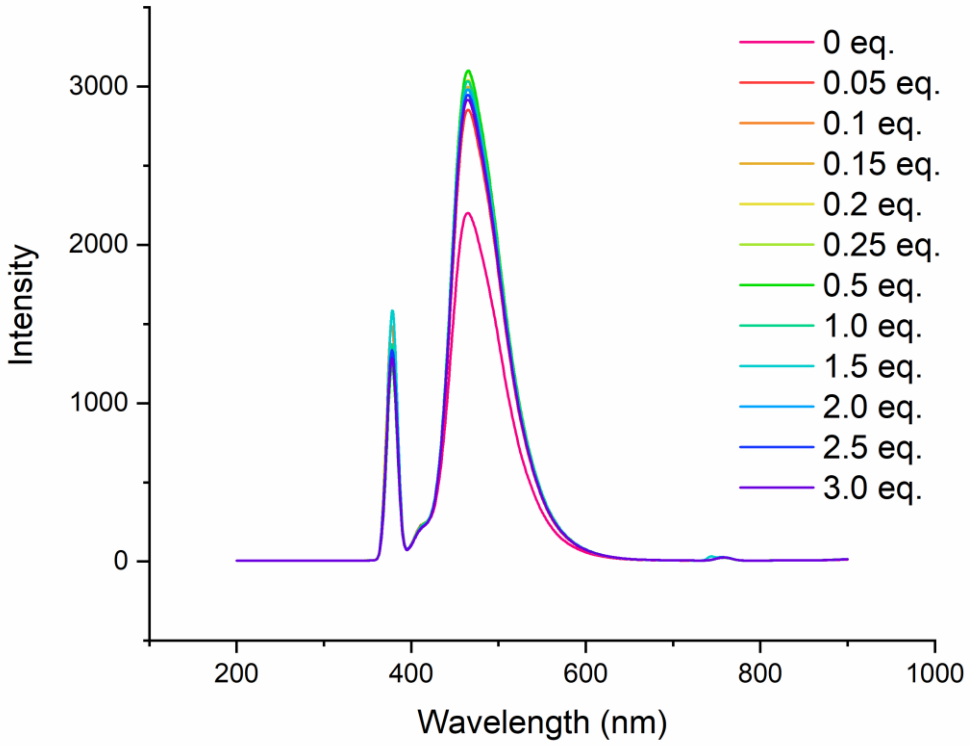

Figure S67. Fluorescence emission spectra of **1a** (100 μM) titrated with different equiv. $LiClO_4$ in $CHCl_3$ / CH_3CN = 5:1 (v/v). (λ_{ex} : 378 nm, $\lambda_{em\ Max}$:465 nm)

4.5 FT-IR spectra of complexes

Fourier transform infrared spectrometry (FT-IR) analyses of biphenyl-cyclo[4]aramide **1a** carried in the absence and presence of $LiClO_4$ produced $\nu_{C=O}$ shifts consistent with the formation of solid phase host-guest complexes.

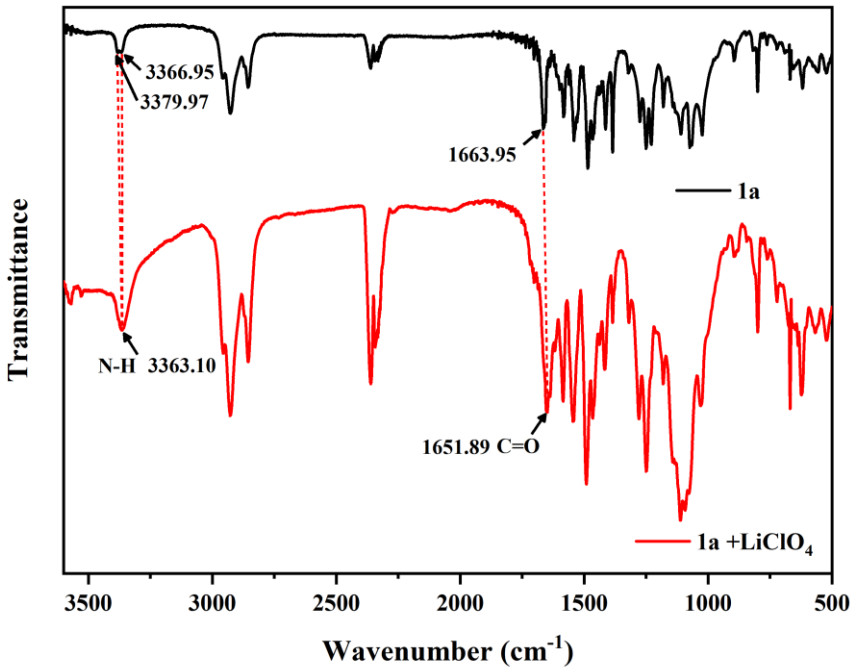

Figure S68. Stacked FT-IR spectra of **1a** and **1a** ⊃ $LiClO_4$.

5. Molecular Modeling

The structure of biphenyl-cyclo[4]aramide was optimized by the density functional theory (DFT) method at the B3LYP/6-31G (d, p) level by employing the Gaussian09 program[7].

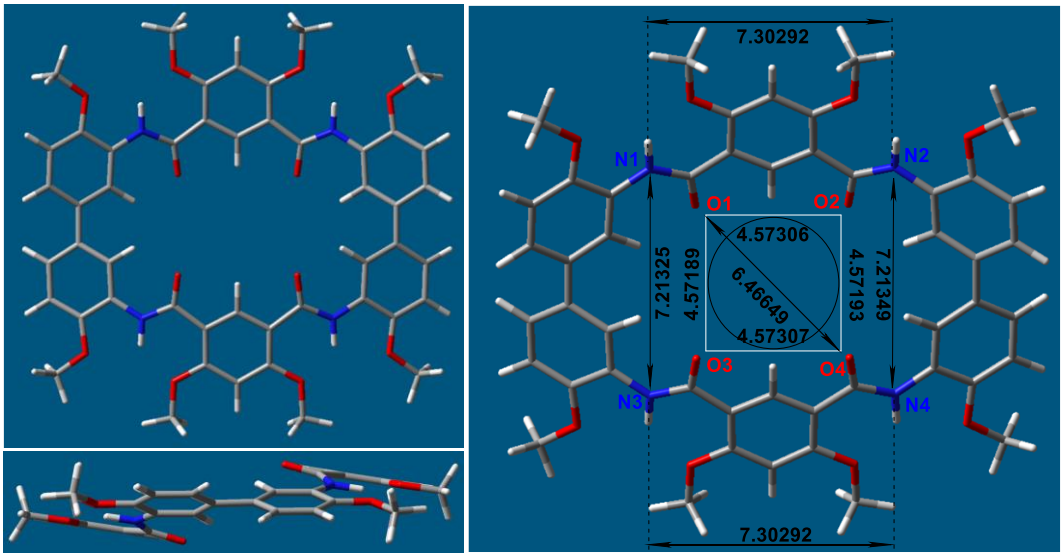

Figure S69. Top view (a) and side view (b) of optimized geometry of biph-**C[4]** at the B3LYP/6-31G (d, p) level. (gray = C, white = H, red = O, and blue = N); (c) Selected interatomic distances (Å) of complexes. For simplicity, all side chains are replaced with methyl groups.

Table S1 Selected interatomic distances (Å) of complexes calculated applying B3LYP/6-31G (d, p) level DFT functional.

atoms	interatomic distances (Å)
O1-O2	**4.57306**
O1-O3	**4.57189**
O2-O4	**4.57193**
O3-O4	**4.57307**
O1-O4	**6.46649**
N1-N2	**7.30292**
N1-N3	**7.21325**
N2-N4	**7.21349**
N3-N4	**7.30292**

Biphenyl-cyclo[4]aramide (Stoichiometry C48H44N4O12)
E(RB3LYP): -2976.48666489 a.u.
Number of negative frequencies: 0
Cartesian coordinates:

Center Number	Atomic Number	Forces (Hartrees/Bohr) X	Y	Z
1	6	0.000006309	0.000062134	0.000005432
2	6	0.000037533	-0.000100350	0.000074107
3	6	-0.000029727	-0.000003082	0.000037071
4	6	0.000010677	-0.000083205	-0.000035214
5	6	0.000007716	0.000033780	-0.000014487
6	6	0.000001652	0.000048767	-0.000086446
7	6	-0.000027398	0.000008532	-0.000034341
8	6	0.000033528	0.000094086	-0.000078589
9	6	0.000000844	-0.000062717	-0.000007403
10	6	0.000008252	-0.000046711	0.000086521
11	6	0.000010968	-0.000038647	0.000005087
12	6	0.000027134	0.000070317	0.000037276
13	7	0.000043248	-0.000022475	0.000049185
14	7	0.000029115	0.000044983	-0.000028763
15	8	-0.000028396	-0.000019400	0.000106885
16	8	-0.000041367	0.000020163	-0.000107792
17	6	-0.000062042	0.000067595	-0.000035808

18	8	0.000042458	-0.000035214	0.000022516
19	6	-0.000027120	0.000024719	0.000030619
20	6	0.000010284	-0.000030145	-0.000033765
21	6	0.000021885	0.000010045	0.000018392
22	6	-0.000048325	0.000014128	0.000046510
23	6	0.000012393	-0.000008646	0.000020182
24	6	0.000047243	0.000007603	0.000021147
25	6	0.000066383	0.000056922	0.000003738
26	7	-0.000014697	-0.000068237	0.000025333
27	8	-0.000017501	-0.000027309	0.000006108
28	8	0.000003053	0.000021376	-0.000105258
29	6	-0.000049063	0.000006484	0.000057494
30	8	-0.000039192	-0.000012522	-0.000078123
31	6	0.000053136	-0.000003369	0.000038012
32	6	-0.000022321	0.000038424	-0.000002553
33	6	-0.000066132	-0.000061447	0.000004192
34	6	-0.000025670	-0.000015391	-0.000019291
35	8	0.000036562	0.000026122	-0.000016844
36	6	0.000045205	-0.000015304	-0.000047856
37	6	-0.000004370	0.000009235	-0.000020416
38	6	-0.000050770	-0.000007416	-0.000021673
39	6	0.000025715	-0.000023737	-0.000028865
40	6	-0.000004926	0.000029615	0.000034297
41	6	0.000061802	-0.000062649	0.000026049
42	7	-0.000033735	0.000043921	-0.000048429
43	8	-0.000011564	0.000038786	-0.000012064
44	6	-0.000019071	-0.000033342	0.000013591
45	6	-0.000036166	-0.000054264	-0.000032365
46	6	0.000028207	-0.000006813	0.000036021
47	6	-0.000037997	-0.000097115	0.000079068
48	6	-0.000002303	0.000066483	0.000007331
49	6	-0.000004732	0.000043631	-0.000088550
50	6	0.000029961	0.000001850	-0.000039382
51	6	-0.000023622	0.000064283	0.000030520
52	6	0.000002977	-0.000046263	0.000089251
53	6	-0.000007814	-0.000066030	-0.000005134
54	6	-0.000042209	0.000103250	-0.000074139
55	6	0.000019760	-0.000012912	-0.000056938
56	8	0.000043791	-0.000017480	0.000107838
57	6	-0.000023282	-0.000014823	-0.000060213
58	8	0.000032408	0.000016401	-0.000108297
59	6	-0.000019231	0.000013162	0.000057953
60	6	0.000023831	0.000013406	0.000059849
61	8	-0.000016205	0.000000756	0.000105896
62	8	0.000030189	-0.000000816	0.000081509
63	6	0.000048550	-0.000004586	-0.000057401
64	6	-0.000053867	0.000001655	-0.000040199
65	1	-0.000011026	-0.000013454	0.000013545
66	1	-0.000012851	0.000005391	-0.000010142

67	1	-0.000027378	0.000065278	-0.000017274
68	1	-0.000011694	-0.000004380	0.000011685
69	1	-0.000011124	0.000014879	-0.000010875
70	1	-0.000024463	-0.000061331	0.000018718
71	1	0.000014466	0.000009943	-0.000018300
72	1	0.000015024	-0.000010182	0.000017365
73	1	-0.000000895	-0.000013071	-0.000011538
74	1	0.000001593	0.000038438	-0.000014264
75	1	-0.000014374	0.000011226	-0.000017550
76	1	0.000003933	-0.000015236	0.000003235
77	1	0.000011737	-0.000004763	-0.000014574
78	1	-0.000009470	-0.000008724	-0.000000686
79	1	-0.000003831	-0.000014011	0.000002309
80	1	0.000005017	-0.000006198	0.000000020
81	1	-0.000012057	-0.000001648	-0.000011040
82	1	-0.000001743	-0.000037749	0.000014202
83	1	0.000001005	0.000011931	0.000011755
84	1	-0.000013354	-0.000012808	0.000019446
85	1	0.000018909	0.000064556	-0.000012566
86	1	0.000012127	0.000002809	-0.000010566
87	1	0.000011289	-0.000014424	0.000010407
88	1	0.000017843	-0.000067030	0.000011290
89	1	0.000010990	0.000013142	-0.000013374
90	1	0.000013052	-0.000003718	0.000009026
91	1	-0.000004821	-0.000000628	-0.000008270
92	1	-0.000003026	-0.000012482	0.000007552
93	1	0.000009877	0.000019482	0.000009047
94	1	0.000004507	0.000000546	-0.000007734
95	1	-0.000006939	0.000023913	0.000010831
96	1	0.000003213	-0.000015354	0.000007791
97	1	0.000005402	-0.000000006	0.000008379
98	1	-0.000009902	-0.000020268	-0.000009133
99	1	0.000002955	0.000013032	-0.000007700
100	1	-0.000003814	0.000000129	0.000007843
101	1	-0.000003079	0.000014940	-0.000007928
102	1	0.000007159	-0.000023072	-0.000010914
103	1	-0.000004087	0.000014343	-0.000003116
104	1	0.000009003	0.000008230	0.000000963
105	1	-0.000011901	0.000003667	0.000014816
106	1	0.000004049	0.000015314	-0.000002468
107	1	0.000012502	0.000002477	0.000011328
108	1	-0.000005777	0.000006675	0.000000080

References:

[7] Gaussian 09, Revision B.01, Frisch, M.J.; Trucks, G.W.; Schlegel, H.B.; Scuseria, G.E.; Robb, M.A.; Cheeseman, J.R.; Scalmani, G.; Barone, V.; Mennucci, B.; Petersson, G.A.; Nakatsuji, H.; Caricato, M.; Li, X.; Hratchian, H. P.; Izmaylov, A. F.; Bloino, J.; Zheng, G.; Sonnenberg,J.L.; Hada, M.; Ehara, M.; Toyota, K.; Fukuda, R.; Hasegawa, J.; Ishida, M.; Nakajima, T.; Honda, Y.; Kitao, O.; Nakai, H.; Vreven, T.; Montgomery, J.A., Jr.; Peralta, J.E.; Ogliaro, F.; Bearpark, M.; Heyd, J. J.; Brothers, E.; Kudin, K. N.; Staroverov, V. N.; Keith, T.; Kobayashi, R.; Normand, J.; Raghavachari, K.; Rendell, A.; Burant, J. C.; Iyengar, S.S.; Tomasi, J.; Cossi, M.; Rega, N.; Millam, J.M.; Klene, M.; Knox, J.E.; Cross, J.B.; Bakken, V.; Adamo, C.; Jaramillo, J.; Gomperts, R.; Stratmann, R.E.; Yazyev, O.; Austin, A.J.; Cammi, R.; Pomelli, C.; Ochterski, J.W.; Martin, R.L.; Morokuma, K.; Zakrzewski, V.G.; Voth, G.A.; Salvador, P.; Dannenberg, J.J.; Dapprich, S.; Daniels, A.D.; Farkas, O.J.; Foresman, B.; Ortiz, J.V.; Cioslowski, J.; Fox, D. J. Gaussian, Inc., Wallingford CT, **2010**.

Supplementary Table S2:

Table S2 The binding constants of reported macrocyclic receptors serving as Li^+ ionophores.

Number	References	Contents
1	J. A. Chen, J. L. Lai, G. H. Lee, Y. Wang, J. K. Su, H. C. Yeh, W. Y. Lin and M. K. Leung, *Org. Lett.*, 2001, **3**, 3999-4002.	Solvent: CH_3CN; Complexation model: only lithium cation; Stoichiometry (Host:Guest) : 1:2; The binding constant between ureyleno crown ether **3** and Li^+ was found to be 3.0×10^7 $(L/mol)^2$.
2	Y. Luo, N. Marets and T. Kato, *Chem. Sci.*, 2018, **9**, 608-616.	Solvent: $CDCl_3$: CD_3CN = 1 : 1 (v/v); Complexation model: only lithium cation; Stoichiometry (Host:Guest) : 1:1; The binding constant between CE derivatives **1** and Li^+ was found to be 2359 M^{-1} and the binding constant between CE derivatives **2** and Li^+ was found to be 610 M^{-1}.
3	Z. Grote, M. L. Lehaire, R. Scopelliti and K. Severin, *J. Am. Chem. Soc.*, 2003, **125**, 13638-13639.	Solvent: D_2O; Complexation model: only lithium cation; Stoichiometry (Host:Guest) : 1:1; The binding constant between metallamacrocycle **2** and Li^+ was found to be

		$(8.4 \pm 0.6) \times 10^2$ M^{-1} and the binding constant between metallamacrocycle **3** and Li^+ was found to be $(2.3 \pm 0.4) \times 10^3$ M^{-1}.
4	K. Roy, C. Wang, M. D. Smith, P. J. Pellechia and L. S. Shimizu, *J. Org. Chem.*, 2010, **75**, 5453-5460.	Solvent: CD_3CN; Complexation model: only lithium cation; Stoichiometry (Host:Guest) : 1:1; The binding constant between pyridyl macrocycle **2** and Li^+ was found to be 6600 M^{-1} and the binding constant between pyridyl macrocycle **3** and Li^+ was found to be 10^6 M^{-1}.
5	C. Ren, V. Maurizot, H. Zhao, J. Shen, F. Zhou, W. Q. Ong, Z. Du, K. Zhang, H. Su and H. Zeng, *J. Am. Chem. Soc.*, 2011, **133**, 13930-13933	Solvent: $H_2O/CHCl_3$ system; Complexation model: only lithium cation; Stoichiometry (Host:Guest) : 1:1; The binding constant between pentamer **2** and Li^+ was found to be $(2.28 \pm 0.10) \times 10^8$ M^{-1}.
6	Q. He, N. J. Williams, J. H. Oh, V. M. Lynch, S. K. Kim, B. A. Moyer and J. L. Sessler, *Angew. Chem. Int. Ed.*, 2018, **57**, 11924-11928.	Solvent: THF-d_8/D_2O (9/1, v/v); Complexation model: ion pair; Stoichiometry (Host:Guest) : 1:1; ^1H NMR spectroscopic titration of ion-pair receptor **2** with LiCl was found $K_a = (8.3 \pm 0.3) \times 10^2$ M^{-1}.
7	K. Kang, J. A. Lohrman, S. Nagarajan, L. Chen, P. Deng, X. Shen, K. Fu, W. Feng, D. W. Johnson, L. H. Yuan, *Org. Lett.,* 2019, **21**, 652-655.	Solvent: $CHCl_3$: CH_3CN = 1 : 1 (v/v) ; Complexation model: ion pair; Stoichiometry (Host:Guest) : 1:1; The binding constant between convergent ditopic receptor **1a** and Li^+ was found to be $(5.5 \pm 0.4) \times 10^4$ M^{-1}.
8	This work.	Solvent: $CHCl_3$: CH_3CN = 1 : 1 (v/v) ; Complexation model: only lithium cation; Stoichiometry (Host:Guest) : 1:1; The binding constant between biphenyl-cyclo[4]aramide **1a** and Li^+ was found to be $(1.92 \pm 0.05) \times 10^4$ M^{-1}.